A Three-Dimensional (3D) *In Vitro* Model of Ehlers-Danlos Syndrome

A Major Qualifying Project Report

Submitted to the Faculty of Worcester Polytechnic Institute

In partial fulfillment of the requirements for the

Degree of Bachelor of Science

By

Madison Donahue

Maya Evohr

Morgan Foltz

Abigail Holmes

Spencer Whitford

March 2024

Approved by:

Professor George Pins, Advisor

Table of Contents

Authorship

Section	Primary Writer	Primary Editor	Final Editor
1.0 Introduction	Morgan	Madison	All
2.1 Ehlers Danlos Syndrome	Spencer	Maya	All
2.2 Clinical Need	Madison	Maya	All
2.2.1 Mechanisms of Cutaneous Wound Healing in Individuals without EDS	Abigail	Spencer	All
2.2.2 Collagen and Wound Healing in Classical Ehlers-Danlos Syndrome	Abigail	Spencer	All
2.2.3 Treatments for Cutaneous Surgical Wounds	Madison	Maya	All
2.3 EDS Cutaneous Wound Healing Models	Morgan	Abigail	All
2.3.1 Standard Cutaneous Wound Healing Models	Morgan	Abigail	All
2.3.2 EDS Cutaneous Wound Healing Models	Madison	Maya	All
2.4 Need Statement	Maya	Abigail	All
3.1 Initial Client Statement	Spencer	Maya	All
3.2 Stakeholders	Abigail	Maya	All
3.3 Initial Objectives	Maya	Abigail	All
3.4 Constraints	Abigail	Maya	All
3.5 Final Objectives	Madison	Abigail	All
3.6 Revised Client Statement	Maya	Abigail	All
3.7 Project Approach	Madison	Abigail	All
4.1 Needs Analysis	Madison	Maya	All
4.1.1 Design Needs	Madison	Morgan	All
4.1.2 Design Needs	Spencer	Morgan	All

4.1.3 Needs and Wants Design Matrix	Madison	Abigail	All
4.2 Functions and Specifications	Maya	Madison	All
4.3 Conceptual/Preliminary Design Phase	Maya	Madison	All
4.3.1 Brainstorming Design Elements	Morgan	Spencer	All
4.3.2 Evaluation of Design Elements: Cell Type	Madison	Spencer	All
4.3.2 Evaluation of Design Elements: Model Style	Morgan	Madison	All
4.3.2 Evaluation of Design Elements: Matrix Material	Morgan	Madison	All
4.3.2 Evaluation of Design Elements: Wound Induction	Spencer	Abigail	All
4.3.3 Quantitative Assessment of Design Elements	Abigail	Maya	All
5.0 Development and Verification of Final Design	Madison	Morgan	All
5.1 Cell-Laden Hydrogel Design	Madison	Abigail	All
5.2 Micro-TUG Design	Maya	Madison	All
5.3 Wound Induction Method Designs	Morgan	Abigail	All
5.4 Preliminary Testing of Overall Design Ideas	Morgan	Maddie	All
5.4.1 Well Plate Mask	Spencer	Abigail	All
5.4.2 Cell Growth Assay	Abigail	Madison	All
5.4.3 Monolayer Scratch Assay	Abigail	Madison	All
5.4.4 Fibrin Gel Design	Madison	Abigail	All
5.4.5 Fibrin Dot Assay	Abigail	Madison	All
5.4.6 Punch Prototyping	Abigail	Madison	All
5.4.7 3D Gel Indentation Testing	Spencer	Abigail	All
5.5 Experimental Contribution to Final Design	Maya	Madison	All

6.0 Final Design and Validation	Maya	Morgan	All
6.1 Final Wound Healing Model is Representative of cEDS Function	Morgan	Abigail	All
6.2 Final Wound Healing Model Allows for Efficient Imaging Over Time	Morgan	Abigail	All
6.3 Fabrication Analysis	Morgan	Abigail	All
6.4 Viability and Useability Analysis	Morgan	Abigail	All
7.1 Final Device Analysis	Morgan	Abigail	All
7.2 Gel Structural Properties	Spencer	Abigail	All
7.3.1 Economics	Maya	Abigail	All
7.3.2 Environmental Impact	Maya	Abigail	All
7.3.3 Societal Influence	Maya	Abigail	All
7.3.4 Political Ramification	Maya	Morgan	All
7.3.5 Ethical Concerns	Morgan	Spencer	All
7.3.6 Health and Safety Issues	Maya	Abigail	All
7.3.7 Manufacturability	Maya	Morgan	All
7.3.8 Sustainability	Maya	Morgan	All
7.3.9 Industry Standards	Maya	Morgan	All
8.0 Conclusions and Recommendations	Madison	Spencer	All

Acknowledgements

The team would like to acknowledge the following people for their contributions, expertise, and assistance throughout this project:

Worcester Polytechnic Institute

George D. Pins, PhD

Sakthikumar Ambady, PhD

Andrew Leverone

Lisa Wall

Ian Anderson

University of North Carolina at Chapel Hill

Elizabeth Doherty, PhD

University of Massachusetts Medical School

Raymond Dunn, MD

Mayo Clinic

Dacre Knight, MD

Ghent University Hospital

Fransiska Malfait, MD, PhD

Center for Multisystem Disease

Jill Schofield, MD

Hartford HealthCare Bone and Joint Institute

Sara Strecker, PhD

Peyton Manning Children's Hospital

Brad Tinkle, MD, PhD

Abstract

Classical Ehlers-Danlos Syndrome (cEDS) disrupts collagen structure, leading to delayed wound healing which negatively impacts patients' quality of life. There exists a need to create treatments to aid in the cEDS wound healing process; however, the mechanisms behind this impaired wound healing are not fully understood. Wound healing models provide an opportunity to further identify disease characteristics and serve as a tool for pharmacological testing. Existing wound healing models are either not sufficiently representative of the disease or are expensive and complex to fabricate. This project aimed to engineer a 3D *in vitro* wound healing model of cEDS. A 3D *in vitro* cell-seeded fibrin gel model was engineered, supported by cell-count studies, wound healing monolayer assays, outgrowth assays, and indentation tests. Initial findings demonstrate the model may serve as a representative tool to improve the general understanding of wound healing in cEDS.

Table of Figures

Table of Tables

1.0 Introduction

The Ehlers-Danlos Syndromes are a collection of connective tissue disorders that are prevalent in at least 1 in 5,000 individuals globally, affecting patients' quality of life through collagen I, III, or V defects (Miklovic & Sieg, 2023). Commonly characterized by clinical presentations of skin hyperextensibility, joint laxity, and irregular wound healing, the thirteen recognized types of Ehlers-Danlos Syndromes (EDS) are described as multisystem disorders that have varied clinical presentations within each subtype (Malfait et al., 2020). Clinical presentation ranges from complications of chronic pain and failure to arterial rupture, organ rupture, and joint dislocation (Miklovic & Sieg, 2023). Delayed wound healing is a major presentation of EDS, in which the fibrous collagen structure is distinctly different from the fine collagen fibers seen in patients without collagen complications (Mao & Bristow, 2001). Due to this delay in wound healing caused by impaired tissue strength, surgery is often avoided in EDS patients although there are various injuries such as connective tissue tears which would require surgeries (Wiesmann et al., 2014). There exists a need to further understand the mechanisms behind wound healing in EDS patients, to inform potential treatments that may enable the use of surgery to treat debilitating conditions.

Wound models, either using *in vitro* or *in vivo* studies, are commonly used to visualize and better understand the behavior of skin. These models offer an opportunity to gain knowledge about dermal and epidermal characteristics, as well as the skin’s response to various methods of treatment, such as suturing, surgical glue, or various therapeutics for tissue growth and response. The standard method of representing wound healing behavior *in vitro* incorporates either the use of monolayer cell culture scratch assay, co-cultured cell culture assays, and skin explants and 3-dimensional cultures (Hofmann et al., 2023). Within monolayer cell cultures, a single layer of

either dermal fibroblasts or epidermal keratinocytes are cultured separately. Co-culture models involve a combination of keratinocytes and fibroblasts separated by a porous insert placed between the cell layers. Three-dimensional models are cultivated using keratinocytes and fibroblasts on a porous membrane, serving to partition the various layers within the model, above a matrix, and human skin equivalents involve keratinocytes grown above a scaffold composed of dermal fibroblasts in a matrix (Hofmann et al., 2023).

The goal of this project is to develop a 3D wound healing model for Ehlers-Danlos Syndrome. This design aims to represent cell growth and wound healing using a 3D wound model incorporating human Ehlers Danlos Syndrome dermal fibroblasts in a biomaterial scaffold representative of native tissue. Most available *in vitro* and *in vivo* wound healing studies focus on the regular function of human keratinocytes and dermal fibroblasts in wound healing behavior, in contrast with cells with impaired or slower function during wound healing. However, for disease pathologies, this is more difficult. The only existing models for wound healing in EDS include *in vitro* scratch wound assays on a monolayer of COL5A1 haploinsufficient EDS fibroblasts, as well as an *in vivo* rat model with a full thickness stamp wound. This project seeks to aid in the understanding of wound healing in EDS by offering an *in vitro* model that is more complex than existing 2D assays, and more accessible than existing *in vivo* models. By evaluating this, the team identified six design objectives to aid in this goal: the model must be reproducible, imageable, representative of EDS pathology, versatile for future testing of different wound healing conditions and treatments, easily useable, and affordable. From there, the team defined the four design elements needed for a 3D wound healing model: cell type, model type, matrix material, and wound induction method.

To begin development of the final design, alternatives for each design element identified were proposed within a group setting. After initial brainstorming, feasibility studies and comparison of each method were conducted using pairwise comparison charts and general discussion. A final preliminary design of a 3D *in vitro* hydrogel model composed of classical EDS dermal fibroblasts embedded within a fibrin matrix was developed. To represent a surgical cutaneous wound, a thin sterilized punch is used for wound induction.

Once the overall design idea was developed, the team progressed through a series of evaluations to ensure that the final model would meet its designated objectives and specifications for overall functionality. The needs and wants of the design were initially noted in addition to constraints and objectives, followed by functions and specifications of how the model would be supported within a laboratory environment, including imageability and overall ease of use. The following preliminary design phase assessed the design options based on previously determined functions, specifications, objectives, and constraints. The final design was then developed, and validation and verification experimentation were conducted to evaluate the model's success.

Throughout the duration of the study, it was observed that the cell count assay revealed increased growth of control neonatal dermal fibroblasts (NHF) in comparison to the experimental cEDS patient-derived fibroblasts. Verification testing using a scratch assay conducted within a confluent monolayer of fibroblasts observed 80% total wound closure by the end of the 24-hour study. Three-dimensional testing of fibrin dot outgrowth observed both NHF and cEDS gel outgrowth by day 5, in which further indentation testing of NHF- and cEDS-seeded gels revealed a difference in structural modulus. Gels seeded with cEDS fibroblasts experienced a higher variability and increased stiffness compared to NHF and acellular, unseeded, fibrin gels, with increased stiffness among all samples over time. The final cEDS wound healing model

successfully observed outgrowth of fibroblasts beginning at day 2 and continuing until final gel degradation on day 6.

Through the development and further optimization of a three-dimensional *in vitro* wound healing model of Ehlers-Danlos Syndrome, an increased understanding of this disease can be observed regarding the wound healing response of impaired connective tissue healing within patients. In addition to this, future pharmacological testing may be conducted to test novel treatments in healing wounds both safely and effectively.

2.0 Literature Review

2.1 Ehlers-Danlos Syndrome

The Ehlers-Danlos Syndromes are a collection of heterogenous, heritable connective tissue disorders. More commonly referred to simply as Ehlers-Danlos Syndrome or EDS, this collection of disorders is characterized by skin hyperextensibility, joint laxity, and irregular wound healing, among other symptoms (Malfait et al., 2020). There are multiple genetically defined subtypes of EDS, most of which exhibit defects in the fibrillar collagen types I, III, or V or have altered enzymatic management of these proteins (Mao & Bristow, 2001). Collagen plays a vital role in the structural components of the extracellular matrix (ECM), and it is a central building block of connective tissue and various organ systems such as the skin, blood vessels intestines, and more (Chiarelli et al., 2019). Due to the essential presence of collagen as a structural protein in nearly all tissues, EDS presents as a multisystem disorder (Malfait et al., 2020; Raspanti et al., 2018). There are thirteen specifically recognized types of EDS, all of which have extensive and varied clinical presentations. While there is no quantified prevalence of different EDS subtypes, the prevalence of three most common forms of EDS are estimated to

be at least 1:5,000 individuals for the hypermobile type (hEDS), 1:10,000-1:20,000 for the classical type (cEDS), and 1:50,000-1:200,000 for the vascular type (vEDS) (Miklovic et al., 2023; Malfait et al., 2020). Each type of EDS has certain hallmark symptoms specific to that type. In hEDS, patients typically have some form of generalized joint hypermobility, stretchy skin, and GI issues (Malfait et al., 2020). In cEDS, patients will experience severe skin fragility leading to tears with minimal trauma, frequent bruising, and are prone to hernias and prolapsed organs (Ehlers Danlos Support UK, 2022). Patients diagnosed with vEDS will experience some similar symptoms of hEDS and cEDS however vEDS patients typically suffer from severe gastrointestinal and vascular/arterial fragility (Malfait et al., 2020).

In addition to the different characteristics of each EDS subtype such as those mentioned above, nineteen distinct causal genes have been identified (Chiarelli et al., 2019). Most notably, classical EDS is associated with defects in the genes COL5A1 (α1(V) procollagen chain), COL5A2 (α2(V) procollagen chain), and rarely COL1A1 (α1(I) procollagen chain). Vascular EDS is associated with mutations in COL3A1 (α1(III) procollagen chain) and COL1A1 (α1(I) procollagen chain) (Malfait et al., 2020). Hypermobile EDS remains molecularly unresolved as the underlying genetic mutation and mechanisms are still unknown (Malfait et al., 2020).

Diagnosis of EDS requires a multifaceted approach often beginning with the identification of major clinical factors such as hypermobile joints and fragile skin (Sobey, 2015). To identify which subtype of EDS a patient has, a genetic test is required, and if it is negative, a clinical hEDS diagnosis may be made. The Ehlers Danlos Society estimates it takes an average of 10-12 years to receive an accurate diagnosis (Sobey, 2015; The Ehlers Danlos Society, 2023). While a patient is undiagnosed or misdiagnosed, the treatment they receive will be uninformed and potentially ineffective at addressing the extensive clinical presentations of EDS.

Clinical presentations and complications of EDS are extensive and vary widely from patient to patient. Major presentations of EDS include but are not limited to hyperextensible skin, joint hypermobility, atrophic scarring, chronic pain, fatigue, gastrointestinal dysmotility, tissue fragility and abnormal or delayed wound healing (Malfait et al., 2020; Viglio et al., 2008; Miklovic et al., 2023). Clinical presentations across types are often complex and overlapping. **Figure 1** provides an extensive overview of the potentially affected bodily systems.

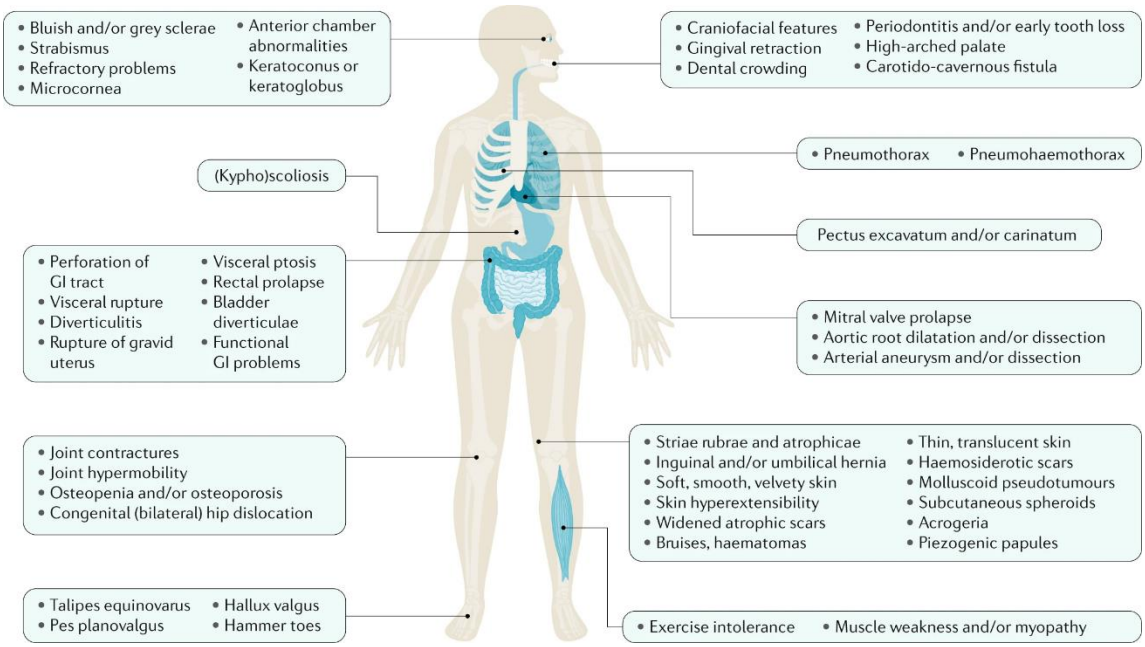

Figure 1. Bodily systems affected by EDS. From Malfait, F., Castori, M., Francomano, C. A., Giunta, C., Kosho, T., & Byers, P. H. (2020). The Ehlers–Danlos syndromes. *Nature Reviews Disease Primers*, 6(1), 64. https://doi.org/10.1038/s41572-020-0194-9

2.2 Clinical Need

Treatment of EDS patients depends on the severity of the case and symptoms, but in some instances, surgery may be the best option for improving quality of life. Patients with EDS can encounter more extensive orthopedic complications such as joint instability and/or nerve compression as well as GI complications such as hiatal hernias (where the stomach protrudes through the diaphragm) or spontaneous perforation in the GI tract (Greenfield, 2021; Burcharth

& Rosenberg, 2012). When addressing these complications, initial treatments are typically minimally invasive and may involve physical therapy or pain relief medications (Greenfield, 2021). However, because of GI complications, many patients experience Gastroesophageal Reflux Disease and cannot handle the long-term ingestion of anti-inflammatory drugs. Opioids are often prescribed for pain management, but continued use can lead to tolerance and decreased effectiveness or addiction (Gunendran & Uma Dwarakanath, 2023). Opioids can also lead to a change in patient sensitivity to stimuli, causing typical environmental stimuli to become painful for patients (Ericson & Wolman, 2017). Medications like these can often treat pain on an as-needed basis, but the primary cause of pain is not addressed (Greenfield, 2021).

Unfortunately, these treatments will only provide relief from pain and other complications for a finite period. Physical therapy is usually encouraged for hypermobile patients; however, it is often preventative, allowing for EDS patients to condition and strengthen muscles before a ligament/muscle tear or joint dislocation occurs. Some EDS patients will require intense rehabilitation through physiotherapy to maintain satisfactory quality of life and mobility (Keer & Simmonds, n.d.). While orthopedic surgery may be clinically indicated, it is typically avoided for patients with Ehlers Danlos Syndrome due to the additional risks associated with the condition. Establishing an exact diagnosis for the joint injury as well as creating a technical plan for surgery can be difficult and requires a surgeon who has experience with EDS to be successful (Ericson 2017). Additionally, if the tissues surrounding the injured joint are too loose, the surgery may fail despite the expertise of the surgeon. There is also an element of unpredictable healing in EDS patients, and they typically have a longer healing process, are more prone to bleeding, and can experience wound healing complications (Ericson 2017). Cutaneous wound healing in EDS patients is often prolonged because of wound dehiscence, inability of

wounds to properly maintain suture holds, and wider scar formations (Baik et al., 2019). For any EDS-related complication, if it is determined that surgery is the best course of action despite the increased risks in EDS patients, it must be done by an experienced surgeon with the knowledge that the surgery might fail. Due to these risks, surgery is always the last resort for EDS patients, despite the potential for surgery to improve these patients' quality of life (Ericson & Wolman, 2017).

2.2.1 Mechanisms of Cutaneous Wound Healing in Individuals Without EDS

Wound healing is a complex and closely regulated process essential for restoring injured tissue (Almadani et al., 2021). As seen in **Figure 2**, wound healing follows a sequence comprised of four stages: hemostasis, inflammation, proliferation, and remodeling (Enoch & Leaper, 2008).

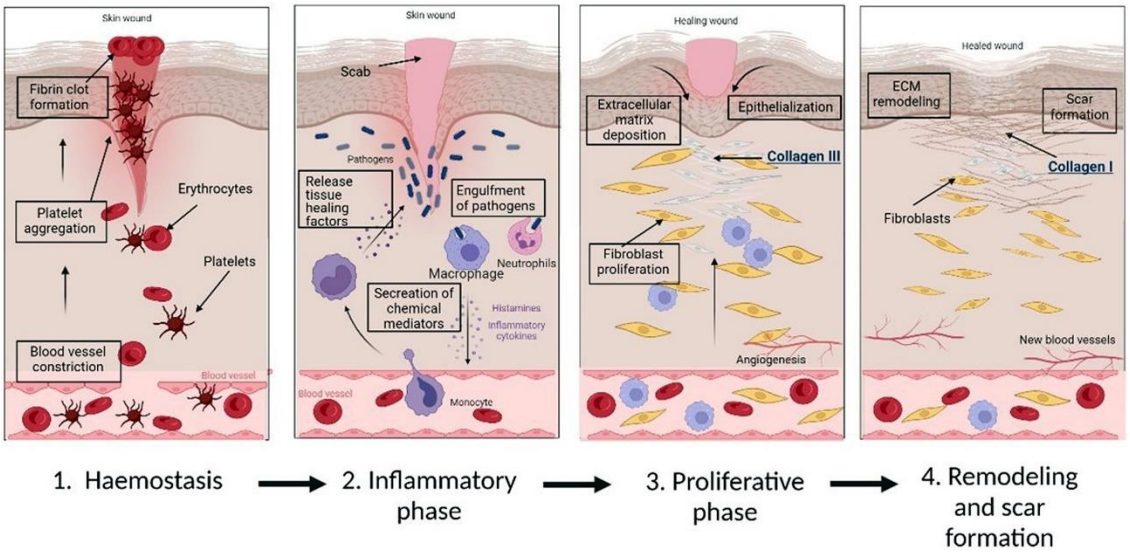

Figure 2. Mechanism of action of wound healing with a role of collagen. From Gajbhiye, S., & Wairkar, S. (2022). Collagen fabricated delivery systems for wound healing: A new roadmap. *Biomaterials Advances, 142*, 213152. https://doi.org/10.1016/j.bioadv.2022.213152

The first phase of wound healing is hemostasis, which begins immediately after injury to control bleeding. Vasoconstriction occurs to reduce blood flow, followed by the formation of a

temporary hemostatic plug to seal the wound (Almadani et al., 2021). Collagen III provides a scaffold for platelet adhesion and fibrin formation (Yates et al., 2012). Platelets adhere to the injured vessel walls and release factors that promote clot formation. This plug is reinforced by a fibrin network, which helps stabilize the wound site and control bleeding (Yates et al., 2012).

The inflammation phase occurs next, occurring within the first 24 hours after injury and lasting up to two weeks after (Schultz et al., 2011). In this phase, the body's inflammatory response is triggered. White blood cells, such as neutrophils and macrophages, migrate to the wound site to remove debris, pathogens, and damaged tissue (Almadani et al., 2021). Inflammatory cytokines and growth factors are released to signal the next stages of healing.

The proliferative phase of wound healing begins approximately four days after the injury and can last up to 21 days (Landén et al., 2016). During this phase, re-epithelialization takes place as epithelial cells detach, migrate, proliferate, and differentiate under the influence of growth factors including epidermal growth factor, keratinocyte growth factor, and transforming growth factor alpha (Schultz et al., 2011). Concurrently, fibroblasts and endothelial cells become prominent in the wound, supporting type I and III collagen synthesis, capillary growth, and the development of granulation tissue, with myofibroblasts contributing to wound contraction. New blood vessels form through angiogenesis, ensuring adequate oxygen and nutrient supply (Schultz et al., 2011).

During the remodeling phase, which can last from weeks to years dependent on the severity of the wound, several critical changes occur in the healing tissue (Gonzalez et al., 2016). Initially, granulation tissue, characterized by an intense network of blood vessels, elevated cellular density of fibroblasts and macrophages, and randomly organized collagen fibers, gradually matures into a scar (Schultz et al., 2011). This transformation involves a reduction in

the density of capillaries, a decrease in the levels of glycosaminoglycans and the associated water content, and a shift from the production of type III collagen to more stable type I collagen (Schultz et al., 2011). This transition significantly enhances the tensile strength of the tissue as it heals. During this phase, many of the newly formed capillaries in the wound gradually regress, returning vascular density to levels seen in uninjured tissue. Additionally, the wound undergoes physical contraction, driven by contractile fibroblasts known as myofibroblasts (Guo & DiPietro, 2010). This contraction process plays a role in scar formation and contributes to the reduction in wound size. It is important to note that while the tensile strength of the healed scar tissue reaches approximately 80% of that of normal, uninjured skin, the healed scar tissue never fully matches the strength of the original, uninjured tissue (Almadani et al., 2021).

2.2.2 Collagen and Wound Healing in Classical Ehlers-Danlos Syndrome

Collagen fibers are essential for maintaining the structural integrity of the skin and other tissues throughout the body. In their normal state, collagen fibers display a highly organized structure. They consist of individual collagen molecules that assemble into a triple helical structure, with each molecule composed of three polypeptide chains. The collagen molecules are stabilized through different types of cross-links (difunctional, trifunctional, and tetrafunctional cross-links), which provide mechanical strength and stability to the fibers (Tanzer 1973). Collagen fibers possess a hierarchical structure, with collagen molecules forming larger fibrils that, in turn, aggregate to create fibers, which range from 1 to 20 microns in diameter (Ushiki 1992). As seen in **Figure 3**, in normal tissue, these fibrils exhibit a basketweave-like, three-dimensional network, contributing to tissue flexibility and mechanical strength (Mathew-Steiner et al., 2021).

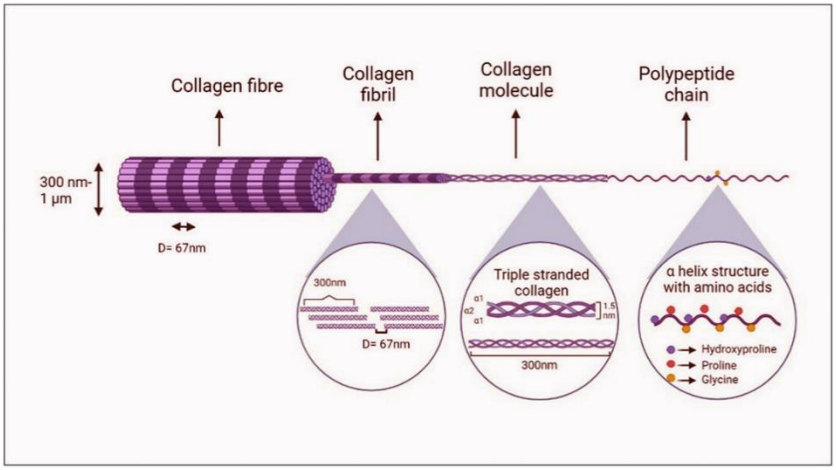

Figure 3. Structure of collagen. From Gajbhiye, S., & Wairkar, S. (2022). Collagen fabricated delivery systems for wound healing: A new roadmap. *Biomaterials Advances, 142*, 213152. https://doi.org/10.1016/j.bioadv.2022.213152

In EDS, there are significant deviations from this normal collagen fiber structure. Notably, individuals with cEDS exhibit a distinctive increase in fibril diameter of approximately 25% compared to that of unaffected patients, resulting in thicker collagen fibrils that significantly deviate from the usual, fine collagen fibrils (Mao & Bristow, 2001). An additional anomaly observed in cEDS is the presence of composite fibrils, which exhibit an abnormal structure characterized by irregularities in size and organization. These composite fibrils are commonly referred to as "collagen cauliflowers," and are depicted below in **Figure 4**. These structural aberrations in collagen fibers compromise tissue strength and impair the wound healing process.

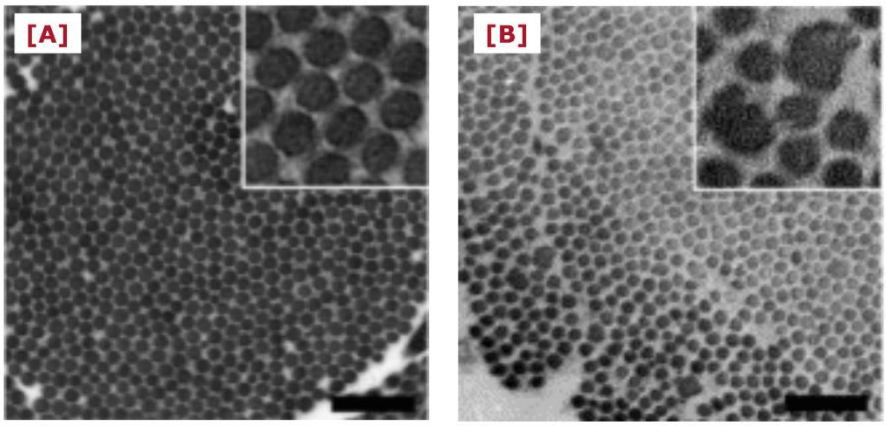

Figure 4. [A] Control presenting with tightly packed collagen fibrils with uniform diameters [B] Large collagen fibrils with irregular contours ("collagen cauliflowers") presented in cEDS patient with heterozygous mutation in COL5A2. Modified from Malfait, F., Vroman, R., Colman, M., & Syx, D. (2021). Collagens in the Physiopathology of the Ehlers–Danlos Syndromes. In F. Ruggiero (Ed.), *The Collagen Superfamily and Collagenopathies* (pp. 55–119). Springer International Publishing. https://doi.org/10.1007/978-3-030-67592-9_3

The impaired wound healing observed in individuals with cEDS can be attributed to a variety of intricate biological mechanisms, dependent on where the cEDS-causing genetic mutation lies. Patients with cEDS most commonly present with a mutation in the COL5A1 gene, followed by COL5A2, and rarely, COL1A1 (Malfait et al., 2020). Mutations in the COL5A1 gene result in haploinsufficiency, which causes an approximate 50% reduction in collagen V levels (Malfait et al., 2020). Collagen V is a crucial regulator of fibrillogenesis, the process of creating fibrils, playing a pivotal role in maintaining tissue structure and integrity (Mao & Bristow, 2001). Collagen V has distinct isoforms, with the [α1(V)2α2(V)] heterotrimer being the most prevalent, regulating fibril diameter within type I collagen fibrils (Viglio et al., 2008). COL5A1 haploinsufficiency limits proper heterotrimer production, impacting fibril assembly. The presence of atypical type V collagen homotrimers or heterotrimers is also postulated to further disrupt the normal ECM organization (Viglio et al., 2008).

The pathophysiology of poor wound healing in cEDS is closely linked to the decreased collagen V levels and its associated consequences. Using fibroblasts from cEDS patients, Chiarelli et al. identified the disorganization of various ECM components including collagen V, collagen III, fibronectin, and fibrillin *in vitro* (Chiarelli et al., 2019). Additionally, there is a disorganization of collagen- and fibronectin-specific receptors for integrins α2β1 and α5β1, which are crucial for cell-ECM interactions (Malfait et al., 2020). Additionally, transcriptome profiling of cEDS fibroblasts show disturbances in ECM modeling and wound healing, as well as dysregulated gene expression related to endoplasmic reticulum homeostasis and autophagy (Chiarelli et al., 2019). The reduced collagen V availability also results in decreased fibroblast proliferation and migration (DeNigris et al., 2016). The precise mechanism by which collagen V affects fibroblast proliferation is yet to be fully understood, but it is likely related to alterations in ECM structure or substrate attachment (DeNigris et al., 2016).

Another mechanism contributing to poor wound healing in cEDS is the decreased attachment of cEDS fibroblasts to components of the wound matrix including collagens I and III, as well as fibronectin (DeNigris et al., 2016). Collagen I and collagen III are pivotal components of the ECM during different phases of wound healing, with collagen I prominent in the remodeling phase. Fibronectin plays a crucial role in various stages of wound healing, including initial matrix formation, fibroblast attachment, and cell migration. The altered interactions of cEDS fibroblasts with the wound ECM affect wound closure and strength (DeNigris et al., 2016). Disruptions in cell-substrate interactions can also impact the biosynthetic profiles of these fibroblasts, causing additional complications in the healing process.

2.2.3 Treatments for Cutaneous Surgical Wounds

Table 1. Summary of Needs and Limitations (Baik et al., 2019)

Wound Care Need for EDS Patients	**Current Treatment Limitations**
Ability to maintain wound closure after surgical incision	• Sutures and staples must remain in the patient for double the typical healing period • Additional tears can form around sutures
Wound dressings that protect the wound as it heals	• Dressings can pull at skin, causing the skin to tear • Tape and other adhesives can cause skin tears so are often avoided

There are many different options for wound care that are commonly used in the medical field. Standard surgical wound closure techniques for unaffected individuals include sutures, staples, and adhesives such as glue or tape. Staples and sutures may be used interchangeably, though staples are often used for larger linear surgical wounds. Otherwise, sutures will be used for wound closure, and suture material may or may not be degradable. Staples are often used for large linear surgical wounds, and for other wounds degradable or non-degradable sutures can be used. Adhesives may be used jointly with either method if added support is required. Adhesives can also be used as standalone treatments for smaller wounds, such as minor cuts and other minor lacerations (Azmat & Council, 2023). When using any of these methods to close cutaneous wounds in EDS patients, alterations must be made to limit complications regarding wound closure and delayed wound healing in patients. Sutures are often preferred over staples and are often left in patients for twice the typical length of time as compared to a non-affected patient (Shirley et al., 2012). To prevent additional tears in the fragile tissue from sutures, the

location where the procedure was conducted can also be temporarily immobilized, though this is not always feasible (Shirley et al., 2012).

In a case study conducted on a cutaneous wound of a patient with EDS, the patient presented with a wound caused by an injury a month prior that had not healed. The wound was excised and sutured using a nylon material. Around three weeks after the initial procedure, the wound was re-sutured to address additional tears that had been caused by the initial suturing. Bolster sutures were added to the excision location to alleviate tension of the fragile tissue. These sutures were partially successful, however they led to partial necrosis of soft cutaneous tissue of the wound as indicated by the yellow arrow in **Figure 5**, below (Baik et al., 2019). In this instance, suturing a cutaneous surgical wound caused prolonged wound healing in the EDS patient, even with multiple EDS specific adaptations to treatments.

Figure 5. Wound conditions of EDS patient A) one month after injury B) immediately after surgical wound treatment and C) 10 days after re-suturing. The yellow arrow in image C points to partially necrotized tissue. From Baik, B. S., Lee, W. S., Park, K. S., Yang, W. S., & Ji, S. Y. (2019). Treatment of the wide open wound in the Ehlers-Danlos syndrome. *Archives of Craniofacial Surgery*, *20*(2), 130–133. https://doi.org/10.7181/acfs.2018.02334

Surgical tapes may also be used to treat surgical wounds. However, removal of the tape adhesive is known to cause cutaneous injuries such as skin stripping, blisters, and skin tears (Fumarola et al., 2020). These injuries can become prolonged in the wound healing process for EDS patients with fragile tissue.

Wound dressings can also be used to treat cutaneous surgical wounds and promote healing. While wound dressings may help to expedite the healing process in EDS patients, there are no wound dressings that specifically cater to the delayed cutaneous wound healing present in EDS patients. One case study reported that an EDS patient with a cutaneous surgical wound was provided FIBRACOL™ Plus, which is an alginate wound dressing containing collagen (Baik et al., 2019). The dressing changes were completed every 3 days instead of every day, in order to prevent complications that could arise from irritation of the fragile tissue (Baik et al., 2019). In another case study of an EDS patient with a cutaneous wound, the patient had experienced prolonged wound healing when using conventional dressings Using an intermittent negative-pressure dressing seemed to help speed up the healing process, however, they are often costly (Law et al., 2020).

To find novel treatments for closing and healing cutaneous surgical wounds in EDS patients that specifically address complications such as skin tears from fragile tissue and delayed wound healing, preliminary testing must first occur. Novel treatments for wound healing must first be tested on wound healing models, which allows for the analysis of treatment efficacy. There are a variety of wound healing models that can be used to assess the impact of treatment on wound healing, but there are no adequate EDS-specific models (Brať ka et al., 2022).

2.3 Wound Healing Models in Ehlers Danlos Syndrome

Amidst the continuous development of new wound healing treatments, it is critical that appropriate models are utilized to mimic the process of wound healing, specifically that of initial wounding and progressing through the proliferative phase until reaching complete wound closure. These models are instrumental tools for testing new therapies, especially when tailored to replicate the pathology specific to a particular condition (Masson-Meyers et al., 2020). In

cEDS specifically, this is observed in the decreased rate of wound closure as well as complications within the connective tissue healing phase that results in regular wound healing.

Models for cutaneous wound healing include *in silico, in vitro, in vivo* (i.e., animal models), as well as clinical human models and volunteers (Wilhelm et al., 2017). Each model mimics various aspects of the wound healing process, from wound contraction to closure, in which information about healing and non-healing can be evaluated without observation from patients first-hand.

Wound healing models for standard re-epithelialization and collagen proliferation have been extensively studied, and mechanisms of wound behaviors have been determined. However, for Ehlers Danlos Syndrome, these models are limited in both the overall understanding and translational ability to human patients. Current models for Ehlers Danlos Syndrome wound healing are primarily focused on monolayer cell culture modeling and have limitations in efficacy and accuracy. Due to mutations and haploinsufficiency in collagen expression, such as collagen V for classical EDS patients, overall wound healing behavior and function is reduced (DeNigris et al., 2016). There is a disparity in wound healing between individuals with and without EDS, which is notable in several aspects, including the delayed duration of the wound healing process as well as the skin fragility and weakened mechanical strength both during and after the healing period. Wound healing behaviors vary among patients, resulting in the need for representative models that will accurately represent Ehlers Danlos Syndrome and can be translated to human subjects (Guo and DiPietro, 2010).

The following *in vitro* and *in vivo* models provide a general review of current systems used to observe wound healing, in which subsequent methods of wounding for each model are reported in **Table 2** below.

Table 2. Overview of reported existing models and wound methods for *in silico*, *in vitro*, and *in vivo* wound healing experimentation.

General Model/Wound	**Model/Wound Classification**
In Silico Models	*In Silico* Computational
In Vitro Model Types	Monolayer Cell Culture
	Co-culture Model
	Skin Explant Model
	3D Matrix Culture
In Vitro Wound Methods	Scratch Assay
	Stamp Assay
	Thermal Injury Assay
	Electrical Injury Assay
	Optical Injury
In Vivo Model Types	Animal Model
	Human Volunteer and Clinical Model
In Vivo Wound Methods	Open Skin Ulcers
	Burn/Thermal Wound
	Ischemic Skin Wound
	Excisional Wound
	Incisional Wound

2.3.1 Standard Cutaneous Wound Healing Models

In Silico Models

In silico wound healing models are computational models of a particular structure or function within the body. These models are particularly valuable because they do not involve animal or human experimentation, and instead rely on cell culture and laboratory analysis.

Advances in bioinformatics and systems biology have promoted the development of models that simulate both sub-cellular and cellular processes (Barh et al., 2014). This approach enables researchers to describe virtually every interaction within the various components of a given system based on the known mechanisms and functions, making fast predictions for a given scenario as a result. This method offers a foundation for formulating hypotheses and understanding the mechanisms that govern cell functions.

In silico computational models do not serve to replace existing experimental models of a disease or system, but instead complement existing experimental data. *In silico* models require parameterization, calibration, and validation through experimental data (Barh et al., 2014). For wound healing, these parameters include components such as half-life of activated inflammatory cells, fibroblast density, rate of pathogen growth, baseline damage repair rate, and level of tissue oxygenation (Menke et al., 2010). These parameters are obtained through predetermined calculations and equations from previous research, and can model a wound healing scenario over time, focusing on a specific variable and its effect/response within the model.

Within a wound with normal perfusion over a duration of two weeks, the computational responses of pathogens, inflammation, damage, and fibroblasts can be visualized, such as in **Figure 6** (Menke et al., 2010). These responses are analyzed to observe wound healing, and further variables can be adjusted to stimulate different wound environments, which is critical due to variability within patients. Using *in silico* models informs wound healing through response of different components within the system over a designated duration of time. Pathogenic response over time is critical in understanding its specific effect on the resulting wound healing and growth, and general evaluation of wound closure and decrease in ‘damage’ will be the main components in any wound healing model. In addition to quantification of inflammation or

number of present fibroblasts within the given sample, a representative understanding of wound healing can be developed, containing many variables that would normally be actively changing within a live model.

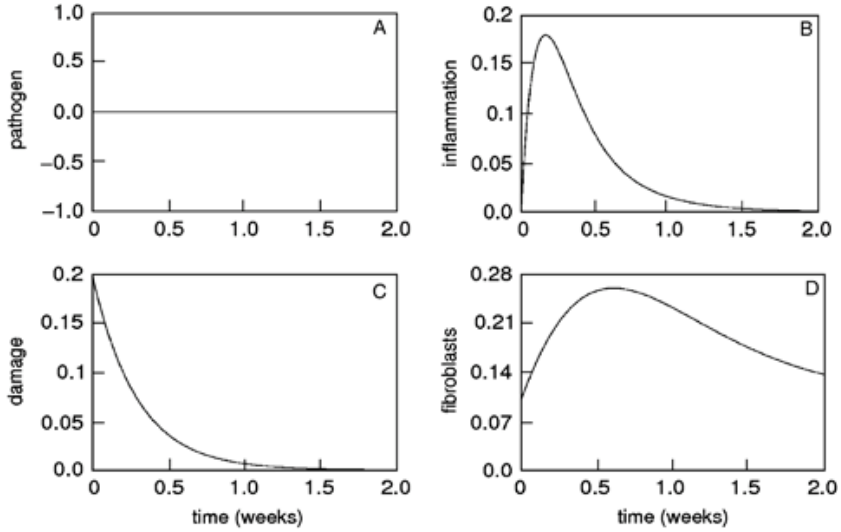

Figure 6. Healing behavior of a baseline wound healing stimulation in an uncontaminated wound with regular perfusion levels From Baik, B. S., Lee, W. S., Park, K. S., Yang, W. S., & Ji, S. Y. (2019). Treatment of the wide open wound in the Ehlers-Danlos syndrome. Archives of Craniofacial Surgery, 20(2), 130–133. https://doi.org/10.7181/acfs.2018.02334.

While *in silico* models for wound healing are critical for understanding wound healing and predicting the immunological response from the body using statistical analysis, these models lack the essential biophysical characteristics of human skin. These models observe components of the wound healing process; however, the biological properties and components of the skin and body cannot be exactly replicated by this method. This is a result of the model creation being limited through only having access to the data that is inputted into the software. *In silico* models are thus theoretical until confirmed via either *in vitro* or *in vivo* experimental data (Sami et al., 2019). The accuracy and reliability of these models are questioned as a result, in which definitive evidence towards the system must be used as a basis for the resulting computational models

beforehand. For medical conditions that have no defined or distinguished mechanisms on wound healing function, *in silico* models are distinctly inferior to biological disease models.

In vitro Models

Human *in vitro* skin models designed for wound healing studies encompass the essential cellular and structural components necessary for analyzing wound healing in humans. These models provide effective means to observe wound healing behaviors in laboratory environments over time, as well as for testing potential treatments and therapeutics before progressing to animal testing and clinical trials (Hofmann et al., 2023). Three primary models for *in vitro* studies include monolayer cell cultures, co-cultured cell cultures, and skin explants or 3D cultures. **Figure 7** provides a visual representation of these *in vitro* models of human skin, illustrating the distinctions between them in terms of their benefits and capabilities.

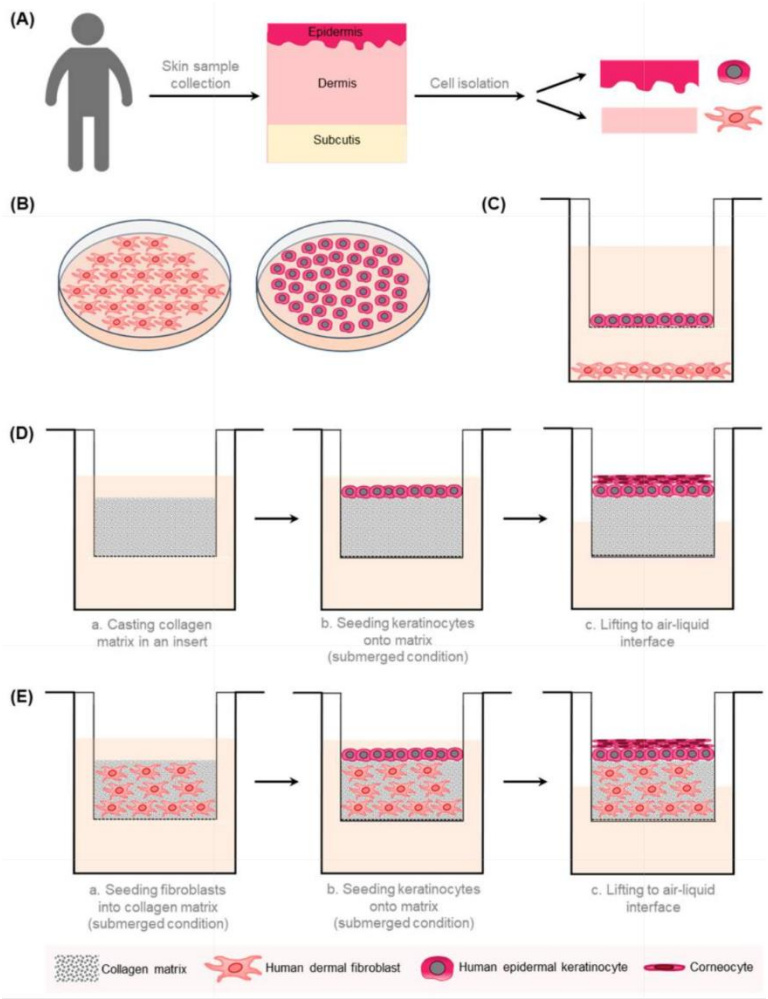

Figure 7. Schematic overviews of 2D monoculture, co-culture, and 3D modeling. (A) Initial isolation process of human dermal and epidermal cells from a human sample. (B) 2D monolayer models' human separate dermal fibroblasts and keratinocytes. (C) Co-culture systems are observed comprised of fibroblasts on the well bottom and keratinocytes grown in a porous insert within the system. (D) Reconstructed human epidermis model is cultivated in a porous membrane above a collagen matrix. (E) Human skin equivalent using keratinocytes grown on top of a dermal model composed of embedded fibroblasts in a collagen matrix. From Hofmann, E., Fink, J., Pignet, A.-L., Schwarz, A., Schellnegger, M., Nischwitz, S. P., Holzer-Geissler, J. C. J., Kamolz, L.-P., & Kotzbeck, P. (2023). Human In Vitro Skin Models for Wound Healing and Wound Healing Disorders. Biomedicines, 11(4), 1056. https://doi.org/10.3390/biomedicines11041056.

Monolayer cell cultures, often referred to as 2D modeling, are simple and cost-effective tests. For wound healing assays, this involves a sequence of four main steps: initial culture preparation and cell seeding, inducing a wound in the cell layer via a scratch, capturing images

and measuring the “wound” gap, followed by data analysis. Limitations of many 2D cultures include primarily the lack of cell-to-cell interactions, vasculature, and cell-to-environment interface (Hofmann et al., 2023). As a result, there is rarely an immune response representative of native tissue, which is a critical limitation in 2D models (Hofmann et al., 2023). For 3D *in vitro* wound healing models, these aid in representing a particular component of the skin more effectively than 2D models, as a scaffold is used to replicating the 3D architecture of the body. However, limitations in 3D model development and analysis include model reproducibility, adaptability, and, like 2D models, there are still areas of wound healing that cannot be fully represented in these models (Randall et al., 2018).

One common approach for 2D wound healing models is the use of scratch assays. These assays are technically non-demanding and inexpensive, making them a popular choice for evaluating cell migration across a 2D surface once mechanically inducing a pseudo wound (Hofmann et al., 2023). The process involves growing a confluent monolayer of cells, and once the cells have reached peak confluency, a pipette tip is used to mechanically create a scratch in the cell layer (De Ieso & Pei, 2018).

Additional methods of 2D wound healing models include the stamp wound assay, thermal injury assay, electrical injury assay, and optical injury assay, all focused on inducing a ‘wound’ to the cell monolayer (Urciuolo et al., 2022). Stamp wound assays focus on creating a lesion within the cell culture using mechanical pressure in the center of the plate, and cell proliferation and migration can be observed following the wound formation (Urciuolo et al., 2022). Similarly, thermal, electrical, and optical injury assays induce a wound by subjecting a specific region of the cell monolayer to high or low temperatures, electrical current, or laser exposure, as seen in **Figure 8** (Urciuolo et al., 2022). 2D wound healing models generally are not

able to replicate the complex conditions of an actual wound, including the intricate wound healing mechanisms. This limitation originates from the use of a single cell line and the absence of the ECM (Urciuolo et al., 2022).

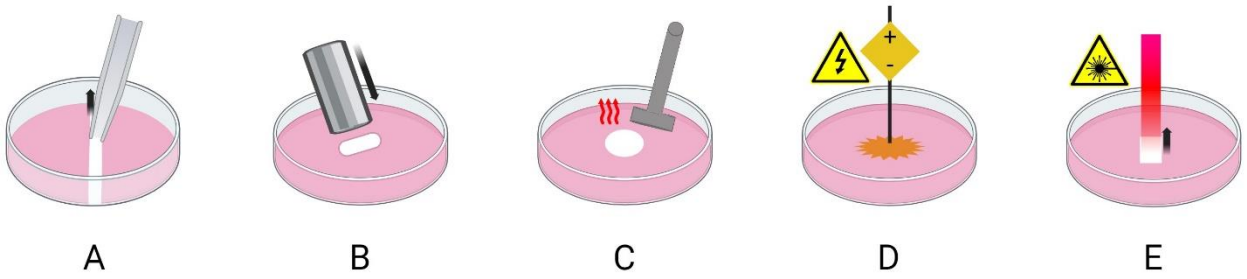

Figure 8. Examples of *in vitro* 3D wound healing models: (A) scratch assay, (B) stamp wound assay, (C) thermal injury assay, (D) electrical injury assay, and (E) optical injury assay. Created using BioRender.

In Vivo Animal Models

Preclinical *in vivo* models for wound research involve various laboratory animals; mice, rats, rabbits, and pigs are the species commonly used in wound model research (Parnell & Volk, 2019). Zebrafish and guinea pigs are also studied. These animal models serve as an effective tool for assessing the intricate nature of wound healing given its multifaceted and complex processes. To mimic wound healing, wounds are induced on the animal through different techniques including incision or excision. Researchers employ specific analysis methods tailored to each, ensuring reproducibility for monitoring the healing process over time. These methods include tracing, photographic documentation and image analysis, biophysical techniques, and other invasive protocols requiring wound biopsies (Masson-Meyers et al., 2020).

In vivo models are widely regarded as the most predictive means for studying wound healing due to their ability to provide a realistic representation of the wound environment. These

models capture the specific cell types, environmental stimuli, and hormonal interactions involved in the wound healing process (Masson-Meyers et al., 2020). When considering the various types of preclinical animal models, it is crucial to choose a model which accurately represents a particular aspect of human physiology while reducing the amount of human involvement and handling. This decision process is additionally reliant on the type of model and purpose of research. All tests involve inducing a wound on the given animal model, though the protocols vary depending on the method. Open skin ulcers, burn wounds, ischemic skin wounds, as well as excisional and incisional wounds are often used in models to observe the ability for skin regeneration and healing (Grada et al., 2018).

While *in vivo* models are the most predictive model of wound healing, a disadvantage is the documented difference between the structure and physiology of skin in animal models and humans. Human skin, specifically in areas of wounds, heals via re-epithelialization and granulation tissue formation. Wound healing in animal models is not identical to wound healing in humans; however, relationships between both humans and animals can be analyzed and used to improve understanding of wound healing (Grada et al., 2018). **Table 3** evaluates the benefits and limitations of each commonly used animal *in vivo* model for wound modeling and behavior.

Table 3. Evaluation and comparison of common animal *in vivo* models for wound healing purposes (Grada et al., 2018; Sami et al., 2019; Summerfield et al., 2015).

Model	Advantages	Limitations
Rodent (Mouse, Rat)	• Availability • Low cost • Small size • Low statistical error • Ease of handling • Ability to be genetically modified	• Thin epidermis • Loose skin adherence • Dense hair (accelerated healing) • Absence of apocrine/eccrine glands • Endogenous source of vitamin C • Subcutaneous panniculus carnosus muscle • Stronger immune system • Poor translational efficacy
Rabbit	• Excisional wound models • Mimics acute healing process • Highly vascularized cartilage	• High breeding cost • Genetic modification difficulties • Scarcity of species-specific reagents
Guinea Pig	• Small size • Relatively affordable • No endogenous vitamin C production	• Not commonly used • Limited number of strains • Lack of transgenic modifications
Porcine	• Thick epidermis/dermis layers • Sparse hair • Apocrine glands • Wound healing via re-epithelization • Burn wound model (low cost and simplicity) • Blood supply similarities	• Small sample size • High cost • Large experimental set-ups required
Zebrafish	• Small size • Low cost • Genetic tractability • Isolated study of processes possible	• Relatively underdeveloped model • Limited number of validated species-specific reagents

Acute wound models are critical for studying natural healing processes and drug discovery. Among these, the most popular models include excisional, incisional, and burn models (Grada et al., 2018). These models are valuable due to their well-established protocols,

which contribute to their ability to be translated with relative accuracy for predictions of wound healing behaviors and skin structure. However, for impaired healing models and general chronic wounds, as well as standard functioning systems in general, it must be noted that all animal models have limitations. An example of this is visualized through a recent study using porcine models to analyze prolonged wound inflammation and overall delayed wound healing by applying Resiquimod, an immune response modifier therapeutic, to mimic chronic wound inflammation. As seen in **Figure 9** below, the application of the drug caused a delayed wound healing effect compared to non-treated control groups, highlighting the differences in healing behaviors over the experiment duration (Holzer-Geissler et al., 2022).

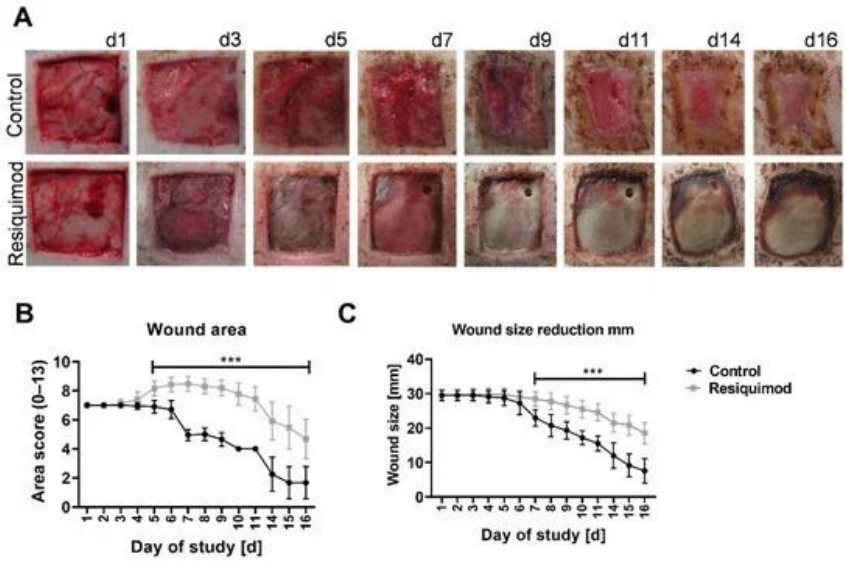

Figure 9. Wound morphology and wound area over the 16-day experiment duration on the back of porcine models is observed. Resiquimod was applied for 6 days at the beginning of the experiment. It can be observed that Resiquimod-induced wounds noted a delay in wound healing/contracture and formation of necrotic scabs. This is representative of chronic wounds. From Holzer-Geissler, J. C. J., Schwingenschuh, S., Zacharias, M., Einsiedler, J., Kainz, S., Reisenegger, P., Holecek, C., Hofmann, E., Wolff-Winiski, B., Fahrngruber, H., Birngruber, T., Kamolz, L.-P., & Kotzbeck, P. (2022). The Impact of Prolonged Inflammation on Wound Healing. Biomedicines, 10(4), 856. https://doi.org/10.3390/biomedicines10040856.

While this model provided valuable insights into the significance of inflammation in wound healing and progression of chronic wounds over time, it also has limitations. These models cannot be directly compared to chronic wounds that develop after a long history of primary diseases, as the study used animals which were not induced with primary chronic diagnoses. Furthermore, the wound samples displayed a high variability in expression patterns, which may result in inaccurate and imprecise translation to humans (Holzer-Geissler et al., 2022).

Chronic wounds and healing complications are relatively rare in animals. The most common chronic conditions induced in animal models include diabetes, mechanical pressure, ischemia, and reperfusion injury (Grada et al., 2018). These chronic wounds additionally differ in their pathophysiology and vary based on the condition, making it difficult to design an accurate and representative model. Consequently, it becomes difficult to apply the findings to human conditions, from overall wound healing to testing of different therapeutics and treatments. Furthermore, the costs associated with animal testing models are significantly higher compared to *in vitro* models, with expenses ranging from 1.5 times as expensive to greater than thirty times as expensive, depending on the chosen model (Van Norman, 2019). This cost discrepancy can pose challenges in replicating studies, contingent on the purpose of the research.

In Vivo Human Volunteer and Clinical Models

Evaluating wound healing behavior is best achieved through human models. These models offer the most relevant and accurate data and are applicable to patients with typical wound healing processes as well as those with chronic illnesses or conditions that affect tissue healing.

When examining chronic wounds in human patients, it's important to consider variability in the uniformity of each wound type within the body (Sami et al., 2019). Limitations in obtaining human models include difficulties in obtaining volunteers, as potential inflicted wounds include partial-thickness wounds, tape stripping, blister models, abrasive models, and full thickness wound models (Sami et al., 2019). Furthermore, a major limitation of using human models for wound healing models is the ethical concerns associated with wounding a healthy volunteer, resulting in animal models being preferred. When wound healing is being studied in patients with impaired function or chronic conditions, these ethical concerns are heightened, and human volunteers cannot be used.

Overall, while standard healing models have been developed and researched, chronic conditions and illnesses involving impaired wound healing are difficult to reproduce with current medical *in-vivo*, *in-vitro*, and in-silico models. For conditions such as EDS, there are limited models that can accurately portray the cutaneous wound healing process and involved mechanisms.

2.3.2 EDS Cutaneous Wound Healing Models

There are a few models that are representative of the delayed cutaneous surgical wound healing that EDS patients experience. Viglio et al. (2008) conducted experiments on a monolayer of COL5A1 haploinsufficient EDS fibroblasts to study their behavior when compared to unaffected fibroblasts. A wound assay was conducted on both effected and unaffected cells by scraping cells in the petri dishes with a plastic cap placed on a stir rod. The cells were then cultured in media supplemented with type V collagen and observed at multiple time points (Viglio et al., 2008). While this model allows researchers to study how cells react on a 2D level, it does not represent the multilayered tissue of a wounded patient (Urciuolo et al., 2022).

A separate study by DeNigris et al. (2016) discusses a 2D *in vitro* model of wound healing in COL5A1 haploinsufficient cells (COL5A1+/-) and a 3D *in vivo* model of wound healing in mice that are COL5A1 haploinsufficient. In the 2D model, dermal fibroblasts isolated from the haploinsufficient mice were placed in petri dishes and a model wound was inflicted on the cells by scratching the monolayer with a plastic pipette as seen in **Figure 10**. The same wound was inflicted on unaffected murine dermal fibroblasts (COl5A1+/+) (DeNigris et al., 2016). Proliferation and migration of each cell assay was then observed to determine the impact of impaired COL5A1 on the wound healing process. It was found that haploinsufficient dermal fibroblasts did not migrate or proliferate as rapidly as unaffected fibroblasts.

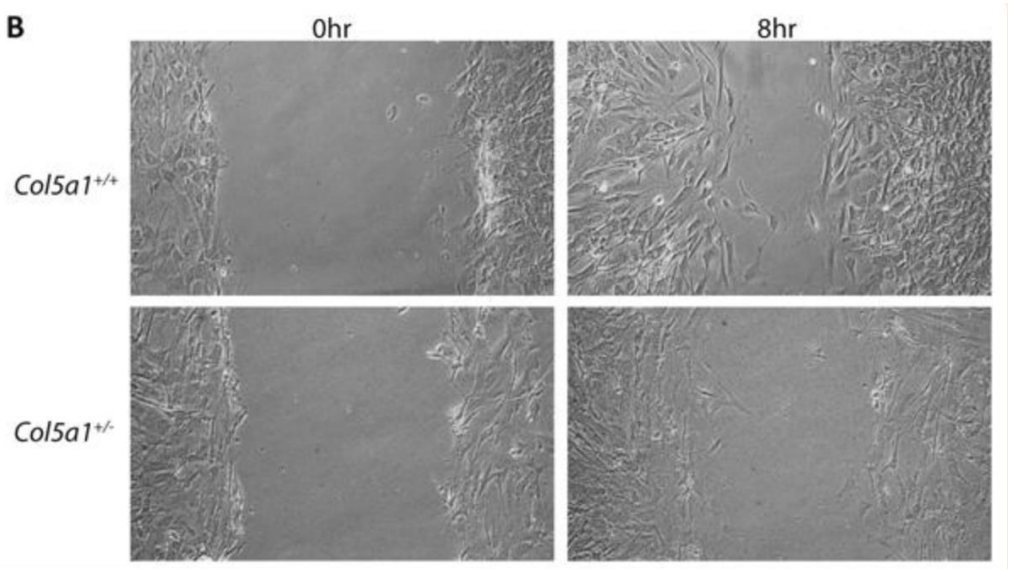

Figure 10. Unaffected dermal fibroblasts (COl5A1+/+) and COL5A1 haploinsufficient dermal fibroblasts (COL5A1+/-) 0 hours and 8 hours after scratch model was inflicted. From DeNigris, J., Yao, Q., Birk, E. K., & Birk, D. E. (2016). Altered dermal fibroblast behavior in a collagen V haploinsufficient murine model of classic Ehlers-Danlos syndrome. *Connective Tissue Research*, *57*(1), 1–9. https://doi.org/10.3109/03008207.2015.1081901

A 3D *in vivo* wound healing study was also conducted on these COl5A1+/+ and COL5A1+/- mice. Full thickness wounds were made on both unaffected and haploinsufficient mice, and the wound healing process was observed at multiple timepoints. Measurements and

photos of the *in vivo* wound models were collected, and it was found that wound closure occurred faster in unaffected mice than in haploinsufficient mice, as seen in **Figure 11** (DeNigris et al., 2016).

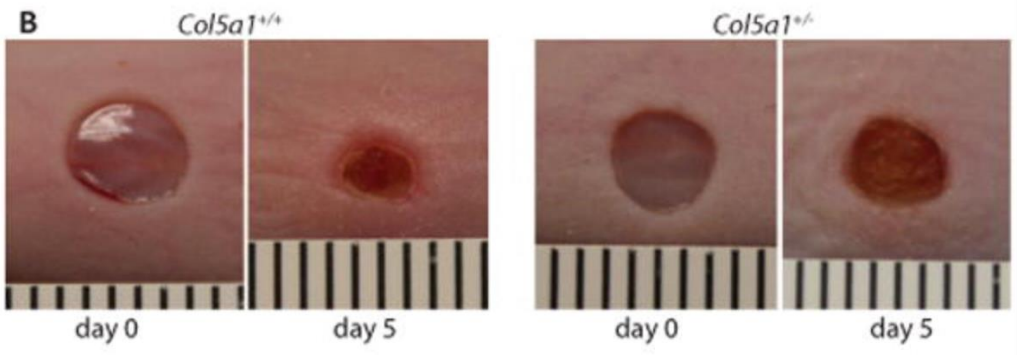

Figure 11. 3D *in vivo* murine wound healing models of unaffected mice (COl5A1+/+) and COL5A1 haploinsufficient mice (COL5A1+/-) at day 0 and day 5 after wound formation. From DeNigris, J., Yao, Q., Birk, E. K., & Birk, D. E. (2016). Altered dermal fibroblast behavior in a collagen V haploinsufficient murine model of classic Ehlers-Danlos syndrome. *Connective Tissue Research*, *57*(1), 1–9. https://doi.org/10.3109/03008207.2015.1081901

This *in vivo* model of EDS wound healing demonstrates the utility of *in vivo* models for assessing the impact of type V collagen mutations on wound healing. It is also much more representative of wound healing in human EDS patients than a 2D *in vitro* model. However, maintaining these *in vivo* models does come with some drawbacks, as they are more costly and time consuming to manage in studies than 2D *in vitro* models (Kapałczyńska et al., 2018). When testing mechanisms and therapies for different medical complexities, some studies utilize 3D *in vitro* models. Use of 3D *in vitro* models can replace the need for *in vivo* models, while still retaining some integrity of the function displayed in *in vivo* conditions. This allows 3D *in vitro* models to overcome the limitations of 2D monolayer cell models (Pozzi et al., 2021).

2.4 Need Statement

There are no targeted treatments for impaired wound healing in Ehlers-Danlos Syndrome. While there have been attempts to modify existing treatments for cutaneous incisional wounds to meet the needs of EDS patients, current techniques do not address the unique complications that arise from prolonged cutaneous wound healing in EDS patients (Gupta & Kumar, 2014).

To produce and test novel therapeutics targeted towards cutaneous wound healing in EDS patients, an experimental model for wound healing is needed. Currently no robust *in vitro* wound healing model of EDS exists. Such a model would allow for researchers to further understand the mechanisms of cutaneous wound healing in EDS tissue and allow for testing of future treatments (Masson-Meyers et al., 2020). Initial models of EDS wound healing have been produced, but only as expensive *in vivo* animal models or as basic 2D culture systems (DeNigris et al., 2016). A 3D *in vitro* model would allow researchers to study cutaneous wound healing mechanisms such as proliferation and migration, without the cost and materials that are required to obtain and maintain an *in vivo* model (Ravi et al., 2015).

3.0 Project Strategy

3.1 Initial Client Statement

The design team developed and pitched a project to identify and address a clinical need in Ehlers Danlos Syndrome. The design team has no outside sponsors and was therefore tasked with developing an initial client statement to drive the project. The team conducted an extensive literature review and interviewed researchers and medical experts associated with Ehlers-Danlos Syndrome to identify a clinical and engineering need. The interview questions can be found in

Appendix A and synopses of the interviews are in **Appendix B.** The team then developed the following initial client statement:

> *Design, develop, and validate a proposed 3D wound healing model to further understand and simulate delayed cutaneous surgical wound healing in patients with Ehlers-Danlos Syndrome.*

3.2 Stakeholders

The team has identified the project's primary stakeholders as the designers, the client, and the users. The designers are the undergraduate biomedical engineering students responsible for creating the model: Madison Donahue, Maya Evohr, Morgan Foltz, Abigail Holmes, and Spencer Whitford. The client for this model is Dr. George Pins. He is a primary investigator with a lab space capable of utilizing a finalized model of dermal wound healing in EDS. The users are researchers who will utilize the model to study and address improper wound healing in EDS. Bryanna Samolyk, a current graduate student in Dr. Geroge Pins' lab, acted as a representative user for this project.

Additional stakeholders may include those in academia and the pharmaceutical industry who are actively involved in EDS research and wound healing studies, particularly relating to treatments for improper wound healing. Doctors and researchers focused on understanding and treating patients with Ehlers-Danlos Syndrome, such as the ones the team interviewed, may also be stakeholders. These individuals were critical in understanding current knowledge gaps in disease understanding and what they want to see within the field, such as for treatments and care.

3.3 Initial Objectives

After speaking with a number of clinical and research experts in Ehlers Danlos Syndrome and wound healing, the team identified six primary objectives for the project to focus on. As a result of these interviews (as summarized in **Appendix A**), the initial objectives were that the model would be reproducible, imageable, representative of EDS wound healing, versatile, usable, and affordable (as described in **Table 4**, below). For this model to be used for research purposes as well as for testing treatments for EDS patients with impaired wound healing, the model should be reproducible in a simple and reliable manner. For quantifiable data to be obtained from the model, it should be imageable. For the model to contribute to research on EDS wound healing, it should be representative of complex EDS dermal pathology and healing mechanisms. For the model to be useful for future testing of wound healing treatments, it should be versatile and allow mechanical, chemical, and light stimuli to be tested. For this model to be able to be widely adopted, it should be easily usable without multiple scientists or uncommon materials or equipment. For this model to reasonably be used for future testing of wound healing treatments, the model should be affordable. These initial objectives, together with secondary objectives and constraints, will inform the team's design process and final design decision.

Table 4. Descriptions of Primary Objectives

Primary Objective	**Description**
Reproducible	System represents an accurate and precise model of dermal wound healing that can be consistently fabricated
Imageable	System can be imaged, and quantifiable data can be obtained.
Representative	System is representative of complex EDS dermal pathology and wound healing mechanisms
Versatile	Model can be used for testing of external stimuli including chemical, mechanical, and light
Usable	Model is easy to use by a single scientist with readily available materials and equipment
Affordable	Market value should outweigh production costs

3.4 Constraints

Constraints for the project were established following the identification of the project's objectives by relevant stakeholders. The constraints were then divided into two categories: logistical and technical. Each constraint and their definitions are defined in **Table 5**.

Table 5. Descriptions of Project Constraints

Constraints		Description
Logistical	Timeline	21 weeks for development
	Budget	$1250
	Material Availability	Development only uses materials team can reasonably obtain
	Equipment Availability	Development only uses equipment available on WPI's campus
Technical	Sterilizable	Model can be sterilized
	Biocompatible	Model does not elicit a negative biological response
	Nontoxic	Model is not toxic
	Standardization	Has control and experimental units
	Incubator	A standard incubator can be used at 37° C and 5% CO_2
	Medium	System allows for regular medium changes
	Proliferation	Cell proliferation occurs for long enough that wound healing can be observed
	Confluency	System is sized to prevent over-confluency and under-confluency
	Contamination	Model must be protected from contamination

Logistical constraints are factors outside of the team's control which limited the project's design. The design had to be developed within 21 weeks, as this is the standard timeline for a WPI capstone project. Additionally, the team had a budget of $1250 funded by WPI that could not be exceeded. Due to time and budget constraints, the team had to rely on materials that could be easily obtained, as well as equipment that was readily available on the WPI campus.

Technical constraints involve aspects that specifically affect project design. Considering that the project is intended to be a tissue model encompassing live cells, the design must be sterilizable, biocompatible, nontoxic, and contaminant-free to ensure cell survival. Additionally, the model must be accessible for regular medium changes for the cells to be provided with the nutrients needed for survival. The cells must be able to survive and proliferate for long enough for wound healing to be observed. The project must include both a control and experimental

model in order to allow for statistical comparison. Equipment constraints include that the model must be able to be housed in a standard incubator (37°C and 5% CO_2), as this is the equipment that is available to the team. The design must be appropriately sized such that the cells are not over-confluent or under-confluent, either of which would affect cell survival as well as the ability to observe a wound healing response.

3.5 Final Objectives

Initial objectives and their secondary objectives were analyzed to gain a better understanding of the goals aimed to be achieved by each project objective. The final objectives tree was derived from an initial brainstorm found in **Appendix C**. **Figure 12** demonstrates the team's final objectives tree, with primary objectives located on the left, which branch out into secondary objectives on the right.

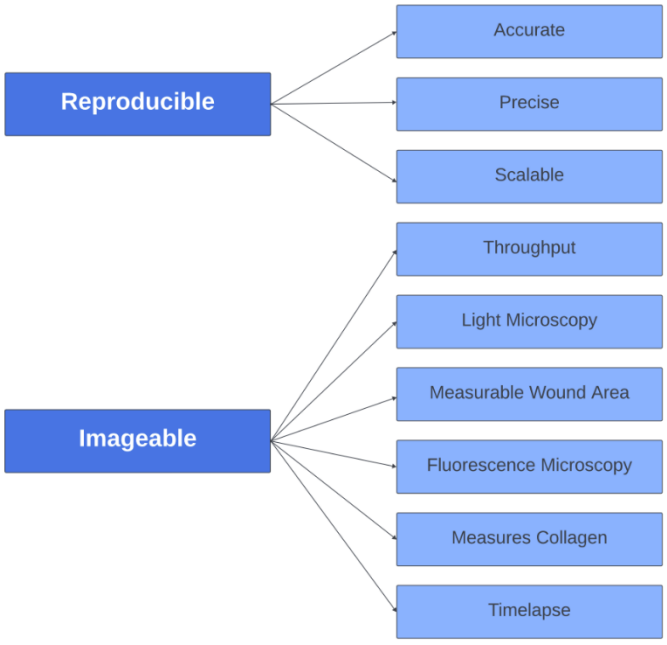

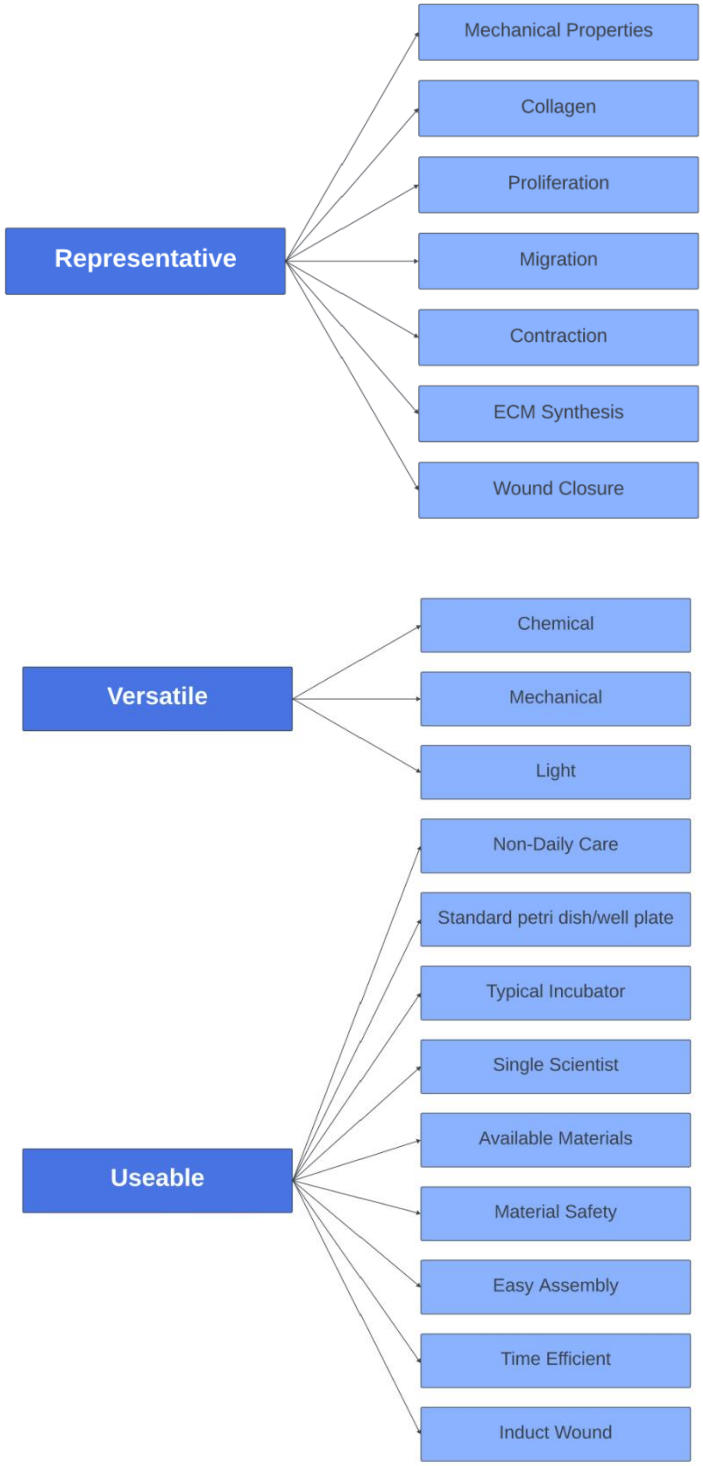
Representative
Mechanical Properties
Collagen
Proliferation
Migration
Contraction
ECM Synthesis
Wound Closure
Versatile
Chemical
Mechanical
Light
Useable
Non-Daily Care
Standard petri dish/well plate
Typical Incubator
Single Scientist
Available Materials
Material Safety
Easy Assembly
Time Efficient
Induct Wound

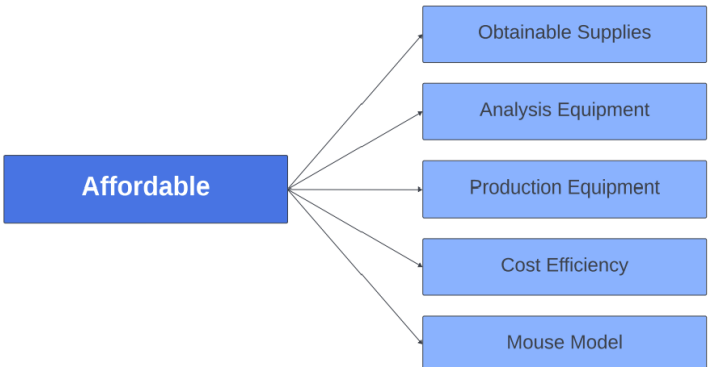

Figure 12. Final Objectives Tree

The primary objectives were ranked using a pairwise comparison chart (PCC) to determine the level of importance of each objective to the overall project. Each objective was given a score of 0, 0.25, 0.5, 0.75, or 1. A score of "0" indicated that the objective ranked is less important than the objective it is compared against. A score of "0.25" indicated that the objective ranked was in some circumstances, but not all, less important than the objective it is compared against. A score of "0.5' indicated equal importance of objectives. A score of "0.75" indicated that the objective ranked was in some circumstances but not all, more important than the objective it is compared against. A score of "1" indicated that the objective ranked was more important than the objective it was compared against. Once all objectives were scored, their totals were calculated. A pairwise comparison chart (PCC) was completed by the design team, client and users. All members of the design team completed a PCC as a collective, and the client and user completed their PCCs without the knowledge of the rankings of the other two parties. **Table 6** summarizes the PCC for the primary objectives. The complete PCCs for each individual stakeholder can be found in **Appendix D**.

Table 6. Pairwise Comparison of Primary Objectives

Primary Objectives	Designers	Client	User	Average
Reproducible	3	3.5	2	2.83
Imageable	4	3.5	1.5	3
Representative	5	3.5	4.75	4.42
Versatile	2	1	2	1.67
Usable	1	3.5	3.75	2.75
Affordable	0	0	0	0

The design team, client, and users all indicated that "representative" was the most important primary objective. Researchers currently lack a 3D *in vitro* model to study cEDS wound healing, making it essential for this device to accurately represent cEDS pathology. This will allow researchers to use the device to understand the mechanisms behind cEDS wound healing. The second, third, and fourth most important objectives were imageable, reproducible, and usable. If the device does not allow for imaging, EDS characteristics such as delayed proliferation and migration cannot be quantified. It is also important for the device to be reproducible, so that data collected from the device can be considered statistically significant. Additionally, it is important that the device is easy to use, so that the data collection from the device is not negatively outweighed by assembly, usage, and testing of device.

Once primary objectives were ranked, PCCs were completed for the secondary objectives of representative, imageable, reproducible, and usable. Definitions for each secondary objective can be found in **Table 7**, **Table 8**, **Table 9**, and **Table 10**.

Table 7. Description of Secondary Objectives for Representative

Primary Objective: Representative	
Secondary Objective	**Description**
Mechanical Properties	The model displays similar mechanical properties of EDS skin
Collagen	The model displays a similar mutated collagen structure to that of EDS skin
Proliferation	System displays mitosis and cell proliferation indicative of EDS
Migration	System displays cell migration and translocation indicative of EDS
Contraction	System displays stress strain and cell contraction through area changes of the matrix and force measurement of the cells/matrix
ECM Synthesis	System displays synthesis of ECM proteins
Wound Closure	System has a measurable rate of closure and wound area reduction

Table 8. Description of Secondary Objectives for Imageable

Primary Objective: Imageable	
Secondary Objective	**Description**
Throughput	System allows for high throughput imaging
Light Microscopy	System allows for light microscopy of live cells
Measurable Wound Area	Still images of the wound can be captured, and ImageJ can be used to measure the area of the wound margin
Fluorescence Microscopy	System allows staining for fluorescent tags and proliferation and allows cell fixation
Measure Collagen	System allows for real-time measurement of collagen deposition
Timelapse	System allows for a timelapse of cell migration and proliferation

Table 9. Description of Secondary Objectives for Reproducible

Primary Objective: Reproducible	
Secondary Objective	**Description**
Accurate	System displays accurate mechanical properties and mutated collagen structure
Precise	The model has precise graft composition, graft thickness and size, wound depth and size, number of cells, and can be consistently fabricated
Scalable	Model production can be scaled up and fabricated repeatedly

Table 10. Description of Secondary Objectives for Usable

Primary Objective: Usable	
Secondary Objective	**Description**
Non-Daily Care	The model does not require daily maintenance and care
Standard Dish/Plate	The model uses a standard 100 mm petri dish or 12-well plate as appropriate
Typical Incubator	System is sustainable in a typical cell incubator at 37°C and 5% CO_2
Single Scientist	The model only requires one scientist for successful model preparation and function
Available Materials	Model materials are found in standard biological labs and can be purchased from standard scientific suppliers as needed
Material Safety	Applicable materials are safe for human handling with no excessive safety precautions and using standard Personal Protection Equipment (PPE) including gloves, eyewear, and laboratory coat
Easy Assemble	The model has a reasonable number of moving parts and efficient assembly time
Time Efficient	Time required for model assembly, care, and short-term maintenance is appropriate
Induct Wound	Wound can be easily induced

The pairwise comparison summaries for these secondary objectives can be found in **Table 11**, **Table 12**, **Table 13**, and **Table 14**. The complete PCC of the design team, client, and user can be found in **Appendix E**. The ranked secondary objectives for representative indicated that ability to model wound closure and ability to test mechanical properties of the model are most important, as seen below in **Table 11**.

Table 11. Pairwise Comparison of Secondary Objectives for Representative

Secondary Objectives for Representative	Designers	Client	User	Average
Mechanical Properties	3.5	2.5	4.5	3.5
Collagen	1	0	4.5	1.8
Proliferation	2	3	1.5	2.2
Migration	4.5	2.5	1.5	2.8
Contraction	4	5.5	0	3.2
ECM Synthesis	0	2	4.5	2.2
Wound Closure	6	5.5	4.5	5.3

Table 12. Pairwise Comparison of Secondary Objectives for Imageable

Secondary Objectives for Imageable	Designers	Client	User	Average
Throughput	3	1	2	2
Light Microscopy	4	4.5	1	3.2
Measurable Wound Area	5	4.5	3.5	4.3
Fluorescence Microscopy	2	3	4.5	3.2
Measures Collagen	0	2	4	3
Timelapse	1	0	0	0.3

Table 13. Pairwise Comparison of Secondary Objectives for Reproducible

Secondary Objectives for Reproducible	Designers	Client	User	Average
Accurate	1	1	2	1.3
Precise	2	2	1	1.7
Scalable	0	0	0	0

Table 14. Pairwise Comparison of Secondary Objectives for Usable

Secondary Objectives for Usable	Designers	Client	User	Average
Non-Daily Care	0.5	1	0	0.5
Standard Dish/Plate	2	0	2.5	1.5
Typical Incubator	3.5	3	6.5	4.3
Single Scientist	5.5	5.5	2.5	4.5
Available Materials	5	2.5	2.5	3.3
Material Safety	7	7	8	7.3
Easy Assembly	0.5	5	4	3.2
Time Efficient	4	5	3.5	4.2
Wound Induction	8	7	6.5	7.2

As indicated, the most important secondary objectives under imageable were the ability to measure wound area, as well as use fluorescent and light microscopy to analyze the device. The most important secondary objective under reproducible was precision, since the devices should all produce similar statistical results with little variation. The most important secondary objectives under usable were material safety, wound induction, and the ability for a single scientist to assemble and utilize the device.

3.6 Revised Client Statement

After identifying stakeholders and objectives, the team, a client, and a user conducted pairwise comparisons charts for all primary and secondary objectives. These scores were averaged, and the most important objectives were identified. These objectives informed the team's revised client statement, which is to:

> *Design, develop, and validate an **imageable** and **replicable** 3D wound healing model to further understand and simulate delayed cutaneous incisional wound healing in patients*

with Ehlers-Danlos Syndrome that displays ***delayed wound closure****,* ***delayed dermal fibroblast proliferation and migration****, and a* ***tensile modulus between 5 and 20 kPa*** *that can be incubated at* ***37 °C*** *with* ***5% CO_2****, requires care* ***less than once per 24 hours****, and can be* ***fabricated in less than or equal to one week****.*

3.7 Project Approach

3.7.1 Management Approach

The team stayed on task and organized by creating a management plan for the project. To establish a timeline for task completion, a Gantt chart was created for each term of the project. The charts can be found in **Appendix F** and observe the timeline from A-Term to C-Term.

Meetings were also crucial to ensuring that the team stayed on track. Weekly meetings with the client were held, which involved a discussion of the current project progress, along with plans for the upcoming week. These meetings ensured that the project continued to move forward, and that the client was satisfied. Meetings with all members of the design team were held multiple times a week. Meetings ensured consistent communication between all stakeholders of the project.

3.7.2 Design Approach

During the design process, the design team brainstormed constraints and objectives for the project to initiate the production of multiple design ideas. The best designs were selected by ranking each design against how well they met the objectives.

3.7.3 Financial Approach

The design team was given a budget of $250 dollars per student, or $1,250 in total by Worcester Polytechnic Institute to complete the entirety of the project. Students were also

required to pay a $50 dollar cost each for utilizing the designated cell culture lab on campus, bringing the final budget to $1,000. As a result of the limited budget, the design team determined what materials were available for usage in the lab before materials were purchased. A list of all materials bought for the project (along with their cost) was created so that the team could ensure they would be able to afford the final design, further specified within **Appendix M**.

4.0 Design Process

4.1 Development of Needs and Wants Analsyis

After reviewing the final objectives, the design team created a list of needs and wants for the design. First, a list of requirements was created to outline how the objectives would be met. Once the requirements were solidified, they were organized into needs and wants based on the importance of the objectives they fell under. Objectives with higher importance were labeled as needs that the design must accommodate, and objectives with lower importance were labeled as wants that did not determine the success of the design. **Table 15** outlines the list of design needs and wants and defines each.

Table 15. Design Needs and Wants

Needs	Definition
Precision	System is capable of reproducibility or repeatability of a result from repeated measurements under unchanged conditions
Accuracy	Data obtained by the model are close to the accepted values
Imageable	System can be imaged, and quantifiable data can be obtained
Representative	System is representative of complex EDS dermal pathology and wound healing mechanisms
Wound Induction	A wound can be induced on the model
Measurable Healing Rate	System can be monitored to quantify a healing rate
Sterilizable	System can be sterilized and maintain sterility
Viable	Model must be able to sustain cEDS cells to maintain accurate representation
3D structure	Model must exhibit a 3D structure
Wants	**Definition**
Scalable	Model production can be reasonably scaled up and fabricated repeatedly
Integrated wound Induction	System contains a component that can induce a pseudo-wound within the model
External Stimuli	Model can be used for additional chemical, mechanical, and light testing
Fluorescent Staining	System allows for staining for fluorescent tags and proliferation
Timelapse	System allows for a timelapse of cell migration and proliferation
Affordable	Market value should outweigh production costs

4.1.1 Design Needs

The team identified nine design needs based on the objectives outlined in **Table 15**. Precision and accuracy are essential to any engineering design. The model system must be able to be consistently replicated. If the model is not replicable, the resulting data obtained from the model system cannot be properly validated. The model must also be accurate. To be accurate, the model must be designed within the previously established and accepted values of EDS. Third, the model must be imageable. This is essential to assess the wound closure and healing of the

model. If the wound closure cannot be imaged and documented, data collection and reporting will be hindered.

The model must be representative of EDS dermal pathology and wound healing. If the model does not represent EDS pathology, then the results obtained from the model will not be relevant to the study of EDS and cannot inform future research. The model must be designed such that the wound healing mechanisms of EDS are not altered. It has been shown introducing collagen V to a haploinsufficient COL5A1+/- cell culture representative of EDS can rescue migratory defects (Viglio, 2008). Causing similar effects must be avoided in the design of this model. The model must be woundable, and a healing rate can be measured. Generating a wound in the model will cause the cells to elicit a healing response and this response must be quantified.

Sterilizing all components of the model is essential to prevent contamination. Contamination can lead to bacterial or fungal growth and destroy the model. The model must be viable for cell culture and sustain cEDS cells throughout. Cells must be alive to exhibit a healing response and produce measurable results. Finally, the model must be three-dimensional. Traditional 2D cell cultures of EDS systems have been conducted and wound healing mechanisms observed. To the best of the team's knowledge, producing a 3D *in vitro* wound model is novel territory. A three-dimensional environment would provide a more representative outcome of *in vivo* wound healing since a 3D model better mimics the body.

4.1.2 Design Wants

Following the identification of essential design needs in **Section 4.1.1**, the design team has prioritized objectives for the wound healing model based on averaged PCC data from

designers, researchers, and potential clients. These objectives, representing priorities of lesser significance, have been translated into designated design wants to guide further development.

Within the "Imageable" primary objective, fluorescence microscopy and fluorescent staining, while ranked lower in priority, hold significant value for the final model. Despite their lesser importance for achieving core objectives, these features offer valuable insights into model structure, function, and collagen growth. Fluorescent staining would enable visualization of cellular processes, particularly collagen deposition, providing crucial data for model validation and analysis.

Similarly, the timelapse functionality, initially ranked low on the PCC, presents valuable opportunities for research. By capturing cell migration and proliferation over time, this feature would facilitate comparisons between non-affected and EDS cells during the wound healing process. This continuous visual record would enable researchers to track cellular movement and outgrowth throughout the experiment, providing a deeper understanding of disease mechanisms and potential therapeutic interventions.

While achieving model scalability within a reasonable timeframe would be ideal within the "Reproducible" objective, the current design phase prioritizes establishing a functional and effective 3D *in-vitro* wound healing model. Validation of this core functionality takes precedence over scalability, as optimizing the design for mass production is often more effective later in the development process. However, recognizing the long-term benefits of inherent scalability, the design team aims to incorporate elements that facilitate future scaling up wherever possible.

Though not prioritized within the immediate "Usable" objectives, integrated wound induction remains a valuable feature for future development. This embedded component, enabling controlled wound creation within the model itself, could significantly improve data consistency across various sample sets. By minimizing human error during wound induction, integrated wound induction can enhance the reliability and reproducibility of experimental results.

While the finalized needs and primary/secondary objectives define the core functionalities of the model, additional features such as affordability and the capacity for external stimuli application could significantly enhance its value and impact. Affordability encompasses both individual components and overall development, such as utilizing readily available supplies, accessible analysis and production equipment, and ensuring justifiable upfront costs that amortize over time. Importantly, commercial distribution should aim for a cost point below that of a mouse model. The ability for external stimuli to be tested is important for future research; however, advances in the understanding of EDS dermal wound healing can still be made without this feature.

4.1.3 Needs and Wants Design Matrix

After defining the needs and wants, a design matrix was created. The design matrix allowed the design team to evaluate which design elements impacted the needs and wants of the design. **Table 16** is the complete design matrix. The needs and wants of the design are placed across the top of the matrix with the design elements listed on the left side. Each X is an indicator of an element impacting the listed need or want.

Table 16. Design Matrix of Needs and Wants

Needs	Precision	Accuracy	Imageable	Representative	Wound Induction	Measurable Healing Rate	Sterilizable	Viable	3D Structure	Wants	Scalable	Integrated Wound Induction	External Stimuli	Fluorescent Staining	Timelapse	Affordable	Total
Culture Matrix Material		X	X	X	X	X	X	X	X					X	X	X	11
Matrix Formation Method	X		X		X			X	X		X				X		7
Cell Culture Media			X				X	X							X	X	5
Cell Type		X		X		X		X	X					X		X	7
Cell Density			X	X		X		X	X					X	X		7
Transparency of Matrix			X			X									X		3
Wound Induction Method	X		X		X		X				X	X			X	X	8
Container Style					X	X	X	X	X		X	X	X			X	9
Container Material			X				X	X	X						X	X	6
Container Coating			X	X			X	X	X		X		X		X	X	9
Container Size	X		X		X			X	X		X	X	X		X	X	10
Wound Size	X		X		X	X		X				X			X		7
Model Size	X	X	X	X	X	X			X		X		X	X	X	X	12

4.2 Functions and Specifications

Based on the team's revised client statement, design needs and prioritized objectives, a list of functions for the wound healing model was created, visualized in **Table 17** below. The wound healing model must be representative of cell function in EDS, allow for efficient imaging of the model over time, allow for accurate and efficient repeated fabrication of model, and integrate standard and easily available materials and equipment. From these functions, a list of specifications was made and a three-point scale for each specification was created to evaluate design options, which can be viewed in **Appendix G.**

Table 17. Functions and Specifications Identified for the Team's Wound Healing Model

Functions	Specifications
Representative of EDS cell functions (DeNigris et al., 2015)	• Dermal fibroblast proliferation rate is 1/3 the rate of unaffected dermal fibroblast proliferation. • Dermal fibroblast migration rate is 1/3 the rate of unaffected dermal fibroblast migration. • Time for full wound closure is twice as long as the time for an unaffected wound matrix. • Model exhibits a tensile elastic modulus of 5 to 20 MPa
Allows for efficient imaging of model over time	• Wound area is measurable to the nearest 0.1 mm • Model can be visualized at 40x objective with at least 80% clarity • Twelve models can be imaged in under 1 hour.
Allows for accurate and efficient repeated fabrication of model	• Model can be replicated with 80% precision greater than 10 times • Model requires 5 or less components to assemble • Model formation from beginning to cells being seeded takes less than or equal to 1 week • Wound induction takes less than 2 minutes for each sample • Model production and regular care will require only one scientist • Model requires care less than once per 24 hours
Integrates standard and easily available materials and equipment	• Materials take less than two weeks to obtain • Model fits in well plate with 22.8 mm diameter (12-well plate) • Model can be incubated at 37°C and 5% CO_2 with zero non-standard specifications for the incubator

In order to represent EDS cell function, the model must have the ability to have dermal fibroblast proliferation and migration rates that are lower than those of unaffected cells. Based on previous literature, this will be defined as having proliferation rates less than or equal to 1/3 of the rates of unaffected cells (Viglio et al., 2008). Additionally, the model must demonstrate delayed wound healing, characterized as taking twice as long as an unaffected model for full wound closure. The model should also exhibit a tensile elastic modulus between 5 and 20 kPa in order to represent the modulus of skin.

To characterize, image, and gather visual data from the model, it must be imageable. The model must have a measurable wound area that allows for measurements with 0.1 mm clarity. Additionally, the magnification setting on any microscope used must allow for individual cells to be visualized with at least 80% clarity. Practically, the model must be able to be visualized on a standard microscope, which is readily available and meets these specifications. This will also inform the model's size, transparency, and ability to be used in a standard petri dish or well plate.

For the model to be useful for research purposes, it must be able to be accurately and efficiently fabricated. The model must be able to be replicated more than 10 times, with 80% precision or higher. The model must require less than or equal to 5 components for easy assembly and should take less than or equal to one week for model formation from the beginning of the process until cells are seeded. The wound induction process must take less than 2 minutes per sample. Additionally, for efficiency, the model production and regular care must only require one scientist and must require care less than once per 24 hours.

For the model to be feasibly created and cared for, it must integrate easily available or standard materials and equipment. All materials must take less than two weeks to obtain. The model must fit in a standard well plate with a 22.8 mm diameter (12-well plate). It must be compatible with incubation at 37°C and 5% CO_2 in a standard incubator.

4.3 Conceptual/Preliminary Design Phase

After determining the functions, specifications, needs, and wants, the team developed a list of design elements that closely aligned with the objectives and functions. The design elements considered were cell type, model style, matrix material, and wound induction method. An extensive list of means was developed by the team for each design element. A subset of

means was eliminated by the team based on the previously defined constraints of the project. The team then developed pros and cons for each remaining means.

Each mean was categorized by design element, and relevant objectives and constraints were assigned to each design element. If a means violated any constraints, it was immediately eliminated from the design matrix. All means that did not violate any constraints were ranked on a three-point scale for each pre-defined specification as seen in **Appendix G**. The top-ranked means were later considered for the final design concept.

4.3.1. Brainstorming Design Elements

The initial step within model design included collectively developing four main categories as a group that encompassed the components of the model based on the previously determined functions. These included cell type, model style, matrix material, and wound induction method. The design team explored the potential options and wrote out ideas on a whiteboard within the meeting space. As there were many elements that could compose a viable 3D *in vitro* EDS wound healing model, all design means were accounted for and noted within **Table 18** below.

Table 18. Means Chart for Design Elements

Element:	**Means:**
Cell Type	- Human-derived EDS fibroblasts - EDS mouse/animal model fibroblasts - Unaffected human fibroblasts in EDS-derived matrix - Unaffected human fibroblasts in chemically altered matrix
Model Style	- Micro-TUG model - Self-assembling tissue model - Cell-laden (hydro/micro) gel model - Microfluidic model - Hanging drop model - Magnetic suspension model - 2D monolayer model
Matrix Material	- Cell-derived matrix using fibroblasts - Fibrin - Collagen I - Matrigel - Alginate - Hydroxyapatite (HA) - Hyaluronic acid (HA)
Wound Method	- Scratch pipette tip - Scratch rubber policeman - Scalpel scratch - Stamp (punch biopsy) - Thermal wound via hot rod/branding - Laser (optical wound) rotating drill - Electric cell-substrate impedance sensing (ECIS) (electrical wound)

The design elements were evaluated in the order noted above, as the team recognized that the cell type determination would be the preliminary step, as the cell type would guide the ability of the model to accurately represent EDS disease pathology. The cell design options were followed by a compatible model that would support the cell growth. The model style was then evaluated, followed by the matrix material. Finally, wound induction methods that could be applied to at least one of the viable models were brainstormed. The pros and cons of each design

element were evaluated within the section below, in which the final designs were determined via a thorough design matrix with a 1-3 scaled ranking for each design element.

4.3.2 Evaluation of Design Elements

Cell Type

Incorporating dermal fibroblasts derived from a human EDS patient would serve to ensure the model is representative of EDS pathology. Having these cells present in the model would be a direct representation of the focus population. They are also accessible and within the budget of the project, with the ability to be obtained from the Coriell Institute Biobank in New Jersey. The cells can also be placed in the model as is, with no further modification or treatment required besides having access to culture media. EDS fibroblasts have been documented to proliferate and migrate at a slower rate which may elongate length of studies; however, delayed growth rate reflects EDS pathology. **Table 19** summarizes the pros and cons of using human dermal EDS fibroblasts in the model.

Table 19. Pros and Cons of Human Dermal EDS Fibroblasts

Derived From Human EDS Patient	
Pros:	***Cons:***
• Human patient (representative of population focus) • Less translation required for in-vivo models • Easily acquirable from Coriell Institute • Exhibit pathology of interest	• Potentially slow growth rate

Utilizing EDS dermal fibroblasts derived from an animal model is another way to incorporate a representation of EDS pathology into the model. Haploinsufficient murine models have been created to obtain haploinsufficient COL5A1 dermal fibroblasts from the models

(DeNigris et al., 2016). Genetically modified animal models are commonly used in research, and there are often several options for model types beyond murine models. The drawback of using animal model derived dermal fibroblasts is that animal models must often be genetically modified which requires additional/expensive materials. It also requires researchers to obtain necessary materials and resources to contain animals during periods of research. Since the cells would be derived from animal cells and not human cells, they would also not be fully representative of EDS pathology. The complete list of pros and cons can be visualized below in **Table 20**.

Table 20. Pros and Cons of EDS Dermal Fibroblasts Derived from Animal Model

Derived From EDS Mouse/Animal Model	
Pros:	***Cons:***
• Commonly used within research studies • Several options for animal models (rodents primarily mice, zebrafish)	• Difficult to genetically modify models to exhibit EDS • Not fully representative of EDS in human patients

Another way to include representative of EDS pathology in the model would be to use non-affected dermal fibroblasts placed in an EDS derived extracellular matrix so that they may be influenced by the ECM to behave in a way that is similar to EDS pathology. Using unaffected cells would be representative of human cell function, however they would not be representative of EDS pathology. They would be easy to obtain, either from a bio bank or from *in vivo* isolation. Cells may also have the potential to remodel the matrix, creating a new, properly formed matrix. A complete summarization of the pros and cons of using unaffected human cells in an EDS derived matrix is shown in **Table 21**.

Table 21. Pros and Cons of Unaffected Human Cells in EDS Derived Matrix

Unaffected Human Cells in EDS Derived Matrix	
Pros:	***Cons:***
• Matrix mechanical properties match EDS • Representative of human cell function • Easy to obtain	• Cell phenotype is not representative of EDS • Cells have potential to remodel matrix with new matrix material

Using unaffected human dermal fibroblast that are chemically altered may also be helpful incorporating a design element that is representative of EDS pathology. Since the cells would be human, they would represent human dermal cell function. They may also be treated in a way that allows them to demonstrate phenotypes of EDS, such as delayed proliferation and migration. While this would in some ways model EDS phenotype, the chemically altered cells would not contain all characteristics of EDS pathology. The chemicals used to alter the phenotype of the cells may also be difficult/expensive to acquire depending on chemicals required. The summary of the pros and cons of the chemically altered human fibroblasts is summarized in **Table 22**.

Table 22. Pros and Cons of Unaffected Human Cells

Chemically Altered Unaffected Human Cells	
Pros:	***Cons:***

• Matrix environment would stimulate EDS environment/factors including:
  ○ Mechanical properties
  ○ Support
• Representative of human cell function
	• Cells do not contain characteristics of EDS pathology

Model Style

In addition to the given cell type used within the model, the model style will significantly influence the resulting components of the overall model, such as imaging ability, analysis, type of wound, as well as the cost and feasibility of the model in general as well. The proposed

models have been commonly used as wound healing models and more general tissue models in the past, and these may be adapted to support EDS cell growth within the provided timeline.

The micro-TUG (micro-scale tissue gauge) is a possible model for cellular growth and observation of wound healing in tissue models. This model allows for the sample to be under constant and stable tension during the healing process. Furthermore, this model allows for the evaluations of mechanobiology and the interactions between the mechanical stimuli applied via the posts within the model and the resulting biological effects on the sample. This model is also highly customizable and can be adapted for EDS cells, however there is an intensive preparation for the development of this model, including PDMS fabrication for the customized posts, specifically at a high precision. There are additionally many variables that need to be considered to ensure that the model has the highest degree of accuracy and precision throughout the experiment. The discussed pros and cons are noted in **Table 23** below.

Table 23. Pros and Cons of the Micro-TUG Model

Micro-TUG Model	
Pros:	***Cons:***
• Allows for sample to be under consistent tension while healing • Allows for application of mechanobiology study during wound healing (Javor et al., 2021) • Team member has extensive experience with this system • Highly customizable	• Requires PDMS fabrication of customized posts • Requires high precision due to small size of posts • Many variables must be taken into consideration (size and shape of posts, number of posts, PDMS stiffness, etc.)

The self-assembling tissue model is beneficial as this completely relies on the sample cells to produce the final matrix, thus not requiring the addition of a synthetic or natural matrix that may not represent the disease pathology as accurately as possible. As a result, this model does not require a synthetic scaffold and thus requires overall fewer materials for the model

production overall, including design components for the maintenance of the model, and there are recent protocols that would aid in the increase rate of ECM formation, which would be ideal based on the given project constraints for time availability. A potential complication with this model includes that there is no known matrix production behavior when using this 3D model style. Furthermore, while there are fewer needed materials, the model remains costly and has a long assembly time. The pros and cons for a self-assembling tissue model are further explained within **Table 24** below.

Table 24. Pros and Cons of the Self-Assembling Tissue Model

Self-Assembling Tissue Model	
Pros:	***Cons:***
• Uses cell produced matrix • Does not require use of synthetic scaffold • Requires fewer materials for model production • New protocols increase rate of ECM formation (Saba et al., 2018)	• Unknown EDS matrix production behavior • Costly • Large time duration for assembly

The cell-laden hydrogel model is a common model used within biomedical research applications and provides support to the cells using a hydrogel scaffold which surrounds the sample cells within a cross-linked network. Through the structure of this model, it can accurately mimic the native structure and function of cells. This model is additionally highly customizable regarding the large size range of hydrogel formation, ranging between less than 1 μm to greater than 1 cm. A variety of testing can additionally be used with this model, as the physical characteristics such as the well-defined shape of the model, resulting mechanical strength, and being biodegradable, are all extremely compatible with the aim of developing an EDS wound healing model. However, limitations of this model include not being able to apply a random packing process, which would prove to be difficult in evaluating native EDS tissue complexity. It

is also technically difficult, and natural hydrogels have the potential to vary in composition and properties, which would influence the accuracy and precision of the data. A complete overview of the pros and cons of cell-laden hydrogels are observed within **Table 25** below.

Table 25. Pros and Cons of the Cell-Laden Hydrogel Model

Cell-Laden Hydrogel Model	
Pros:	***Cons:***

• Provides support via hydrogel scaffold encapsulating cells within cross-linked network
• Aids in mimicking native tissue-like structure/function
• Large size range: <1 um to >1 cm
• Effective physical properties:
  ○ Well-defined shapes
  ○ Mechanical strength
  ○ Biodegradable
	• Cannot apply a random packing process (essential in recreating biomimetic tissue complexity in EDS) (Du et al.)
	• Technically difficult and slow to scale-up
	• Natural hydrogels vary in properties and composition (accuracy and precision)
	• Limited transport of nutrients and oxygen across dense hydrogels influence viability of cells

A microfluidic model is a model that provides a complex structure to aid mimicking the in-vivo environment of cells while within a 3D *in vitro* model. There are a variety of studies used with these models, and it can be designed to provide a model of the complex cellular environment observed within EDS. However, this model notes a difficulty in maintaining the cells in-vitro specifically for EDS cells, which is difficult based on the nature of an EDS wound healing model that should represent the native tissue. There are additional complications with long-term stability within the physiological conditions, and there is limited background research for the purpose of this project, as the primary microfluidic techniques focus on using alginate for fiber production. A complete overview of the microfluidic model with designated pros and cons are explored in **Table 26** below.

Table 26. Pros and Cons of the Microfluidic Model

Microfluidic Model	
Pros:	***Cons:***
• Provides micro-scale complex structures to mimic the in-vivo environment of cells • Applications include cell analysis, protein studies, intracellular signaling, cell culture and tissue engineering • Can be developed to provide a complex environment mimicking EDS • May include a gel-free model • Potential for future low-cost alternative to animal models for research	• Difficulty maintaining cells *in-vitro* in a state like physiological condition to *in vivo* EDS cells • Limited long-term stability in physiological conditions • Primary microfluidic techniques focus on alginate for fiber production

The hanging drop model is a novel 3D tissue model that effectively allows for the development of specialized tissues. As EDS has a difficult pathology to model, this method would be beneficial for accurately representing the components of native EDS cells and tissue. This is a scaffold-free culture technique, requiring fewer model components as a result, and this model does not require any specialized equipment. This is ideal as this can be fabricated and analyzed within a standard laboratory environment. Complications within this model include the observation that this method is both labor- and time-intensive, in addition to being low throughput and costly due to the specialized equipment needed. The goal for this project is to develop a model that would accurately represent dermal EDS cellular structure, and the potential for producing spheroids using a scaffold-free technique for this model would not be ideal. The complete evaluation of hanging drop model pros and cons is noted below in **Table 27**.

Table 27. Pros and Cons of the Hanging Drop Model

Hanging Drop Model	
Pros:	***Cons:***
• Controls the desired environmental factors for modulating the behavior of cells (via PANDA system) • Allows for development of specialized tissues • Scaffold-free culture technique (Biju et al., 2023) • Does not require any specialized equipment • Modifications can be made based on the cell type	• Requires specialized plates • Labor - intensive (Cho et al., 2020) • Time-intensive • Costly • Low throughput • Requires a second manipulation for transferring the formed microtissue into a different culture vessel for additional assays (not fully inclusive within one plate) • Formation of spheroids using scaffold-free method

The magnetic suspension model is a system that exposes cells to magnetic fields, which promotes 3D structure formation via cellular aggregation (Parfenov et al., 2020). These models are successfully able to both introduce and manipulate various components of the model due to the sample suspension within the medium. However, limitations of this include the observation that resulting wound induction is a complex process for the model, and the presence of the magnetic field being applied on a sensitive sample has the possibility to result in artifact-formation in the data analysis. The additional combination of high cost and complex materials notes the difficulties of using the magnetic suspension model as well. The complete pros and cons of this model are observed in **Table 28** below.

Table 28. Pros and Cons of the Magnetic Suspension Model

Magnetic Suspension Model	
Pros:	***Cons:***
• Easy to introduce and manipulate various reagents and factors due to cell suspension in liquid medium	• Wound induction is complex • The presence of the magnetic field can potentially affect cell behavior and introduce artifacts into the data • High cost • Requires complex materials that are not readily available

The final evaluated model is the 2D monolayer model, and this was considered based on the model simplicity and low equipment costs. The model could be developed and there would be a wound that could be induced with relative ease, in which observation and analysis could be conducted to evaluate the wound healing behavior in EDS cells. However, the nature of a 2D model does not allow for a fully representative observation of cell-cell and cell-matrix interactions. The pros and cons of this model are further explained in **Table 29** below.

Table 29. Pros and Cons of the 2D Monolayer Model

2D Monolayer Model	
Pros:	***Cons:***
• Simple • Low equipment costs	• 2D model does not exhibit fully representative cell-cell interactions

Model Matrix Material

To construct a viable wound healing model that would accurately model dermal wounds within EDS tissue, the matrix material that will be incorporated in addition to dermal fibroblasts is critical in influencing and controlling the cellular processes such as cell migration, wound healing, and differentiation. These matrices serve to provide the essential physical scaffolding for the cells as well. The following matrix options provide options for final a wound model

component that would help to represent the pathology of EDS and have the potential to benefit the model for the duration of project development.

Incorporating cell-derived matrix using fibroblasts would serve as relevant and accurate alternative for the study of EDS cell behavior within an in-vitro model. As this is a cell-derived matrix, this will allow for the model to have an increased physiological relevance because of the observation that the matrix is produced from natural materials instead of synthetically created materials that may not represent the disease pathology as well. This matrix specifically will be able to observe cell migration and proliferation in addition to being able to be imaged through a variety of methods. However, this model is hindered by the long duration of preparation and formation of the cell-derived matrix, ranging between 8-22 days. Given the time constraint for this project, it is infeasible to produce accurate and precise results by creating and analyzing samples within 7 weeks. Furthermore, this model would require materials that would need to be ordered and may not be readily available. The pros and cons of this design are noted in **Table 30** below.

Table 30. Pros and Cons of a Cell-Derived Matrix Using Fibroblasts

Cell-Derived Matrix via Fibroblasts	
Pros:	***Cons:***
• offers a more physiologically relevant alternative for studying *in vivo*-like cell behavior *in vitro* (Kaukonen et al., 2017) • Proliferation and migration can be observed within matrix • Can be visualized using immunofluorescence and brightfield	• Time consuming (8-22 days for CDM formation). • Requires multiple materials not readily available • Derivation is impacted by cell-type and cell behavior

Using fibrin is a common method of matrix production, defined as a provisional matrix that is developed through the formation of fibrin clots and fibronectin, seen in the first phase of

wound healing. Fibrin as a material itself is critical within the ECM within biological tissue during wound healing processes. It plays an important role in cellular tissue repair, including leukocyte cell adhesion and migration of cells during the angiogenesis process and development of new blood vessels using endothelial cells (Laurens et al., 2006). Furthermore, the use of fibrin as a matrix provides a good structural matrix for the cells. However, the development of the fibrin matrix is a complicated process, as it includes multiple components such as thrombin, as well as an involved method of production specific to these materials. As the formation of fibrin clots of critical in the development of the matrix construct, an inhibitor must be used to ensure that the clots do not break down over time. The pros and cons of this design are noted in **Table 31** below.

Table 31. Pros and Cons of a Fibrin Matrix

Fibrin	
Pros:	***Cons:***
• Natural adhesive properties • Represents healing response • Provides good structural matrix for cells	• Complicated formation (requires thrombin) • Requires plasminogen inhibitor to prevent clot breakdown

Collagen is a natural and abundant protein located within the human body, and its fiber-like structure is beneficial for making tissues. This material has natural adhesive properties, and cellular growth and overall model survival can be supported through integrin receptor activation. However, complications of this material used within an EDS wound healing model include the potential for EDS cell function "rescue," in which the collagen V behavior may represent non-affected tissue (Viglio et al., 2008). This may result in poor data or misrepresentation of EDS cell behavior, both overall and during the wound healing process. Evaluation of the complete pros and cons of collagen are noted in **Table 32** below.

Table 32. Pros and Cons of a Collagen Matrix

Collagen	
Pros:	***Cons:***
• Natural adhesive properties • Integrin receptor activation promotes cell survival and growth	• Evidence of "rescue" of EDS cell function in collagen V • Possible misrepresentation of cell behavior

Matrigel is a commercial extract derived from an Engelbreth-Holm-Swarm (EHS) tumor and contains all major components of many common tissue basement membranes, leading this material to be an impressive matrix when mimicking *in vivo* ECM characteristics (Passaniti et al., 2022). Furthermore, the material promotes cell survival and growth when the integrin receptor is activated, similar to a collagen matrix. Like collagen, a limitation of this matrix is seen by having the potential to interfere with various defective aspects of integrins within the pathology of EDS. The complete list of pros and cons of a Matrigel matrix is observed in **Table 33** below.

Table 33. Pros and Cons of a Matrigel Matrix

Matrigel	
Pros:	***Cons:***
• Integrin receptor activation promotes cell survival and growth • Good mimic of *in vivo* ECM	• May interfere with defective aspects of integrins in EDS pathology • Batch to batch variability

Alginate is a naturally occurring polymer obtained from seaweed that is used for a variety of applications within both biomedical science and engineering (Lee & Mooney, 2012). Benefits when using this material as a matrix include the gel pore network, as it allows for the efficient diffusion of both nutrients and waste, which is critical in cell and overall model survival. Furthermore, alginate has a structural similarity to extracellular matrices in tissues and can be adjusted accordingly depending on the purpose of the research being accomplished. However,

alginate dressings have been recorded to impact the healing rate of tissues, and when making a model to accurately represent the ability for native EDS to heal from a wound, this is not ideal. A comprehensive pros and cons list for alginate matrices are noted in **Table 34** below.

Table 34. Pros and Cons of an Alginate Matrix

Alginate	
Pros:	***Cons:***
• Gel pore network allows diffusion of nutrients and waste materials in addition to its non-animal origin (Anderson et al., 2013) • Ability to image proliferation using antibody staining • Biocompatible • Easy to manipulate properties of gel • Structural similarity to ECM in tissues	• Not highly commercialized • Alginate dressings can impact healing rate (Agarwal et al., 2011)

Hydroxyapatite (HA) is an inorganic mineral found within the body, specifically in bone and teeth, and using this material for the model matrix is effective through successfully being able to increase the bioactivity of the cell, including proliferation, adhesion, and differentiation more effectively than non-porous materials (Anil et al., 2023). This is a direct result of the porous nature of HA, and the resulting improved cell adherence will serve to integrate the cells within the matrix lattice and HA coating. However, this material displays weak mechanical properties with a high fragility, which may not be fully representative of the EDS pathology. These pros and cons are summarized in **Table 35** below.

Table 35. Pros and Cons of a Hydroxyapatite Matrix

Hydroxyapatite (HA)	
Pros:	***Cons:***
• Porous nature of HA • Increases bioactivity of cell (proliferation, adhesion, differentiation) ○ Resulting cell adherence to the surface of the HA coating and production of ECM	• weak mechanical properties • High fragility

Hyaluronic acid (HA) is a common substitutive and regenerative matrix material that can replace the dermis, and this material has been historically used to modulate tissue mechanics, ECM protein organization, and cellular remodeling. The matrix is also beneficial because it supports cell survival, proliferation, migration, and adhesion, which are all critical components when developing a viable 3D *in vitro* wound healing model. However, limitations in sourcing this material are present, as naturally occurring (animal) sourcing often contains hyaluronidases and industrially produced HA contains high endotoxin levels. Furthermore, constraints within the project note a higher cost of HA than other matrix materials. The pros and cons for using a hyaluronic acid matrix are noted below in **Table 36.**

Table 36. Pros and Cons of a Hyaluronic Acid Matrix

Hyaluronic Acid (HA)	
Pros:	***Cons:***
• Historically used to modulate tissue mechanics and remodeling (and organization of ECM proteins) • Signals triggered in HA to influence cell survival, proliferation, adhesion, and migration (Wolf & Kumar, 2019) • Provides 3D scaffold	• Difficulty obtaining HA from animal sources • Difficulty obtaining HA from industrial production • High costs

Wound Induction Method

The wound induction method is how a wound is created on the model. Choosing an efficient and accurate wound method is critical to designing a wound healing model. The chosen method will inform the final design as well as potentially influence the healing response of the cells. The team must choose a method that is feasible, simple, and accurately represents an incisional wound.

The first method the team considered was a scratch wound using a pipette tip. A scratch model is when the chosen instrument is dragged across the tissue culture and mechanically disrupts the cells and matrix. This is a standard method used in 2D monolayer culture throughout literature. The protocol is simple, cost effective and can produce a consistent wound size between samples. Additionally, there is extensive previous literature on scratch models. The scratch model using a pipette tip is also widely applicable to many model styes and culture conditions (Stamm et al., 2016). A drawback of the manual pipette scratch model is the potential for human error in creation of the scratch. This can lead to a lack of precision between samples. The pipette scratch is also typically associated with a 2D assay, and the team would be trying to apply the 2D scratch methodology to a 3D model. Finally, there is potential for mechanical disruption of the plate coating, encouraging cells to remain stuck at the edge of the wound margin and not migrate into the wound margin. The list of pros and cons for the scratch pipette wound is summarized below in **Table 37**.

Table 37. Pros and Cons of a Scratch Pipette Tip Wound

Scratch Pipette Tip	
Pros:	***Cons:***
• Technically simple protocol for wound induction • Cost effective for samples • Consistent size of wound area • Previous literature on various ECM components including collagen I, IV, laminin, fibronectin • Widely available culture conditions and equipment	• Potential for human error • Typically used to study migration of cells on a 2D assay • Cells may stick to the border of the scratch • Potential for mechanical disruption of plastic surface or ECM coating, affecting cell migration behavior

The scratch model with the rubber policeman is very similar to the scratch model with the pipette tip. Compared to the pipette tip, a benefit to the rubber policeman is it more effectively cleans and removes debris from the wound site. The pipette tip is widely applicable to model style and a variety of culture conditions because it is readily available, sterilizable, and not costly. The cons for the rubber policeman scratch are analogous to those of the pipette tip. The scratch can disrupt specialized coatings on the bottom of the well plate, there is potential for human error in scratch replicability, and it is typically used for 2D cultures so it may not effectively cut through the 3D matrix. The complete list of pros and cons for the scratch rubber policeman wound induction method is summarized below in **Table 38**.

Table 38. Pros and Cons of a Scratch Rubber Policeman Wound

Scratch Rubber Policeman	
Pros:	***Cons:***
• Allows for effective cleaning/removal of cells without scratching plate • Widely available culture conditions and equipment	• Potential for human error • May mechanically disrupt plastic surface • Often disrupts the underlying ECM coating on culture surface • Typically used for monolayer cultures

Similar to the two previous scratch models, the scalpel scratch is a simple procedure. It is easily reproducible and has been used to cut cell-laden hydrogels previously. As the scalpel is often used in surgeries, it may act as a highly representative option for producing an incisional wound. A major con of the scalpel is the introduction of a potentially dangerous blade to the system if handled improperly. Precautions must be taken to ensure the safety of all team members if the scalpel is used. A list of pros and cons for the scalpel scratch is summarized below in **Table 39**.

Table 39. Pros and Cons of a Scalpel Scratch Wound

Scalpel Scratch	
Pros:	***Cons:***
• Simple procedure for wound induction • Reproducible • Been shown to cut cell laden hydrogels effectively	• Primarily used for monolayers • Introduces a potentially unsafe blade to the system • Potential to disrupt the plate coating

The next option the team considered is the stamp punch biopsy. This method involves depressing a stamp of selected shape into the culture area (Stamm et al., 2016). This pressure damages the cells and creates a wound. The stamp has a defined area of prechosen shape. An advantage of the stamp wound is its ability to be combined with thermal wounding if the stamp is heated. This makes it a versatile method. The stamp model results in less damage to the plate coating layer. A major con of the stamp method is inconsistency in manual pressure applied, which can possibly influence the results of the wound (Stamm et al., 2016). A full list of pros and cons for the stamp method can be found below in **Table 40**.

Table 40. Pros and Cons of a Stamp Punch Biopsy Wound

Stamp Punch Biopsy	
Pros:	***Cons:***
• Defined wound area that can be applied with pressure • Can combine with thermal wounding • Any shape possible • Influence of cell debris on migration can be monitored • ECM matrix coating remains intact	• Inconsistent manual pressure applied to stamp may influence results

Thermal wounding occurs when the system is exposed to a heated rod. The rod is pressed against the culture system, and the heat damages the cells. Thermal wound models can be very effective for studying burn models. Thermal wounds allow an investigation of the cellular response to thermo-mechanical damage and the hot rod can effectively remove cells from a designated area. A drawback of the thermal wounding method is the potential to cauterize the wound and create an environment not representative of incisional wound healing. The heat may also damage the surrounding cells and not provide a well-defined wound margin. While an effective wounding method, thermal wounds would not well represent incisional wound healing in EDS. A comprehensive summary of pros and cons can be found below in **Table 41**.

Table 41. Pros and Cons of a Thermal Wound

Thermal Wound via Hot Rod/Branding	
Pros:	***Cons:***
• Studies thermo-mechanical vs. mechanical damage to a cell model • Effectively would remove cells within a designated range of area	• Cauterizes wound – not representative of healing and initial cutaneous injury • Heat may not be restricted to a certain area (accuracy/precision limitation)

Optical wounding is a unique wound method that uses a high-powered laser to damage tissue. Using a laser creates high reproducibility and has the potential for high throughput. The Laser Enabled Analysis and Processing (LEAP) instrument can be valuable for producing highly

accurate and precise defined wound areas (Stamm et al., 2016). Unfortunately, the LEAP instrument is expensive specialized equipment, heat can lead to unintended cell damage, and it has not been shown to produce partial thickness wounds. The optical wound method is also not representative of an incisional wound. A summarized list of pros and cons for the optical wound method can be found below in **Table 42**.

Table 42. Pros and Cons of an Optical Wound

Laser (Optical Wound)	
Pros:	***Cons:***
• High reproducibility • High throughput (use of LEAP system) • Sterile environment • High accuracy and precision with power of laser	• May not be possible to conduct partial depth wounds • Potential damage to cells outside range of wound induction • Specialized equipment needed • Heat development can affect cell viability • Acquisition of LEAP instrument necessary

The rotating drill is a method of mechanical wounding. Similar to a stamp method, the rotating drill is brought in to contact with the tissue and allowed to cause damage. The mechanical damage may be like that of an incisional wound. A rotating drill can remain consistent in size and wounding pattern between wounds. Additionally, the rotating drill has the potential to be automated. A major limitation of the rotating drill is the possibility of the drill to cause damage outside of the anticipated wound area and damage the plate. If the drill incorrectly catches part of the plate, it has the potential to cause catastrophic damage to the model system (Stamm et al., 2016). A summarized list of pros and cons for the rotating drill method can be found below in **Table 43**.

Table 43. Pros and Cons of a Rotating Drill Wound

Rotating Drill	
Pros:	***Cons:***
• Mechanically induces wound • Rotating drill remains consistent size/speed • Potential to be automated	• Potential for damage of cells (outside range of wound induction) • Potential damage to plate

The final wound method the team considered was Electric Cell-Substrate Impedance Sensing (ECIS) to create an electrical wound. In this method, cells are grown over an electrode placed in the bottom of a plate. A large current surge is sent through the electrode and results in cell death. Alternating current is applied through the electrode as the cells return to confluency to monitor the growth. As the cells become more confluent, the impedance measured increases. Some advantages of ECIS include automation, real time measurement, and a well-defined wound margin. Some disadvantages of ECIS include the requirement of specific equipment, high cost, primary application in 2D models, and changes in cell adhesion and density that can affect the impedance output (Stamm et al., 2016). Additionally, an electric wound may not be representative of an incisional wound. A complete list of pros and cons for an electrical wound is summarized below in **Table 44**.

Table 44. Pros and Cons of a ECIS Wound

Electric Cell-Substrate Impedance Sensing (ECIS) (Electrical Wound)	
Pros:	***Cons:***
• Effective at reducing drawbacks of scratch assay • Real-time, label-free, impedance-based method to study cell behaviors in a tissue culture • Defined wound • Increase in impedance over time reflects wound closure via migrating cells • Can be used in medium- to high-throughput screening experiments • Measurement and control of cell destruction • Measurement of regrowth by impedance • Real-time measurement • Automatic wounding – thus eliminating human manual error	• Specific equipment and ECIS device must be purchased if not available ○ Special electrode plates • Not cost effective • Primarily used for monolayer models • Measurement of regrowth by impedance (may influence growth formation) • Low throughput • Change in cell adhesion and density alter impedance • Disruption of confluent cell layer possible

4.3.3 Quantitative Assessment of Design Elements

The team ranked design element ideas using a decision matrix to assess how well each mean achieved the relevant objectives. Design means were categorized into four design element groups: cell type, model style, matrix material, and wound induction method. Relevant objectives and constraints were assigned to each category (abbreviated to O and C respectively, as demonstrated in **Table 45** below). The analysis began by determining if the design means violated any constraints. Means were assigned a value of yes (Y) if they did not violate a constraint or no (N) if they did violate a constraint. If a constraint was violated, the design mean was removed from consideration and assigned a score of zero.

Means that did not violate constraints were given a score of 1 to 3, with 1 being the least favorable and 3 being the most favorable. A full list of metrics for each sub-objective can be found in **Appendix G**. After a score was assigned, the score was normalized by dividing the score by the largest score received by any mean for that specific sub-objective. The sum of the scores for all sub-objectives were multiplied by their respective primary objectives' weight, which was assigned based on the team, client, and user pairwise comparison charts described in Chapter 3.5. The last step was to sum all the sub-objective scores for each mean, which resulted in the final score. These scores were compared to each other to determine the highest-ranked mean for each design objective. **Table 45** below displays an example matrix evaluation for the model style design element.

Table 45. Decision Matrix Example (Model Style)

			Micro-TUG Model			Self-Assembling Tissue Model			Cell-Laden (Hydro/Micro) Gel Model			Microfluidic Model			Hanging Drop Model		
	Constraints	Weight %	Score	Normalized Score	Weighted Sum	Score	Normalized Score	Weighted Sum	Score	Normalized Score	Weighted Sum	Score	Normalized Score	Weighted Sum	Score	Normalized Score	Weighted Sum
C	Timeline			Y			Y			Y			Y			Y	
C	Budget			Y			Y			Y			Y			Y	
C	Material Availibility			Y			Y			Y			Y			Y	
C	Equipment Availability			Y			Y			Y			Y			Y	
C	Sterilizable			Y			Y			Y			Y			Y	
C	Biocompatible			Y			Y			Y			Y			Y	
C	Nontoxic			Y			Y			Y			Y			Y	
C	Standardization			Y			Y			Y			Y			Y	
C	Incubator			Y			Y			Y			Y			Y	
C	Media			Y			Y			Y			Y			Y	
C	Proliferation			Y			Y			Y			Y			Y	
C	Confluency			Y			Y			Y			Y			Y	
C	Contamination			Y			Y			Y			Y			Y	
	Objectives																
O2	**Imageable**	20		3	59.94		3	59.94		3	59.94		3	59.94		2.3	46.6
O	Measurable Wound Area		3	1		3	1		3	1		3	1		1	0.3	
O	Light Microscopy		3	1		3	1		3	1		3	1		3	1	
O	Throughput		3	1		3	1		3	1		3	1		3	1	
O4	**Usable**	18		7.7	137.9		6.7	119.88		8	143.856		5.3	95.904		6.7	120
O	Standard Dish/Plate		3	1		3	1		3	1		1	0.3		3	1	
O	Typical Incubator		3	1		3	1		3	1		3	1		3	1	
O	Single Scientist		3	1		3	1		3	1		3	1		3	1	
O	Available Materials		3	1		3	1		3	1		3	1		2	0.7	
O	Material Safety		3	1		3	1		3	1		3	1		3	1	
O	Easy Assembly		3	1		3	1		3	1		2	0.7		2	0.7	
O	Time Efficient		3	1		1	0.3		3	1		1	0.3		3	1	
O	Induct Wound		2	0.7		1	0.3		3	1			0		1	0.3	
					197.8			179.82			203.796			155.844			167

The final scores for each of the design element categories are displayed in **Table 46** below. The complete design matrices are provided in **Appendix H**. The highest rated elements, highlighted in yellow, were incorporated into the design concepts developed in Chapter 5.

Table 46. Summary of Decision Matrix Results

Cell Type			
Human EDS Fibroblasts	EDS Mouse/Animal Model	Normal Human Fibroblasts in EDS Derived Matrix	Normal Human Fibroblasts in Chemically Altered Matrix
145	0	0	96.9

Model Style					
Micro-TUG Model	Self-Assembling Tissue Model	Cell-Laden (Hydro/Micro) Gel Model	Microfluidic Model	Hanging Drop Model	Magnetic Suspension Model
197.8	179.82	203.8	156	167	0

Matrix Material								
Cell-Derived Matrix via Fibroblasts	Fibrin	Collagen I	Matrigel	Alginate	Polylactic Acid (PLA)	Polyglycolic Acid (PGA)	Hydroxyapatite (HA)	Hyaluronic Acid (HA)
0	152	142	156	0	132	132	131.9	0

Wound Induction Method							
Scratch Pipette Tip	Scratch Rubber Policeman	Scalpel Scratch	Stamp Punch Biopsy	Hot Rod/Branding	Laser (Optical Wound)	Rotating Drill	Electric Cell-Substrate Impedance Sensing (Electrical Wound)
150	150	150	133	130	0	143	0

5.0 Development and Verification of Final Design

Once a quantitative design analysis was completed, the design team met with the client, and the top designs were approved. This allowed the design team to move forward and make a few final design alternatives. The two top model designs were a cell-laden hydrogel and a micro-TUG design, both of which incorporate fibrin and EDS human dermal fibroblasts. While the cell-laden hydrogel did receive a higher analysis score than the micro-TUG, the difference between the two was slight, so final designs of both models were considered. There were also three wound inducting method designs that were considered, with the intent of using the scalpel as the wound induction method. The three designs all included incisional guides to ensure precision of the wounds. The designs included paper incisional guide placed under the well plate, a modified

plate cover that allows for guided induction, and a partially automated lever arm attachment that allows for guided wound induction.

5.1. Cell-Laden Hydrogel Design

The model that was given the highest analysis score was the cell-laden hydrogel design. As mentioned previously, this model-type allows for a wide variety of characteristics to be altered and studied. The hydrogel design ranked well against other designs due to efficient assembly, ease of accessing materials needed to create hydrogel, and ability to analyze many characteristics of the EDS dermal fibroblast phenotype such as migration and proliferation. In this final design, a fibrin gel made of thrombin and fibrinogen had cells embedded in its matrix, as seen below in **Figure 13**. A scalpel was proposed to be used to make the wound incision with one of the three templates mentioned previously.

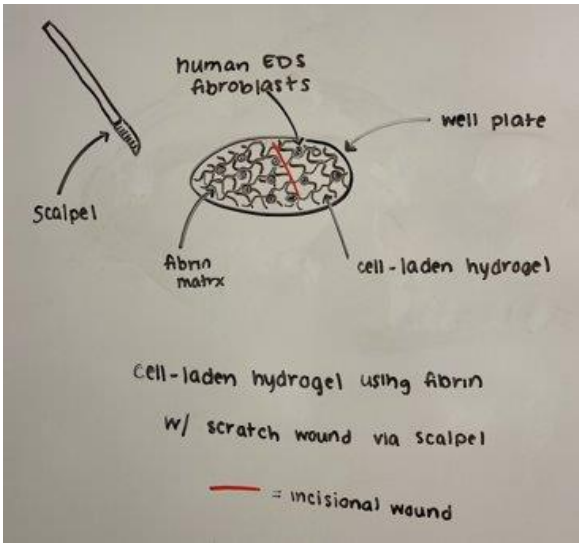

Figure 13. Representative sketch of potential hydrogel model design

5.2 Micro-TUG Design

The second-highest rated design was the micro-TUG design, which is more complex than the cell-laden hydrogel and therefore lost a few points in the design matrix. A benefit of the

micro-TUG model design was that this model provides the user with information relating to the various mechanical forces acting on the wound model. This is a result of the deflection within the 4 support posts. Similar to the primary cell-laden hydrogel design, the micro-TUG design would be composed of a fibrin matrix with embedded human EDS fibroblasts within a well plate.

This model would be under consistent tension and strain during cellular growth and wound healing. This model would therefore be effective to mimic the cellular environment of cEDS and would allow the study of how mechanical stimuli affect the resulting biological processes and behaviors within the model. In **Figure 14** below, the amorphous red area represents the EDS cell-matrix and the four circles on each respective corner represent the circular posts that form the micro-TUG structural support.

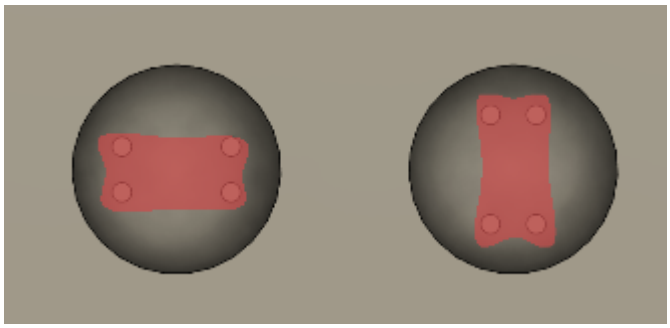

Figure 14. Representative sketch of possible micro-TUG design.

5.3 Wound Induction Method Designs

After determining the various possibilities of model design for tissue, the next step involved focusing on the method of wound induction within the model. This method needed to consistently and precisely create wounds across all samples, ensuring uniformity in wound size, length, and orientation. Among the various possibilities, the scalpel-based scratch method was chosen for its accuracy in mimicking surgically induced wounds. This approach was then

incorporated into the initial model designs. Moreover, given the 12-well plate format for the model experiments, the design dimensions were specifically tailored to this platform.

The advantage of the proposed devices is that each device would aid the induction of a wound with greater control than if a scientist manually induced a wound with only a scalpel and no guide. Furthermore, each design could be reused for multiple samples, as each design is compatible with all standard laboratory 12-well plates, can be sterilized, and can be used within a sterile environment.

Three design concepts were developed to address the potential for human error in wound induction within the final wound healing *in-vitro* model. Visuals of each design concept are available in **Table 47**.

Preliminary Design #1: Printed Wound-Sizing Incisional Guide

This design is inspired by graph paper and will be placed below the well plate as a guide. This design requires manual wound induction by one scientist and contains 12-well plate circumference outlines to line the 12-well plate up accurately before beginning the wound incision process. Furthermore, equal-sized incisional wound markers are located in the center of each well plate with dark ink to be seen through the model and matrix.

Preliminary Design #2: Well Plate Cover with Incisional Guide

As an adaptation of a standard 12-well plate cover, this design will contain 12 equally sized and oriented incision markers for a scalpel to be lowered into the model to make consistent wound lengths. This model requires manual incisions to be conducted by a scientist, and the cover can be removed for imaging as well.

Preliminary Design #3: Scalpel Holder and Wound Induction Lever Attachment

This design will allow the scalpel to the lowered to the model for a full depth wound based on design specifications. A scalpel-holder will be located at the top of the lever for securing the scalpel for stable incisions. There is limited longitudinal movement to ensure the same wound length is conducted for all 12 well-plate samples, and the design can be attached to the side of the designated well-plate and moved for each sample.

Table 47. Summary of Preliminary Wound Induction Designs

Model of Design	**Description**
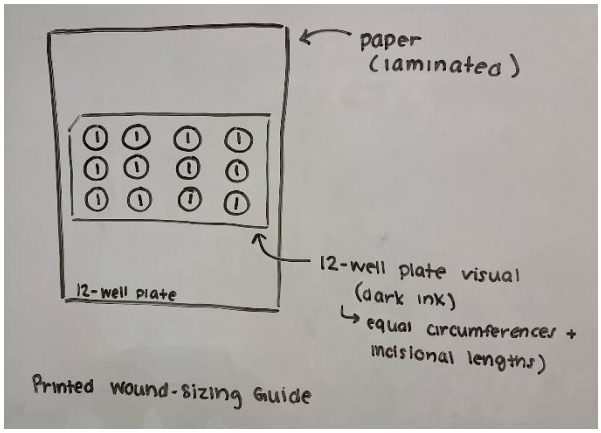	*Preliminary Design #1: Printed Wound-Sizing Incisional Guide* This design is printed on sturdy paper and is laminated for reusability. The printed outline and incisional markings will be on the paper with dark ink for visibility.
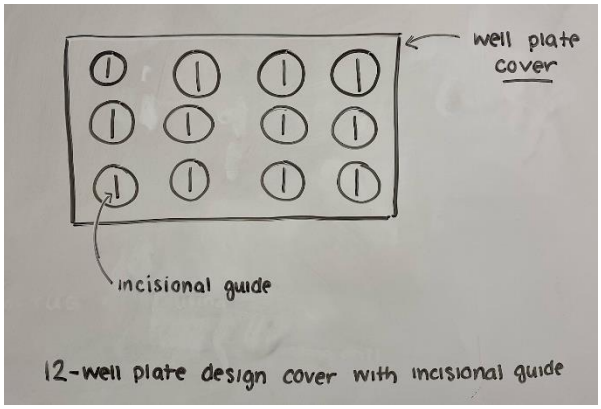	*Preliminary Design #2: Well-Plate Cover with Incisional Guide* This design consists of an altered 12-well plate cover with pre-cut incisions that will be a guide for a scalpel to move through the model with a precise cut throughout all the models at a particular length.
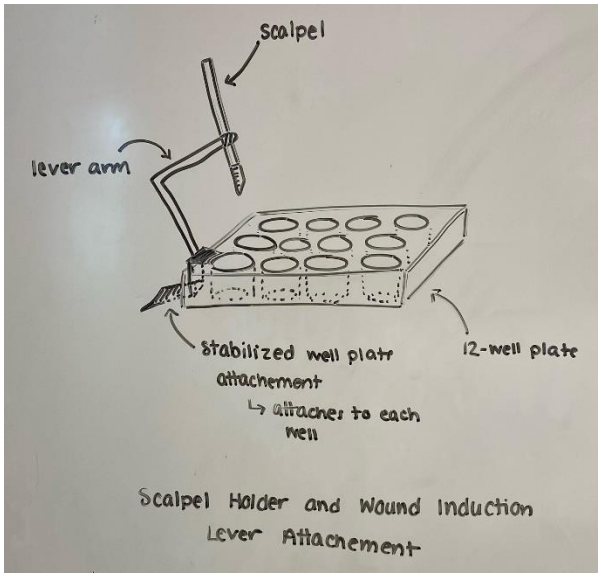	*Preliminary Design #3: Scalpel Holder and Wound Induction Lever Attachment* This design is more automated than previous designs but continues to rely on scientist supervision for wound induction. Furthermore, this design continues with one-well incision. A lever is attached to the side of one well and will have a designated “drop” height to induce a full depth wound, as well as a set length for the incision.

After evaluating different methods for inducing wounds, the team selected *Preliminary Design #2: Well-Plate Cover with Incisional Guide* as the primary choice for use in the initial development and testing phases. This design stood out because it offered a clear guide, could be sterilized, and could be used repeatedly for multiple samples and experiments. Moreover, considering the project's limitations, this design seemed feasible to achieve.

Preliminary Design #3: Scalpel Holder and Wound Induction Lever Attachment is an intriguing option that could be considered for implementation at a later stage due to its potential for adding automated elements. However, the project constraints indicated that this design may be too complex for this stage of the project.

5.4 Preliminary Testing of Overall Design Ideas

Preliminary testing of the final 3D *in vitro* wound model of cEDS was conducted to optimize the functionality of each design component: the wound incision method and guide, the design of the fibrin gel, components of the media, and the system for compression testing. To develop the final model, a variety of cellular experiments were conducted with increasing complexity. Initially, a simple cell growth test was performed, followed by a 2D monolayer scratch assay, and finally, cell-seeded fibrin gels for both wound induction and compression testing. A comprehensive protocol for each experiment is located in **Appendix I**.

5.4.1 Well Plate Mask

The team developed a well plate mask to be utilized during imaging and wound induction. The well plate mask combined and iterated upon the wound induction preliminary design methods #1 and #2 (**Table 47**). The team developed this mask to improve efficiency, accuracy and precision of wound incision and imaging. The mask provided a consistent area to create the wound and greatly restricted the imageable area, allowing the team to identify the

region of interest (ROI) more consistently and in less time. The mask design went through multiple iterations starting from a hand cut piece of paper before achieving the final design of a laser cut acrylic piece.

The team began by marking the bottom of a 12-well plate with sharpie to consistently image the region of interest. The team found the opaque sharpie obscured the plate and prevented imaging. This violated our specification of imageability. Additionally, marking every well was inefficient and inconsistent. The team created the first iteration of a mask by measuring and tracing a 12-well plate outline on a piece of paper. This outline was subsequently cut out and 6 mm square regions were cut from the center of each well using an Exacto™ knife as seen in **Figure 15**. The team utilized the paper cut out as a proof-of-concept verification that masking the well plate created a reduced imageable region. The paper mask was limited in consistency of dimensions and sterilizability.

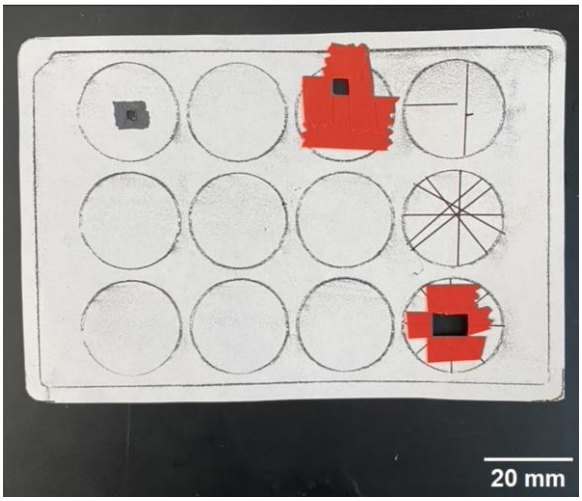

Figure 15. Initial paper well plate mask.

The final well plate mask design was created in SolidWorks and laser cut from white acrylic. The interior base of the well plate was measured, and the mask was designed to fit flush

within the outer walls of the well plate. A 6 mm square region is cut from the center of each well. Wounds for the final model and scratch model are induced over the unmasked region and imaging is performed within the bounds of the unmasked region. The final mask fits within a 12-well plate base, can be sterilized, improves wound induction and imaging, and can be seen in **Figure 16**. Two acrylic masks were created with the same CAD files to improve throughput. Masks were marked in the top left corner with sharpie to maintain orientation and to prevent potential manufacturing discrepancies from affecting the imaging ROI.

Figure 16. Left: Final acrylic well plate mask. Right: The mask fits when placed under a 12-well plate.

5.4.2 Cell Growth Assay

Tests were performed in order to compare the rate of cell growth between the cEDS dermal fibroblasts and neonatal human dermal fibroblasts (NHFs). Three wells of cEDS dermal fibroblasts and NHFs were separately plated, each with 5,000 cells per well. The wells were imaged every 24 hours over a five-day period. The cells present in each well were counted in two 1.26mm by 0.71mm regions of the well using the ImageJ Cell Counter analysis tool, and the

average cell count was recorded. **Figure 17** provides a visual assessment of the cell growth over the five-day period.

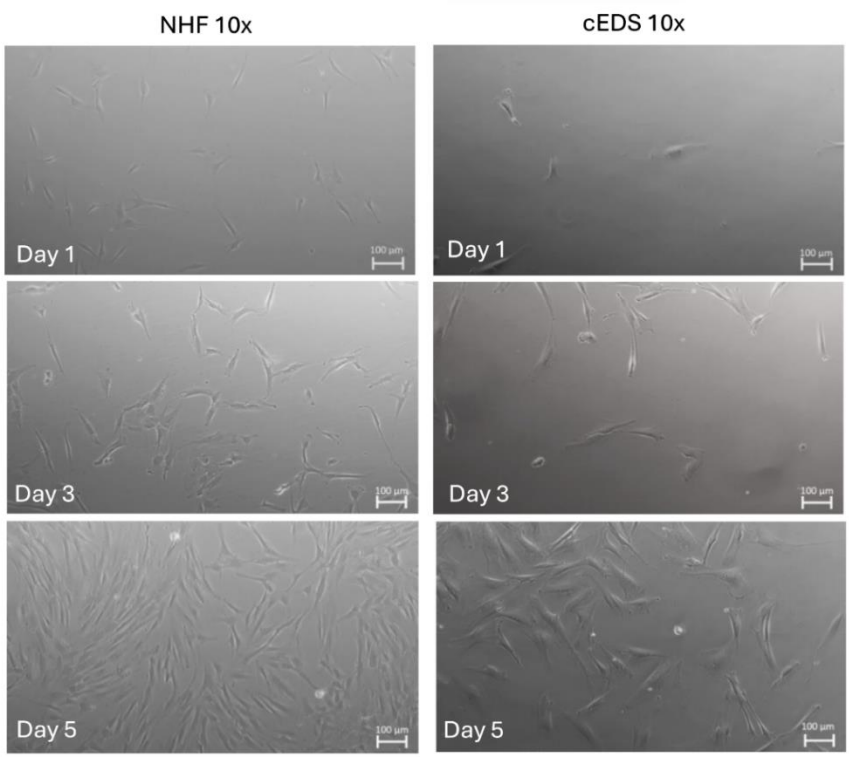

Figure 17. Visual assessment of cell growth in NHFs and cEDS dermal fibroblasts over a five-day period, 10x magnification

To compare the rate of cell growth, the average number of cells per well was recorded in three wells of each cell type every 24 hours for five days. As seen in **Figure 18**, the NHFs had a greater average change in the number of cells present as compared to the cEDS dermal fibroblasts.

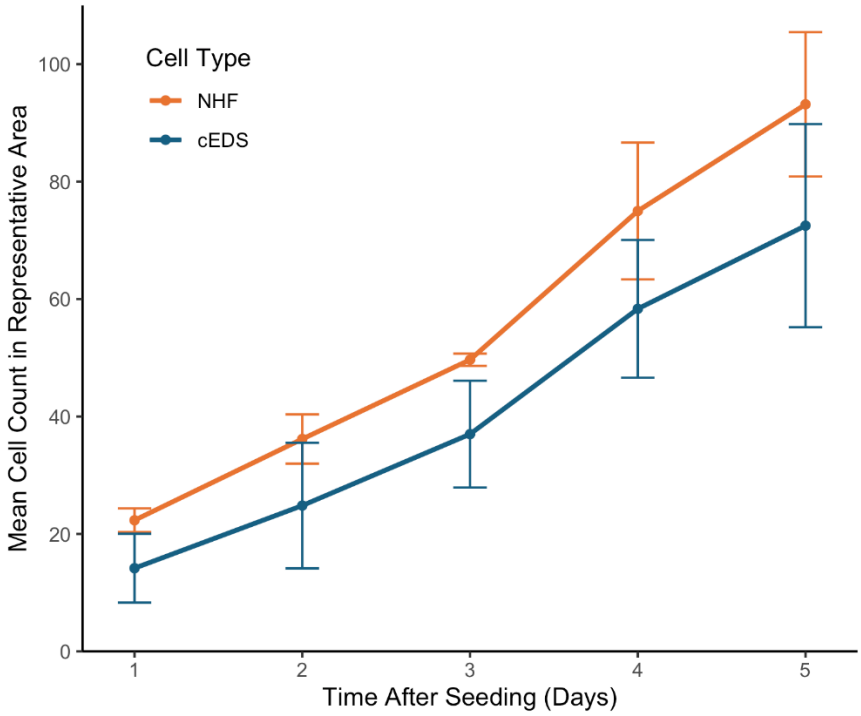

Figure 18. Cell count from Day 1 of cEDS dermal fibroblasts and NHFs over a five-day period.

A two-sample t-test assuming unequal variances for each group comparison at each time point was calculated. No significance was found between the NHF and cEDS groups (p-values ranging from .125 to .2). Details of this statistical analysis can be found in **Appendix L**.

5.4.3 Monolayer Scratch Assay

Monolayer scratch assays were performed with both cEDS fibroblasts and NHFs to act as a benchmark to compare the rate of wound closure with that present in the literature. The method used to induce a wound was a critical component of the design process, since wound induction method would directly affect the study of wound closure.

For the monolayer scratch assay, a pipette tip was used to create the scratch, as this method is consistent with the literature (DeNigris et al., 2016). Scratches from a 200 µL and 1000 µL pipette were compared to determine which was optimal. The team decided to use a 200

µL pipette as this created a smaller wound margin, which was easier to view with a microscope at 10x magnification. To begin the monolayer scratch assays, eight wells of 80,000 cells per well were plated for each cell type. The cells were left to incubate over a 2-day period, or until the cells reached 80% confluence. Once the cells reached 80% confluence, the media was aspirated from each well and replaced with 1 mL of Phosphate Buffered saline (PBS). The mask was placed under each well plate to guide the placement of the wound. A 200 µL pipette was then scraped across the center of the well plate to induce the wound. The wells were imaged every two hours over a 24-hour period using a brightfield microscope at 10x magnification. **Figure 19** provides a visual assessment of the wound area reduction in the cEDS dermal fibroblasts over a 24-hour period.

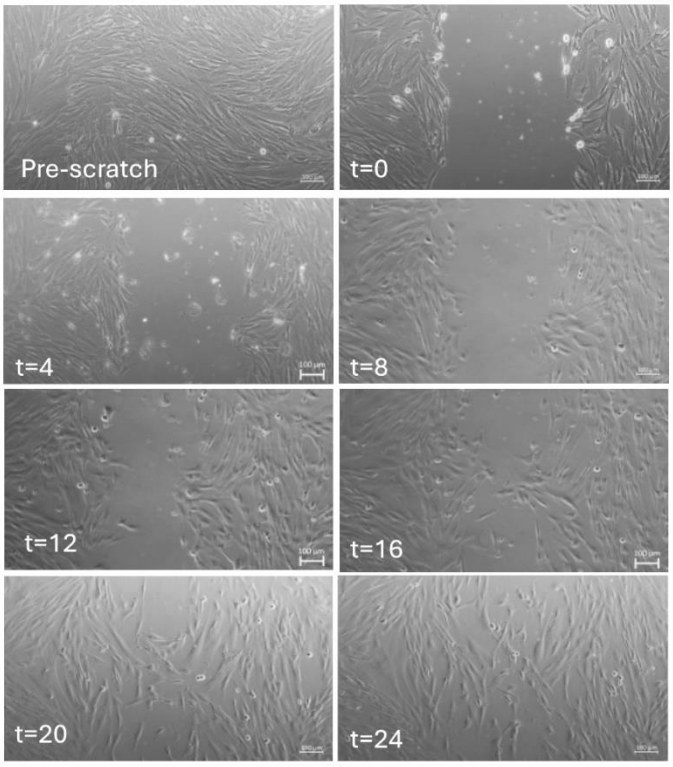

Figure 19. Reduction in wound area of cEDS dermal fibroblasts over a 24-hour period, 10x magnification

To conduct a quantitative analysis on the reduction in wound area, an ImageJ analysis macro developed by Suarez-Arnedo et al (2020) was used. Wacom tablets and pens were used to trace the wound margins in each image. **Figure 20** depicts an example of a wound margin outline using the Wacom pen.

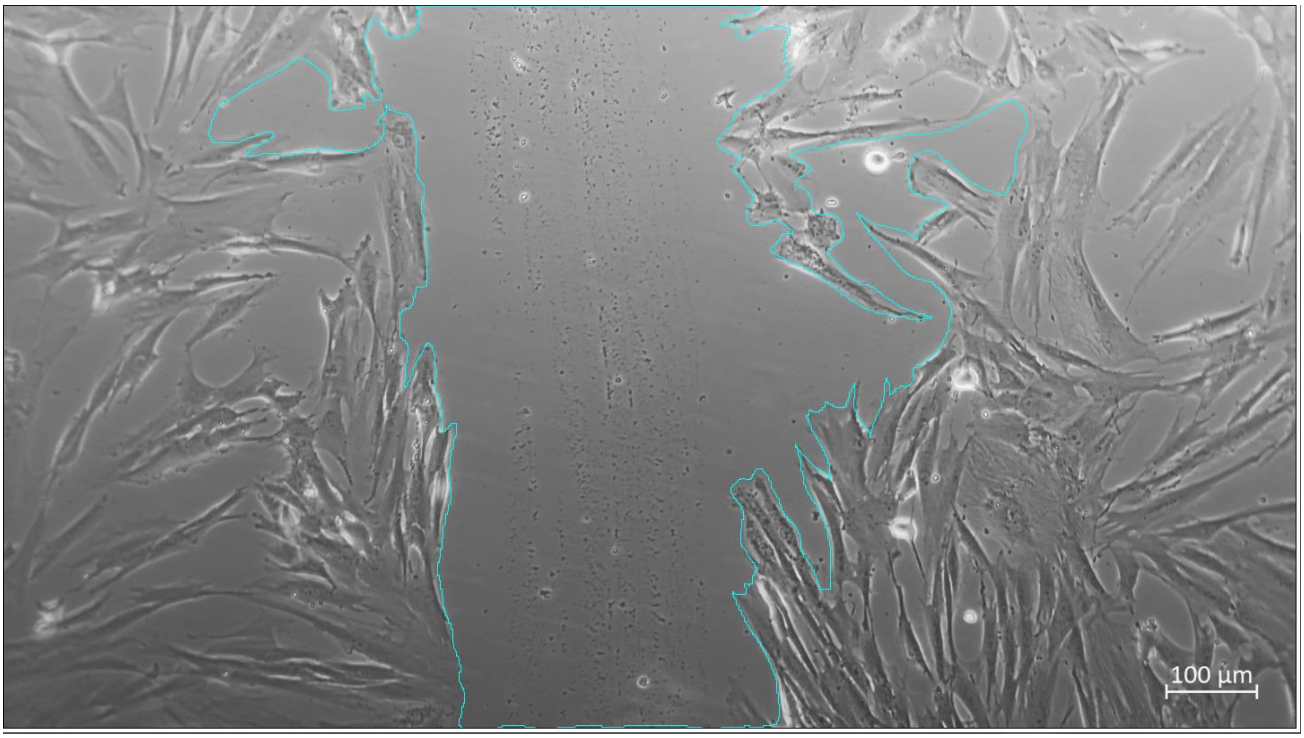

Figure 20. Example tracing of monolayer scratch assay (cEDS dermal fibroblasts) using Wacom pen on ImageJ to evaluate wound area percentage, 10x magnification

After tracing the wound area for each image, the results were converted into a percentage of original wound area by setting the original wound area equal to 100%, and then using the new wound area at each of the two-hour time points to calculate the percentage of wound area remaining. Measurements were taken three times by different people, then averaged together. Time point from 8 hours was excluded due to missing data. **Figure 21** depicts the average percent of open wound margin over time for both NHF and cEDS dermal fibroblasts.

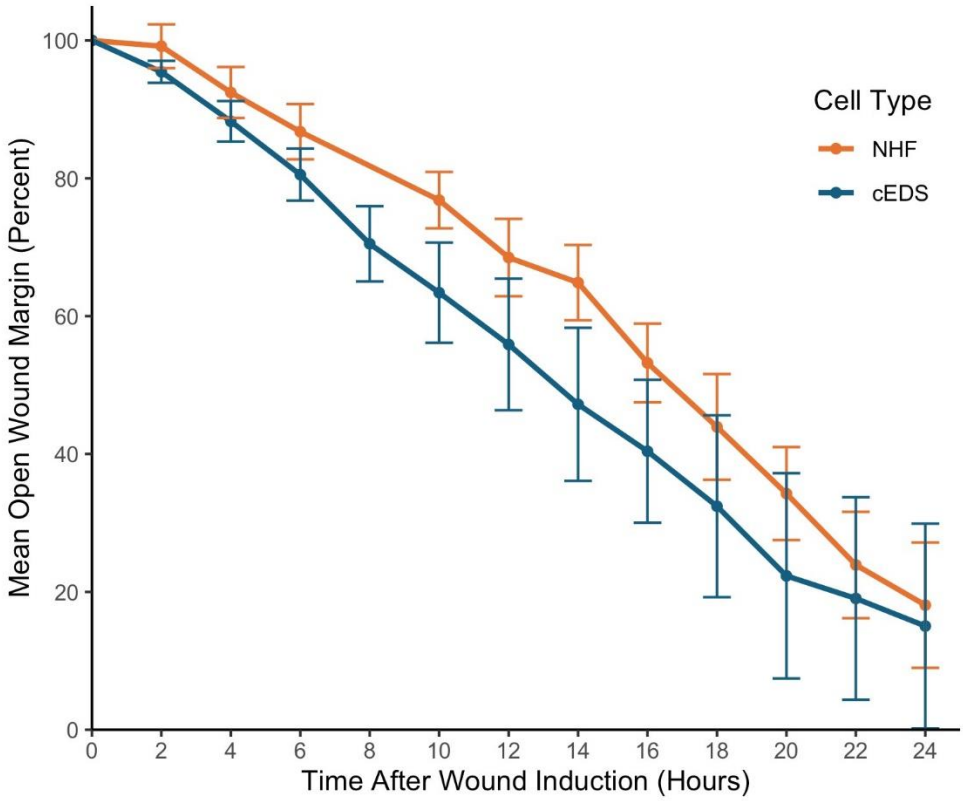

Figure 21. Mean open wound margin (percent) over 24-hour period for NHF (n = 9) and cEDS (n = 8) dermal fibroblast monolayer scratch assay.

Comparison of both NHF and cEDS dermal fibroblast samples reveal approximately 80% wound closure of both cell types, consistent with prior literature (DeNigris et al., 2016). A two-sample t-test assuming unequal variances for each group comparison at each time point was calculated. The percent of open wound margin was significantly smaller in the cEDS group than the NHF group from time two to time sixteen at $\alpha = .05$ (statistical analysis presented in **Table 48**, below). In this table, * indicates that the P value is < 0.05; ** indicates that the P value is < 0.01; *** indicates that the P value is < 0.001.

Table 48. T Test Results for Wound Margin Closure of NHF and cEDS Scratch Assay

Time	Statistic Value	Degrees of Freedom	P Value
2	-3.09	12.06	.009**
4	-2.60	14.84	.020*
6	-3.30	14.93	.005**
8	n/a	n/a	n/a
10	-4.62	10.75	<.001***
12	-3.27	11.06	.007**
14	-4.08	9.94	.002**
16	-3.10	10.60	.010*
18	-2.16	10.98	.053
20	-2.09	9.51	.065
22	-0.84	10.30	.421
24	-0.50	11.33	.626

5.4.4 Fibrin Gel Design

A series of gels with varying volumes and concentrations were tested to determine the final volume of fibrin solution per gel, the final concentration of thrombin and fibrinogen, and the finalized composition of media that the cell-seeded gels will be placed in.

First, multiple gels were made by dissolving a stock of Knox gelatin powder into H_2O using the ratio provided on packaging (0.14 g/mL) to test different wound induction methods. The gelatin mixture was dyed blue with food coloring to better visualize. In a 24-well plate, gelatin was poured into wells with volumes including 100, 200, 300, 400, 500, and 600 µL. In a 12 well plate, gelatin was poured into wells with volumes of 1 mL, 1.5 mL, and 2 mL as seen in **Figure 22**.

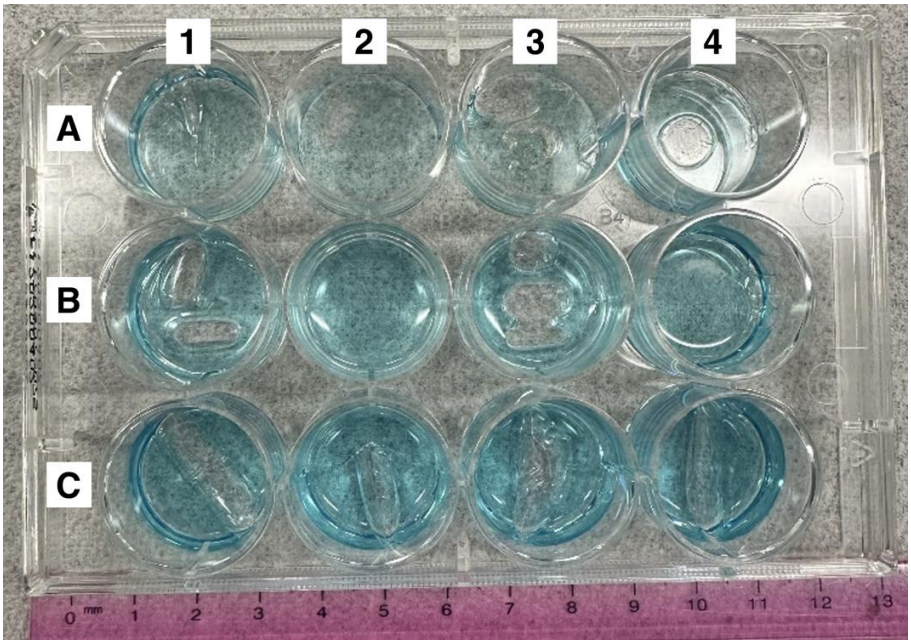

Figure 22. Gelatin in 12-well plate, with volumes of 1 mL (row 1), 1.5 mL (row 2), and 2 mL (row 3). In well A1, a scalpel was used to induce a wound to the gel. In wells A3 and A4, a circular leather punch was used to induce a wound. In well B1, an oval leather punch was used to induce a wound, similar to the wound induced in B3. In all wells of row C, a longer rectangular leather punch was used to induce wounds.

Various volumes of the left-over gelatin solution were placed into petri dishes for wound induction testing to be completed later. Based on the thickness of the dermis, which ranges from 1 to 4 mm, the 1 mL volume of gel solution placed in a 12 well plate was selected for the final volume of the 3D gel model (The University of Texas Medical Branch, 2008). The area of each well was roughly 3.5 cm^2, allowing for a 1 mL volume gel to obtain a thickness of around 0.28 cm, or roughly 3 mm in thickness.

The concentrations of fibrin gels were then evaluated. Using non-sterile aliquots of fibrinogen and thrombin, various concentrations of un-seeded gels were made. All thrombin aliquots were 4 units per 200 µL and fibrinogen aliquots were either 70 mg/mL or 10 mg/mL. Final fibrinogen concentrations were achieved through dilutions while making gels. For example, to create a 1 mL gel with a concentration of 35 mg/mL fibrinogen, 500 µL of the 70

mg/mL aliquot was mixed with the proper amount of thrombin. Gels were therefore created by taking 75 µL of the thrombin aliquot and mixing it with 425 µL 40 mM $CaCl_2$ solution which was then combined with 500 µL of the diluted fibrinogen aliquots. This allowed gels to reach a final volume of 1 mL in each well of the 12 well plates. The final concentration of thrombin was 1.5 units per 1 mL gel, and final fibrinogen concentrations included 5 mg/mL, 17.5 mg/mL and 35 mg/mL as seen in **Figure 23**.

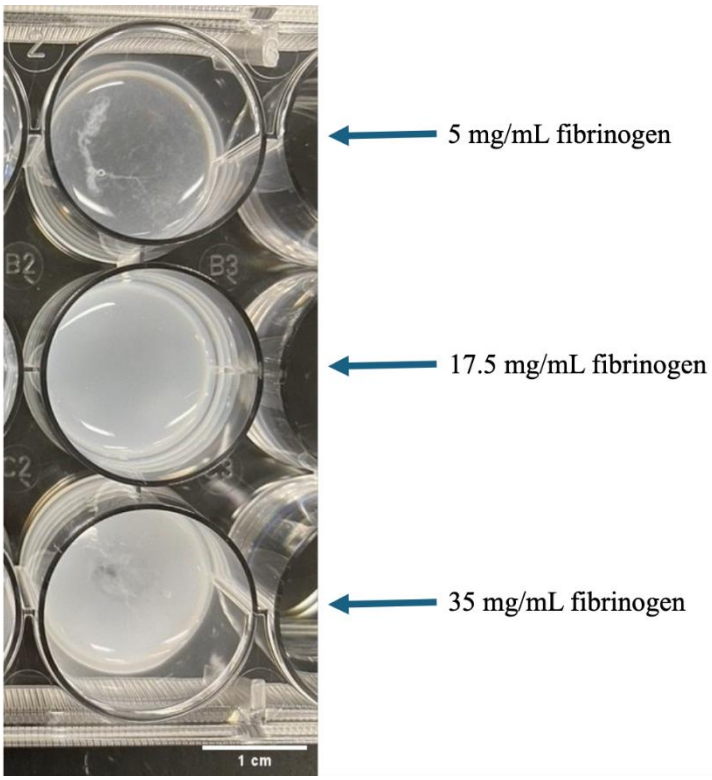

Figure 23. Non-sterile unseeded fibrin gels with varying fibrinogen concentrations of 5 mg/mL (top), 17.5 mg/mL (middle), and 35 mg/mL (bottom).

The three fibrinogen concentrations were evaluated under a microscope to determine what was the most transparent and best for imaging. It was determined that 5 mg/mL was the best for observation under the 10x magnification with the Zeiss microscope. The different concentrations were then compared to cell seeded gels in literature, and it was determined that 5 mg/mL gels correlated with the most cell proliferation (Duong et al., 2009). This confirmed that

the final gel model would have a 5 mg/mL fibrinogen concentration with a 1.5 units/mL thrombin concentration for the best cell growth outcome in the 3D model.

The final step in verifying the final design of the gels was evaluating the best medium composition for extending the integrity of the gels. 200,000 cells were always seeded in each well, suspended in 200 µL of media. At first, DMEM supplemented with 10% FBS was used on the gels after they were polymerized. This led to fast cell growth, however the gels disintegrated in 1-2 days after media was placed on each gel. The concentration of FBS in DMEM was then lowered to 1% to slow cell growth, however this caused what was perceived to be as cell death. The FBS concentration was then increased to 5%, which caused apparent slowed growth, but still lead to a large percentage of apparent cell death. The FBS concentration was then raised back up to 10% FBS in DMEM, however this again resulted in complete degradation of the gels after 1-2 days as seen in **Figure 24.**

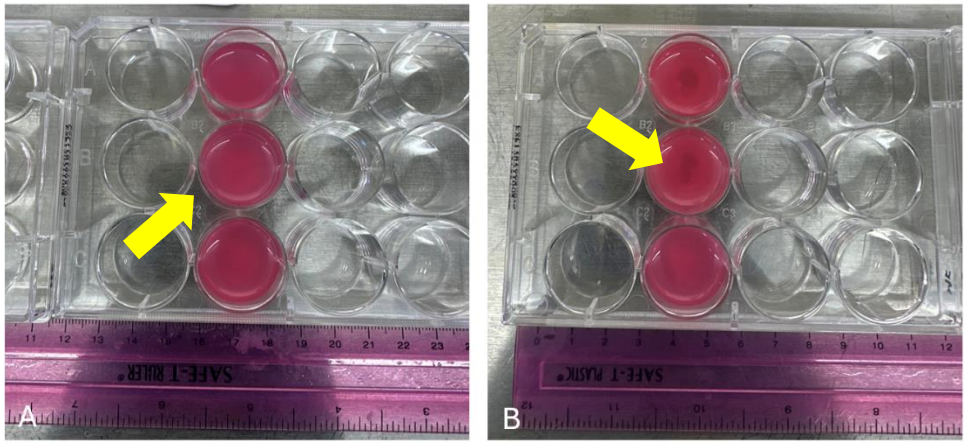

Figure 24. Image A shows a fully disintegrated gel (yellow arrow). Image B shows a partially disintegrated gel that still maintains its shape (yellow arrow).

It was determined that the increased proliferation may be causing cell proteases to break down the fibrin gel, so aprotinin was added to the 10% FBS DMEM media as a protease inhibitor. The completed fibrin gel model was cultured in 10% FBS DMEM with 20 µg/mL of

aprotinin and was developed using a fibrinogen, thrombin, and calcium chloride ($CaCl_2$) solution with initial concentrations of 5 mg/mL and 4U/200 µL, respectively.

5.4.5 Fibrin Dot Assay

To characterize cell outgrowth, dot samples composed of 100 uL cell-seeded fibrin hydrogels were pipetted into a 12-well plate, cultured in complete media with aprotinin (20 µg/mL), and evaluated at 24-hour increments for up to 10 days. NHF dots degraded after 9 days in culture, while cEDS dots degraded after only 6 days in culture. In both cases, cells were observed to proliferate and expand in the matrix area. Outgrowth from the fibrin dots was observed by day 5 for both cell types (Figure 25).

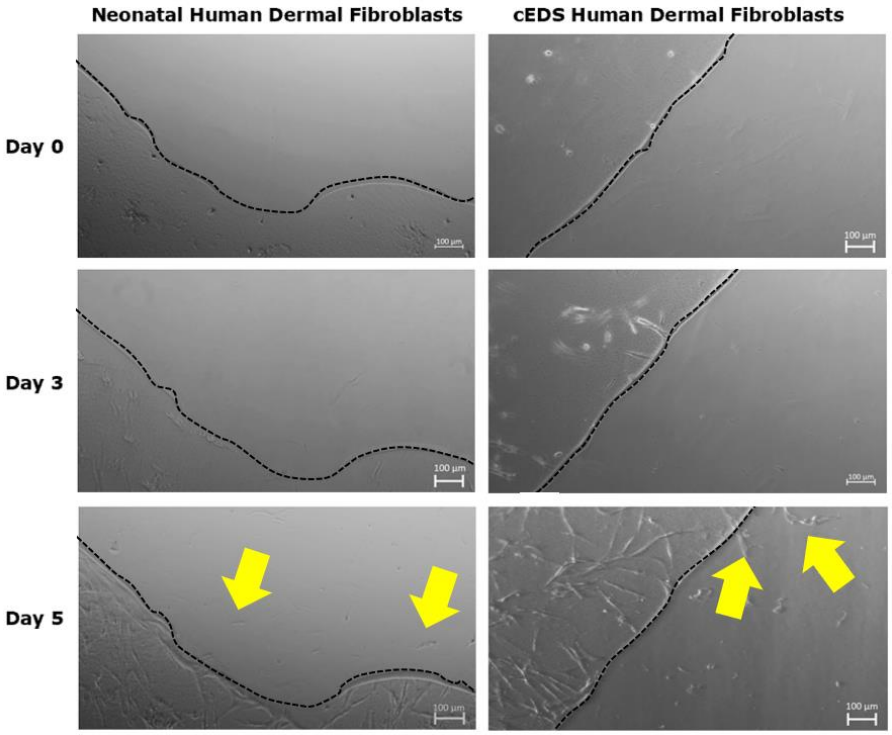

Figure 25. NHF and cEDS fibrin dots, outgrowth observed by day 5 (yellow arrows point to fibroblast outgrowth)

5.4.6 Punch Prototyping

To determine the finalized specifications of the 3D fibrin gel model, four prototypes were tested with various materials to determine wound induction method. The first wound induction method was completed using a scalpel to cut out a rectangle within the gelatin. This method proved ineffective as the scalpel left many scratches on the bottom of the plate, and the wound shape and size were inconsistent. Additionally, the scalpel caused the gelatin to tear upon wound induction, furthering inconsistencies in shape amongst the different trials.

To make the wound more consistent, the team utilized punches from a leather punch kit (**Figure 26**.).

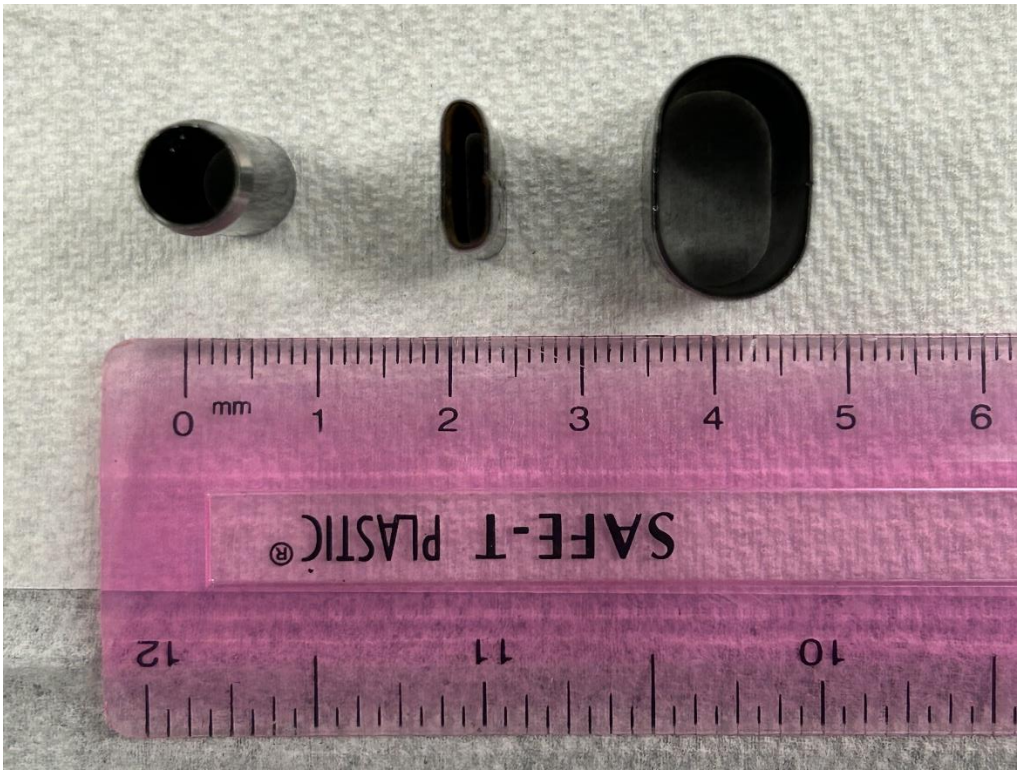

Figure 26. Left to right: 10x10mm (circle), 25x15mm (oval), and 15x6mm (oval) punches from leather punch kit

10x10mm (circle), 25x15mm (oval), and 15x6mm (oval) punches were tested. For preliminary testing, the punches were stamped into the gelatin, and then the inside of the punch was aspirated using a vacuum aspirator. This resulted in uniform punches with defined wound margins. **Figure 27** demonstrates example wounds from punches in 40 mL of gelatin in a 100mm by 15mm petri dish. The 15x6mm oval punch was selected as its smaller wound margins allowed for easier imaging, and the oval shape mimicked that of an incisional wound.

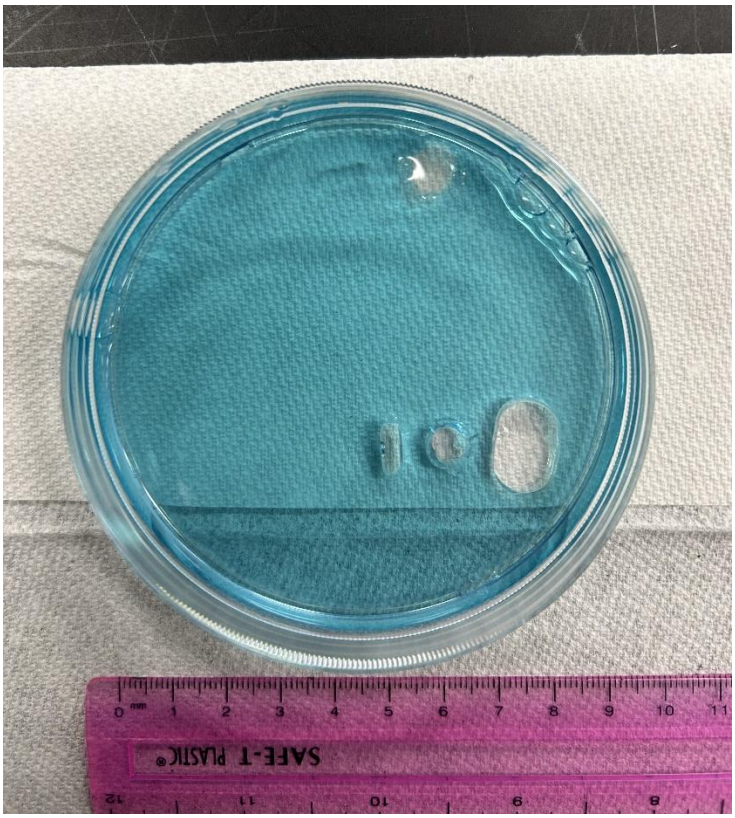

Figure 27. 40 mL of gelatin with 10x10mm (circle), 25x15mm (oval), and 15x6mm (oval) punches

This same methodology of using the leather punch with the aspirator was applied to unseeded fibrin gel. In contrast to the gelatin, the aspirator did not have enough suction to remove the fibrin gel from inside the wound, likely due to the fibrin's higher density.

The final method for inducing a wound in the 3D model involved outlining the wound margins with the leather punch, loosening the edges of the wound with a scalpel, and removing the fibrin gel left inside the wound margins with forceps. While this method proved to be the most effective, it maintained some limitations. The use of the scalpel resulted in slight scratches around the edges of the wound margins. While helpful for cell adhesion on the bottom of the plate, these scratches were inconsistent among samples and therefore introduced variation into the experiments. Additionally, at times, the wound margins were not completely loosened by the scalpel, resulting in minor tears and subsequent changes in wound shape when the inner part of the gel was removed with forceps.

5.4.7 3D Gel Indentation Testing

Previous literature has demonstrated that cell-seeded fibrin gels stiffen over time due to cell proliferation, spreading, and contraction within the gel (Duong et al. 2009). Duong demonstrated fibrin gel stiffness could be modulated and measured using a flat punch indentation method. The team hypothesized an observable difference in change in stiffness over time between cEDS dermal fibroblast seeded gels and NHF seeded gels. The team first developed and verified an indentation material testing method, fixture, and analysis method before validating the cell seeded fibrin hydrogel model.

The team adapted the indentation method from Duong et al. (2009) below in **Figure 28**. A custom cylindrical flat punch fixture with a 6 mm diameter was displaced into the sample of interest contained within an 18mm diameter well of a 12 well plate at a fixed rate of 2 mm/min until 2 mm of displacement was achieved.

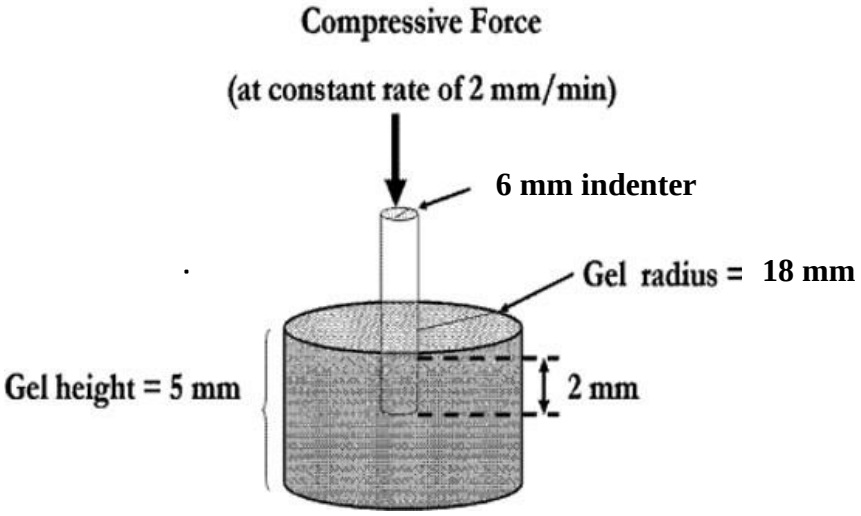

Figure 28. Schematic of the soft gel indentation testing method adapted from Duong, H., Wu, B., & Tawil, B. (2009). Modulation of 3D Fibrin Matrix Stiffness by Intrinsic Fibrinogen–Thrombin Compositions and by Extrinsic Cellular Activity. *Tissue Engineering Part A*, *15*(7), 1865–1876. https://doi.org/10.1089/ten.tea.2008.0319

Initial testing was performed on acellular fibrin gels using an Instron 34SC universal testing system with a 200N load cell. The lower grip of the Instron was removed, and a 12-well plate was taped to the frame of the Instron. Initially, a 3M drill bit was placed in the grips and the flat end was used as a test fixture, as can be seen in **Figure 29**. Data obtained from this initial test was void as the forces experienced were not properly measured by the load cell.

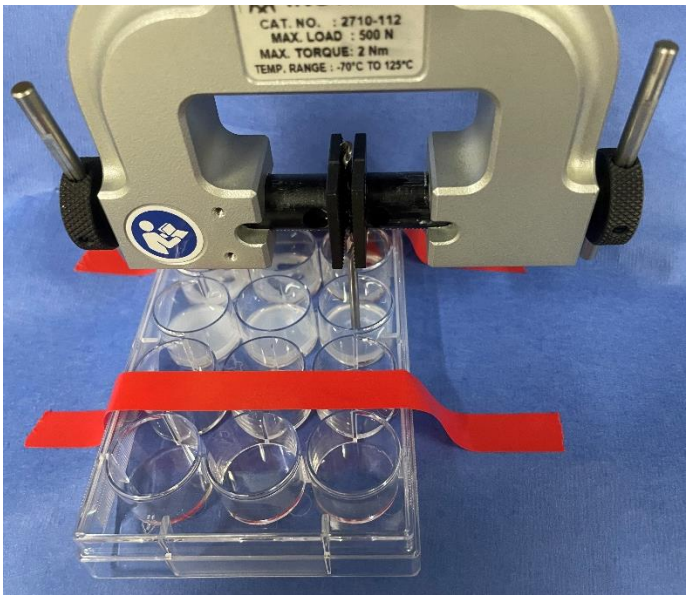

Figure 29. Instron fixture used during the first acellular indentation test.

Indentation testing was transitioned to utilize the CellScale UniVert S mechanical tester to take advantage of the 2.5N load cell. CellScale load cells have a lower limit of 0.02% so loads as low as 0.0005 N can be recorded. Multiple iterations of a custom indentation fixture were created. Initial designs were sketched as seen in **Figure 30** and the team enlisted the help of Ian Anderson in the Goddard Hall machine shop to CNC machine an aluminum flat punch fixture as seen in **Figure 31**. The cylindrical fixture was secured to the 2.5N load cell with a 3M screw. The fixture has a diameter of 6 mm. This size was intentionally chosen to maintain the same indent area-to-sample-area ratio of approximately 2 reported in Duong et al. (2009) despite use of a 12-well plate instead of a 24-well plate.

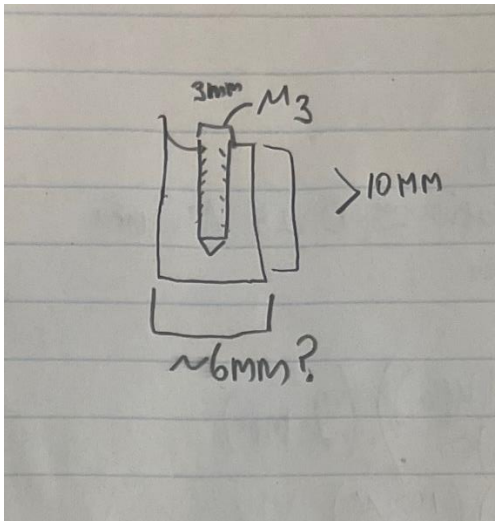

Figure 30. Initial sketch of flat punch indentation fixture.

Figure 31. Final aluminum flat punch indentation fixture.

Verification of the indentation method was performed using an acellular 5 mg/mL fibrin gel. The gel was prepared in a 12-well plate as previously described. To ensure sufficient sample thickness, the volume of the gel was doubled from one mL to two mL. The gel surface was then covered in 1 mL of complete media and left overnight in a 37˚C incubator. Following refrigeration, the well plate was taped to an aluminum block which served as a lower fixture that elevated the well plate. The 2.5N load cell and flat punch fixture were secured finger tight

according to the CellScale manufacturer instructions. The complete set up can be seen in **Figure 32**.

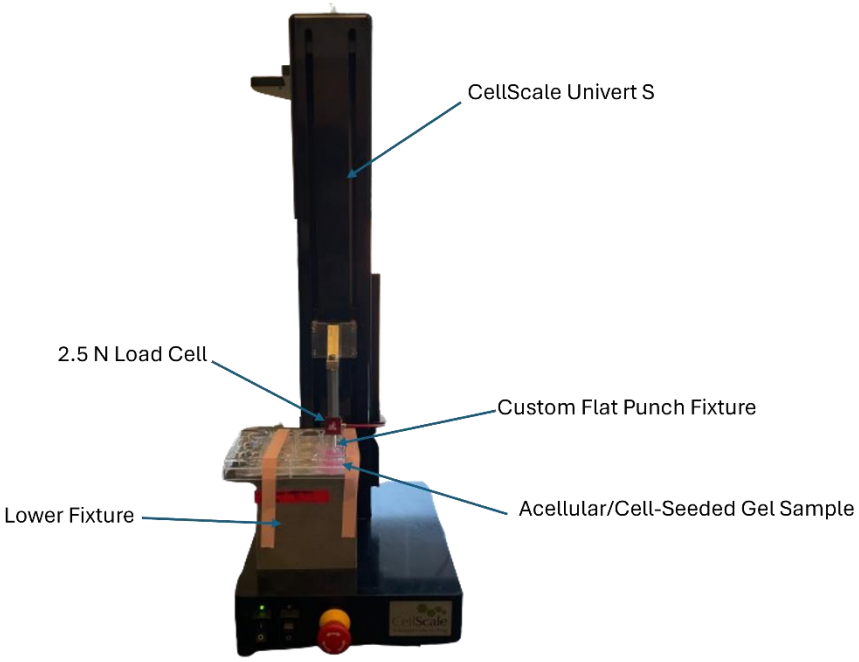

Figure 32. Indentation material testing set up.

The fixture was lowered using the manual jog buttons in the UniVert software until the face of the fixture contacted the surface. A custom displacement-controlled test method was defined and run in the UniVert software to provide a compressive load at 2 mm/min until a maximum displacement of 2 mm was achieved. The fixture then unloaded and recovered the total displacement at a rate of 2 mm/min upwards. Displacement of the fixture into the gel prior to recovery can be seen in **Figure 33**.

Figure 33. Fixture displacement into the acellular fibrin gel prior to recovery.

Load vs. displacement data was recorded and saved in an Excel spreadsheet. The team utilized the Oliver-Pharr method of indentation analysis, because it is widely used for soft material testing to accurately measure the structural modulus of materials (Zhang, 2022). Load vs. displacement was plotted as seen in **Figure 34** to fit a curve to the unloading region.

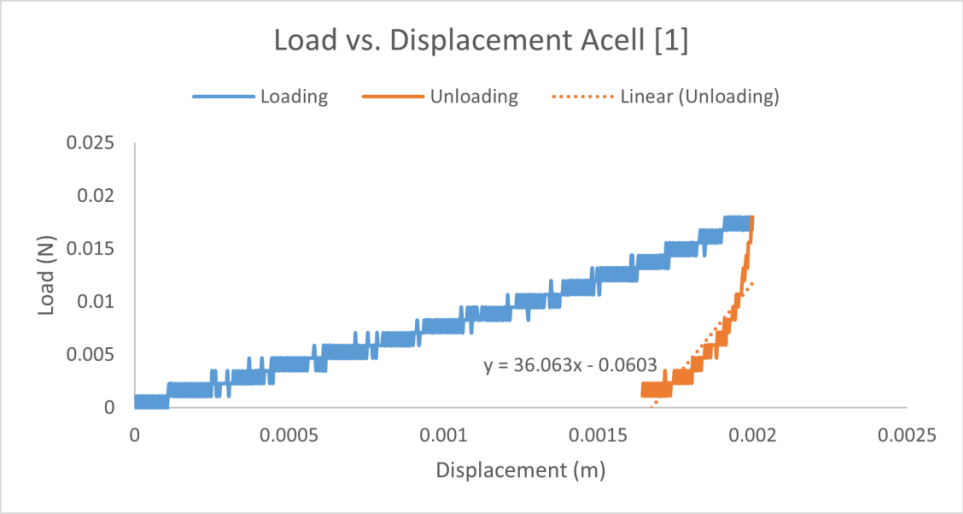

Figure 34. Load vs. Displacement plot for acellular 5 mg/mL fibrin gel at 2 mm/min.

The Oliver-Pharr method was used to determine the structural modulus of the fibrin gel. This can be done using the following two relations:

$$E_r = \frac{\sqrt{\pi}}{2\beta}\frac{S}{\sqrt{A}}$$

$$\frac{1}{E_r} = \frac{1-v^2}{E} + \frac{1-v_i^2}{E_i}$$

Where E_r is the indentation or reduced modulus, S is the measured stiffness, β is a geometric constant according to the indenter geometry, and A is the contact area. Additionally, v is the Poisson's ratio of the indenter, E is the structural modulus of the indenter, v_i is the Poisson's ratio of the sample, and E_i is the structural modulus of the sample. To use these relations, the elastic contact stiffness of the material must be known. The elastic contact stiffness is the slope of the fitted curve of the unloading region at the maximum displacement, h_{max}, as seen in the following equation:

$$S = \left(\frac{dP}{dh}\right)_{h=h_{max}}$$

where P is the applied load and h is the measured displacement. The unloading region of the plot was fitted to a curve according to the following equation:

$$P = B(h - h_f)^n$$

where B is a fitted constant, n is a geometric constant based upon the geometry of the indenter and h_f is the fitted residual indentation depth. In the case of the cylindrical flat punch $n = 1$ and the fitted curve of the unloading region was linear. Finally, in the case of a flat punch the contact area A remains consistent throughout the entire loading and can be calculated using the following equation:

$$A = \pi a^2$$

where a is the radius of the indenter. An example written analysis of the structural modulus can be found in **Appendix J** and an acellular example calculation is summarized in **Table 49**.

Table 49. Relevant Oliver-Pharr analysis values.

Physical Property	Variable	Value
Contact Area	A	$2.83 \times 10^{-5}\ m^2$
Elastic Contact Stiffness	S	$36.063\ N/m$
Indentation/Reduced Modulus	E_r	$6.01\ kPa$
Sample Structural Modulus	E_i	$5.63\ kPa$

Initial indentation testing yielded a structural modulus of 5.63 kPa for an acellular 5 mg/mL fibrin gel. This value falls within reported values for structural modulus values of a fibrin gel, between 0.5 kPa and 6 kPa found in Duong et al. (2009). The team noted this value is more

consistent with higher concentrations of fibrin gel but found the value to be within a reasonable range. This verified the test fixture and method as being capable of successfully measuring the structural modulus of a soft gel material.

After verification of the test method, the team reproduced the procedure and analysis methods on additional acellular samples, NHF seeded gel samples, and cEDS cell seeded samples. All gels were created as previously described at a final concentration of 5 mg/mL fibrin and cellular gels were seeded with 200k cells. Previous literature has suggested this was an optimal cell count to observe gel stiffening (Duong et al., 2009). Gels were tested on days one and four post-polymerization. New samples were tested each day as gels were considered non-viable after indentation due to plastic deformation and open-air contamination. To conserve materials, acellular gels were only tested on day one to establish a baseline as previous literature has demonstrated acellular gels do not exhibit the same stiffening effect over time (Duong et al., 2009). Gels for day 4 were created with residual material, however creation of valid samples was unsuccessful.

Acellular gels tested on day one were found to have an average structural modulus of 5.97 ± 0.47 kPa. Day one NHF and cEDS cell seeded gels both exhibited greater stiffness than the acellular with calculated average structural moduli of 7.00 ± 0.96 kPa and 10.23 ± 2.67 kPa respectively. By day four, both NHF and cEDS seeded gels exhibited an increase in average structural modulus as expected, 7.63 ± 0.90 kPa and 11.31 ± 3.33 kPa respectively. These results are summarized in **Figure 35** and examples of calculations and raw load vs. displacement graphs can be found in **Appendix K.**

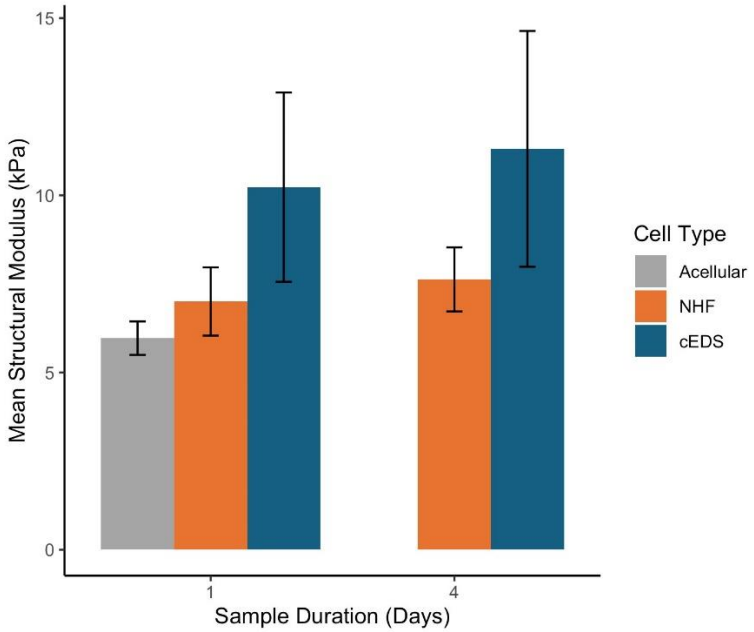

Figure 35. Structural modulus values of acellular, NHF, and cEDS cell seeded gels reported in kPa, n=2

Despite the observable difference, there were no statistically significant differences between experimental groups or across days within an experimental group. Two-sample t-tests assuming unequal variances for each group comparison (acellular vs. cEDS, acellular vs. NHF, and cEDS vs. NHF) on day one were calculated, with no significance found between any of the groups (p-values ranging from .257 to .346). An ANOVA was calculated for day one results, with no significance found ($F(2,3)= 3.58$, p=.161). A two-sample t-test assuming unequal variance comparing cEDS and NHF groups on day four was calculated, with no significance found (p=.349). Two-sample t-tests assuming unequal variance comparing cEDS results from day one to day four and NHF results from day one to day four were calculated, with no significance found (p=.756 and p=573, respectively). The team did note the much larger variability in cEDS seeded gel structural modulus when compared to the NHF seeded or acellular gels.

5.5 Experimental Contribution to Final Design

Each experiment in the team's preliminary testing phase was focused on different elements of the design as well as the functional requirements needed for a wound healing model. Together, these informed and validated each part of the team's final design: the well plate mask, cEDS patient-derived cells, three-dimensional fibrin gel model, and sterile punch for wound induction.

The well plate mask was custom fabricated to allow the model to be imaged in the same part of the well each time. The cell count assay was conducted to obtain a baseline of cellular behavior, evaluating the difference in cell population and growth over time between the control and cEDS experimental cells. The monolayer scratch assay was used to quantify cell outgrowth and movement of experimental and control cells into a wound margin in a two-dimensional setting. The wound induction template created by the team was used initially in the monolayer scratch assay to verify its usefulness for aiding in consistent wound induction and location of wound margin for imaging. Moving to 3D models, a fibrin dot outgrowth assay was conducted to evaluate the outgrowth of cells from a dot located within the center of a well plate. This is critical because our team needed to observe the behavior of cell growth within a three-dimensional environment. The fibrin hydrogel was then mechanically tested in order to investigate how the control and experimental cell-seeded gels differed from acellular gel. In order to verify that a wound could be induced in the fibrin hydrogel, punch prototyping was completed, in which a sterilizable rectangular punch was identified as the most promising option.

All together, these experiments lead to the team's final design: a three dimensional fibrin hydrogel seeded with cEDS dermal fibroblasts with a punch-induced wound.

6.0 Final Design and Validation

The team's final wound healing model design consisted of cEDS patient-derived dermal fibroblasts seeded into a fibrin gel composed of 5 mg/mL fibrinogen, 1.5 U/mL of thrombin, and 40 mM $CaCl_2$ prior to the addition of 100,000 cells in 200 µL of DMEM with 20 µg/mL aprotinin. The cell-seeded gel was created in a 12-well plate, allowed to polymerize for 30 minutes, and then covered with 1mL complete DMEM media with of 10% FBS and 20 µg/mL recombinant bovine-lung aprotinin. After incubating the cell-seeded fibrin gel for 24 hours, a sterile leather punch measuring 15mm by 6mm with a rounded rectangular shape was pressed into the gel to form a wound and the gel was removed using a scalpel and forceps.

This model represents a combination of the team's previous wound healing experiments and 3D fibrin hydrogel experiments. After the initial wounding of the model, gels were imaged daily until they degraded. Outgrowth of cEDS cells from the wound margin was observed beginning on day 2, with continued growth observed through day 4. Cell death and gel degradation were observed on day 6. No data from NHF models was obtained because of time constraints.

6.1 Final Wound Healing Model is Representative of cEDS Function

The model's function to be representative of EDS cell functions was supported by various specifications used to guide our team's device design. These included dermal fibroblast proliferation and migration rates that are 1/3 the rate of unaffected dermal fibroblast behavior. Similarly, the duration of full wound closure in cEDS fibroblasts was specified to be twice as long as the healing duration of full wound closure within unaffected fibroblast healing. Regarding structural properties and mechanical integrity, the specified elastic modulus of the model material was to be within a range of 5 to 20 MPa (Duong et al., 2009).

Based on cell count and monolayer scratch assay testing, it was found that the initial growth of cells within a plate over a course of 5 days exhibited a difference in cell population over time when comparing the control and experimental samples. Per day, there was a 20.2% increase in the change in cell count of NHF samples compared to cEDS samples, suggesting that the team's hypothesis that cEDS fibroblasts grow and populate a wound at a slower rate than unaffected fibroblasts was reasonable. The conducted monolayer assay observed an 80% wound closure over the duration of 24 hours, with higher variability seen in cEDS samples compared to NHF samples. While fluctuations in percentage wound closure were observed from hour 6 to 20, the final wound closure area remained similar at approximately 80%, which was not expected based on prior literature (Figure 21). No statistical significance was reported between cell types in the cell count assay (proliferation study). Statistically significance was observed between NHF and cEDS wound margins in the scratch assay from hours 0 through 16, but were not statistically after the 16 hour time point.

The main obstacle the design team faced with meeting our specification requirements was meeting the initial predicted values for the cEDS fibroblasts behavior in comparison to NHF cellular behavior. These specifications for the model to be representative of cEDS cell function were developed based on prior literature and observation of cEDS migration and proliferation data. However, our team believes that by incorporating pathogenic cEDS dermal fibroblasts within the model as the experimental sample, this serves to represent accurate cEDS cell function, even though the observed behavior of cEDS cells did not meet the proliferation, migration and outgrowth specifications hypothesized in our specfications. Furthermore, variability in cell behavior is a component that will be further observed to develop additional conclusions of cEDS cellular behavior in comparison with unaffected dermal fibroblasts. The

experiments and results of the cell count assay and monolayer scratch assay are discussed above in **Section 5.4.2 and Section 5.4.3**, respectively.

6.2 Final Wound Healing Model Allows for Efficient Imaging Over Time

The function for evaluating the ability of the model to be effectively imaged over time throughout the course of the study was to successfully image the wound margin to the nearest 0.1 mm, visualized with a 40x objective with a minimum of 80% clarity, and effectively image twelve models in under 1 hour.

Using standard Zeiss brightfield microscopy, our team was able to measure all samples using all objective lenses up to 40x magnification, in which cells, each gel, and the resulting wound margins were visualized with a 100-micron scale bar, using the 10x magnification lens. This allowed our team to evaluate the individual cell within each wound model. In addition to this, each image was successfully imaged with adequate clarity, in which exact wound margins, cells, and edges of the gel were visualized for further analysis.

During experimentation, our team was successful in imaging more than 18 wells within an hour, including scratch assays, fibrin dot assays, and the final punch models. The imaging and analysis processes for each set of experiments are further discussed in Section 5.4.1 through 5.4.5.

6.3 Fabrication Analysis

The team's evaluated function to allow accurate and efficient fabrication of the model was accomplished over the study. This was measured through specifications describing that the model can be replicated with 80% precision at least ten times, requiring a maximum of five components to assemble, duration of model formation takes a maximum of one week, and wound

induction taking less than two minutes per sample. Furthermore, the model production and regular care should require a single scientist and only require care less than once per 24 hours.

The final gel model, as explained in Section 6.0 was developed using five overall components, consistent with our specifications. These components include the (1) 12-well plate, (2) fibrin gel, (3) seeded NHF or cEDS fibroblasts, (4) leather punch for wound induction, and (5) acrylic template placed below the well plate. While the fibrin gel was composed of a solution of $CaCl_2$, thrombin, and fibrinogen before the addition of the cell samples, adding to the overall number of components, there were only 5 total components that needed to be developed for a successful gel punch wound healing model.

Due to the use of a defined protocol for gel production, sterile leather punch as the method of wound induction, and an acrylic template for consistent wounding and imaging, 80% precision in both generating an overall gel model and inducing a wound was successful. Scratch wounds using a 200 µL pipette tip and punches using the metal stamp were made using the acrylic template, in which the wounds were cleanly made through the center of each well and were relatively consistent among all samples. Overall development of the model took an average of 25 hours. This time was composed of the initial 30 minutes after combination of the solution for gel polymerization, 24 hours for the cells to settle and integrate within the gel, and the final wound induction before analysis, which was estimated to take 2 minutes per sample to punch, consistent with our team's specifications.

Limitations in this study for final model development involve the use of the punch wound method. As human error is involved, complete consistency and precision among all models was not observed, even though the stamp remained the same.

6.4 Viability and Useability Analysis

The function of integrating both standard and easily available materials and equipment was successful in our team's development of a final wound healing model. Specifications for this included obtaining materials within two weeks, having the ability for the model to fit in a well plate with 22.8 mm diameter wells, and ensuring that the model can be incubated at 37°C and 5% CO_2 with zero non-standard specifications for the chosen incubator.

Components such as calcium chloride, cell culture medium (DMEM), and general laboratory supplies including pipettes, pipette tips, microscopes, cell culture flasks, and well-plates were supplied through the Biomedical Engineering Department at Worcester Polytechnic Institute and were obtained within one week. For components such as cEDS patient-derived dermal fibroblasts, fibrinogen, and aprotinin, order approval processes and shipping took a maximum of two weeks per item, accomplishing the team’s proposed specification. Our final model was successfully integrated within a 12-well plate with 22.8 mm diameter wells and incubated at the desired specifications. The well plates were then only removed from the incubator for a medium exchange, imaging under the microscope, at the end of designated study, or if the cells observed any degradation or contamination.

7.0 Discussion

7.1 Final Device Analysis

The final wound healing fibrin gel model of Ehlers-Danlos Syndrome proved to be an effective proof of concept design to represent pathological classical Ehlers-Danlos Syndrome pathology. Wounds were successfully induced using a leather punch and imaged at 24-hour increments until the end of the study, in which outgrowth from the cEDS gels was evaluated starting at day 2 and further progressing until final gel degradation at day 6. Gel wound induction

via a leather punch was effectively induced in each model with varying levels of consistency due to human error.

Further analysis and optimization of the device will be an accurate way to observe disease pathology regarding wound healing, as well as to evaluate novel pharmacological therapeutics for treating this condition. Limitations observed within the final gel model sample include the behavior of gel degradation and sample contamination. These challenges were difficult to overcome, as many of our studies were designed to be observed for 10 days to 21 days for cellular outgrowth and indentation testing, respectively.

7.2 Gel Structural Properties

Based on the results reported in **Section 5.4.6**, the team noted stiffer cEDS cell seeded gels than control NHF seeded gels and acellular gels. Gels seeded with cEDS cells also exhibited greater variability in structural modulus compared to control NHF seeded gels and acellular gels. Additionally, the team saw the expected stiffening effect of seeded gels. These results did not reach statistical significance due to limited sample size and limited duration of the study. The team believes significance may have been found if more samples were run, and for longer durations. Previous literature suggested the stiffening effect of cell seeded fibrin gels is due to cell growth and proliferation within the gel (Duong et al., 2009). Based on this, the team believes the differences in structural modulus between cell types can be attributed to cell distribution within the gels. However, this result is inconsistent with previous findings and the initial hypothesis. Greater cell count leads to a stiffer gel, therefore the cEDS gels were expected to exhibit lower stiffness due to decrease cell proliferation within the gel (Duong et al., 2009).

There are a few possible explanations for the stiffer and more variable cEDS seeded gels. First, the phenotype of the seeded fibroblasts could contribute varying structural support.

Although the NHF and cEDS cells are both fibroblasts, phenotypic differences of cells at the cytoskeleton or microscale could contribute varying support to the gel. Alternatively, it has been hypothesized the decreased elasticity found in cEDS skin is a result of the altered collagen fibers and not the fibroblast structure (Royer & Han, 2022). Classical EDS fibroblasts have been shown to exhibit a phenotypic change when returned to a more stable collagen matrix and it is possible suspending the cEDS fibroblasts in a fibrin matrix restored mechanobiological cues based on the material properties of the fibrin with little effect from the cell type suspended in the gels (Royer & Han, 2022). Royer & Han (2022) suggests the previously reported lack of mechanical integrity of cEDS skin could be a key player in impaired wound healing and the team believes our findings of stiffer cEDS seeded fibrin gels may provide insight into the mechanobiology of wound healing in cEDS. With further testing and more replicates, it is believed these preliminary findings will contribute to a statistically significant distinction between NHF control seeded gels cEDS seeded gels to help inform further research. Additionally, future studies should incorporate ascorbic acid in the media to promote remodeling and collagen deposition in the 3D matrix. This would allow for greater analysis of cEDS fibroblast collagen synthesis and structural affects of a defective collagen matrix.

7.3 Impact Analysis

7.3.1 Economics

The team's *in vitro* 3D fibrin gel model creates a unique system for researchers, physicians, and industry professionals to study wound healing in Ehlers Danlos Syndrome without needing to use an animal model. This reduces model costs, allows for higher throughput testing, and improves accessibility to a wound healing model. In industry, this model could help reduce the cost of testing treatments for poor wound healing, allowing the product to be

extensively tested *in vitro* before being tested *in vivo*. Additionally, there is not currently a lot of research being done on wound healing in classical Ehlers Danlos Syndrome, as it is a rare condition. However, this model would allow smaller labs and less well-funded companies to do this research, as it is significantly less expensive than an animal model and uses easily obtainable materials and equipment.

On average, patients with Ehlers-Danlos Syndrome and other rare diseases experience healthcare costs ranging between 1.5 to 23.9-times more than patients without rare diseases (Bogachkov, 2021). Between 2006 and 2020, costs per patient per year for those with rare diseases nationwide cost between $8,812 to $140,044, compared to $5,862 for the control group (Bogachkov, 2021). There is a need for treatments, and thus models, that will represent this condition and have the potential to be used for therapeutic evaluation. With use of this model advancing wound healing treatment options for people with cEDS, patient medical costs may be reduced due to more effective treatment options.

7.4.2 Environmental Impact

The model must be cultured in a sterile environment, which leads to negative environmental effects. Because sterility must be maintained, many lab supplies used to care for the models (including well plates, pipette tips, and glass pipettes) are single use items that are not recyclable due to being biohazards, such as plastics or glass that have been in contact with cellular components or hydrogel model. The use of many non-recyclable lab supplies creates plastic waste; however, autoclavable reusable lab supplies could be used to reduce this environmental impact. Additionally, the biosafety cabinet requires electricity to operate, and the incubator requires a supply of CO_2 and constant electricity. There are currently no alternatives

for these pieces of equipment that would reduce the environmental impact of the model, but alternative energy sources may be considered to provide sustainable electricity.

Furthermore, the use of various biomaterials such as fibrin, cellular components such as the cEDS patient-derived dermal fibroblasts and NHF samples, and culture reagents including DMEM, FBS, GlutaMax, and Penicillin-Streptomycin have various environmental impacts depending on the sourcing and type of material. This may be due to materials sourced from animals and antibiotics, which have ramifications in both production and waste processes.

7.4.3 Societal Influence

This model will allow research on wound healing in cEDS patients to be advanced and better treatment options to be developed for wounds. This will positively impact the cEDS patient community, allowing them to spend less time, money, and mental effort tending to their wounds. Specifically, better treatment options will allow patients to save money on physician appointments as well as less time spent off from work, which disrupts the typical income flow. Additionally, this model could be easily adopted for other diseases that affect collagen synthesis or wound healing, positively impacting research and patient populations for other conditions as well. Furthermore, this model will provide an opportunity to provide better treatments for patients that are limited in their options for wound healing treatments. Increase in these individuals' quality of life through an increased understanding of wound healing pathology and resulting treatments can be observed in an improved wound healing treatment, more effective rehabilitation period, and overall costs associated with their treatments.

7.4.4 Political Ramification

The results of high costs of model development for both *in vivo* and *in vitro* experimentations remain a large consideration globally in both research and therapeutic testing.

This engineered model may reduce wound model costs, benefiting the global market for therapeutic testing. Additionally, by increasing accessibility to a wound healing model for a rare condition, the project may bring awareness to rare conditions and possibly spark additional infrastructure to support rare disease research.

7.4.5 Ethical Concerns

Regarding the ethical considerations of an *in vitro* 3D fibrin gel model with seeded human dermal fibroblast cells or classical Ehlers-Danlos Syndrome cells, the concern lies within the potential use of such a model more so than the specific model itself. An *in vitro* model that would aid to accurately represent the wound healing and properties of classical Ehlers-Danlos Syndrome serves to promote an increased understanding of the disease pathology and begin the development of a viable testing method for pre-clinical surgical incision or therapeutic testing. This model may additionally be modified with different cells and thus be able to represent different dermal disease pathologies.

An ethical concern lies within the use of bovine-sourced fibrin gel as well as the fetal bovine serum (FBS) used within the medium. There are possibilities to obtain FBS from companies that aim to limit the use of animal products and testing. However, this model provides an alternative to currently used animal models within EDS research. Furthermore, this model increases efficiency in limiting the number of clinical trial participants and potential consumers involved in disease research studies and wound healing studies. An additional ethical concern is noted within the topic of using patient cells; using a patient's own cells would result in a personalized wound healing model, however the cell sourcing may be a potential ethical concern through the observation of replicating the dermal tissue.

In addition to this, ethical concerns for human and patient interaction using cells to mimic dermal tissue can be mitigated using patient consent forms for initial approval to use the cells, as well as data protection from the resulting gel wound healing model.

7.4.6 Health and Safety Issue

If lab safety requirements are adhered to, this engineered model does not pose a health or safety risk to researchers working with it. There is a slightly elevated risk of laceration due to the use of sharp tools, but this can be avoided by attentive handling of the tools. Additionally, because sterilization processes are required for proper model function, there is minimal risk of model contamination causing harm to the researcher. This model is not intended for patient interaction, and therefore will not cause any negative health or safety impacts on patients. In fact, because the model may be used for pre-clinical testing of wound healing treatments, it may minimize negative impacts of these tests on patients by serving as an additional verification step for treatments before they are tested on humans.

7.4.7 Manufacturability

This 3D wound model is easily reproducible, following the team's clearly defined methods for creating fibrin gels seeded with cEDS dermal fibroblasts, inducing a wound, imaging areas of interest using a well plate mask, and performing 3D gel indentation testing. This reproducibility is visualized through the ability for the cells to be passaged and applied within the model, obtaining multiple thrombin and fibrinogen aliquots from a single bottle, as well as for the protocol to be consistently conducted over time. To scale the team's design up for high-throughput manufacturing, automating parts of the process or creating larger models may be considered.

The cost to specifically manufacture this device has been considered. While not within the top ranked objectives, the team aims to reduce the price of a wound healing model for research and therapeutic testing in comparison to those currently offered in the market. Many current costs for monolayer scratch assays average at approximately $330 for tests such as a cell comb scratch assay (Millipore, 2024). *In vivo* animal models, while effective in evaluating wound healing on a live specimen, can be extremely expensive to produce and overall be a long experimentational process. The model itself can range between $850 to $1,800 (Stone, 2012). However, to represent a particular disease pathology, genetic modification of the models must occur for accurately representing the wound response, resulting in additional costs up to $5,250 for the genetic editing of a transgenic mouse (Yale Genome Editing Center, n.d.). The cost to create one of the 3D *in vitro* wound healing models is about $27.23, including the one-time cost of purchasing the leather punch tool for wound induction. This is lower than both *in vivo* and *in vitro* wound models mentioned, however common lab supplies such as media, media supplements, and cell culture materials were not included in this cost calculation. The full breakdown of model cost and materials purchased is in **Appendix M.**

7.4.8 Sustainability

Two components of the wound healing model must be considered for sustainability. The fibrinogen and thrombin used in the model must be sourced from animals, which impact the environment to raise but are a renewable resource. Additionally, the energy used to sustain the biosafety cabinet, incubator, and other lab equipment may be created from fossil fuels but can be produced using renewable energy sources, such as wind.

An additional design element that makes this model sustainable within a laboratory setting is the overall use of a 3D model that consists of a fibrin matrix. Since this model design

allows for researchers to change the type of cells that are applied within each model for the evaluation of wound healing, this can be applied to further research beyond neonatal human and classical Ehlers-Danlos Syndrome dermal fibroblasts.

7.4.9 Industry Standards

For the team's well plate mask, which was drawn up using Solidworks, a built-in feature was used to ensure that the design met all ISO standards for dimensional specificity. For model therapeutic development, there are multiple ISO, ASTM, and FDA standards required for final development and commercial distribution of the model. For the general requirements for transportation of cells for therapeutic use, the model process must follow ISO standard 21973, and ISO 23033 will observe the requirements for both the testing and characterization of cellular therapeutic products, which may be involved for testing therapeutics on the models (*Standards Development for Regenerative Medicine Therapies*, 2023). Furthermore, the ASTM F2739 standard supports the quantification of cell viability within biomaterial scaffolds. ISO 10993 evaluates biological components of medical devices and must be followed throughout the study as well (*Use of International Standard ISO 10993-1, "Biological evaluation of medical devices – Part 1: Evaluation and testing within a risk management process"*, 2023).

8.0 Conclusions and Recommendations

Using the results obtained through extensive testing of cell behavior and outgrowth using both 2D and 3D modeling, our team developed an effective proof of concept design for a three-dimensional *in vitro* wound healing model of Ehlers-Danlos Syndrome. The model met the functional requirements of being efficiently imaged, accurately and efficiently fabricated, and allowed for integration of standard materials and equipment. While the model did not meet the initial functional specifications for being representative of cEDS pathology, we believe that

using cEDS cells within the model allowed for accurate representation of pathology regardless of unmet specifications. The model costs $27.23 to manufacture, compared to *in vivo* models mentioned in **Section 7.4.7** which can range between $1,800 - $5,250. The model is additionally 3D, ensuring more complexity than similar 2D wound healing models. The model allows for testing of pharmacological treatments specialized for cEDS, is easily imageable and replicable, and represents some characteristics of complex cEDS pathology (such as 3D structure) while still remaining an *in vitro* model.

In the future, more testing could be conducted to further validate the design. While the team was able to successfully observe outgrowth of cEDS cells onto the 2D well plate from the punch wound in the final fibrin wound model, there was no control model with NHFs to compare against the pathological cEDS model. If comparisons can be made between NHF and cEDS *in vitro* seeded 3D wound models, we believe that a statistical significance between the outgrowth, proliferation, and migration of pathological (cEDS) and unaffected (NHF) cells may be observed. Supplemental experiments may also be repeated in hopes of observing statistical significance, including in the cell count assay, fibrin dot assay, and indentation testing.

It was observed that cEDS seeded gels degrade at a faster rate than NHF seeded gels. This led the team to suspect that there may be overexpression of proteases in cEDS cells, since proteases can break down fibrin clots resulting in their disintegration. In the future, it may be beneficial to monitor protease activity in pathological and unaffected cells using a fluorescent labeled substrate. Understanding protease activity can allow for better prevention of gel degradation, which was observed despite the introduction of aprotinin, which acts as a protease inhibitor. Preventing degradation will allow for experiments to run for between 10-21 days,

providing more data at later time points to observe long term proliferation, migration, and outgrowth.

Inconsistencies between punch wounds were observed across replicates. An automatic induction tool should be created/used in future punch wound induction. Ensuring consistency amongst replicates will allow for direct comparison of the same locations within a punch wound between multiple wound models. This consistency can be achieved by creating some sort of automatic machine that can be placed over the well plate in the same location for each well, with a punch wound that allows for consistent removal of excess gel within the punch site.

Analysis of images across all experiments was conducted manually with the aid of ImageJ with analysis completed three times by three different team members to calculate average cell counts and wound margin areas. It is recommended that in the future, a macro script is utilized to rapidly analyze multiple images in a scientific image analysis software such as ImageJ, CellProfiler, or MATLAB. This will decrease time spent on image analysis and allow for more experiments to be run and analyzed.

It is believed that with these modifications, the wound healing model will be a representative 3D *in vitro* wound healing model of complex classical Ehlers-Danlos syndrome pathology while being imageable, easy to replicate, and less expensive than *in vivo* research models.

References

Agarwal, A., McAnulty, J. F., Schurr, M. J., Murphy, C. J., & Abbott, N. L. (2011). 8 - Polymeric materials for chronic wound and burn dressings. In D. Farrar (Ed.), *Advanced Wound Repair Therapies* (pp. 186–208). Woodhead Publishing. https://doi.org/10.1533/9780857093301.2.186

Agarwal, A., McAnulty, J. F., Schurr, M. J., Murphy, C. J., & Abbott, N. L. (2011). 8 - Polymeric materials for chronic wound and burn dressings. In D. Farrar (Ed.), *Advanced Wound Repair Therapies* (pp. 186–208). Woodhead Publishing. https://doi.org/10.1533/9780857093301.2.186

Almadani, Y. H., Vorstenbosch, J., Davison, P. G., & Murphy, A. M. (2021). Wound Healing: A Comprehensive Review. *Seminars in Plastic Surgery*, *35*(3), 141–144. https://doi.org/10.1055/s-0041-1731791

Andersen, T., Auk-Emblem, P., & Dornish, M. (2015). 3D Cell Culture in Alginate Hydrogels. *Microarrays*, *4*(2), 133–161. https://doi.org/10.3390/microarrays4020133

Anil, S., Sweety, V. K., & Joseph, B. (2023). Marine-Derived Hydroxyapatite for Tissue Engineering Strategies. In F. R. A. Maia, J. M. Oliveira, & R. L. Reis (Eds.), *Handbook of the Extracellular Matrix: Biologically-Derived Materials* (pp. 1–26). Springer International Publishing. https://doi.org/10.1007/978-3-030-92090-6_60-1

Azmat, C. E., & Council, M. (2023). Wound Closure Techniques. In *StatPearls*. StatPearls Publishing. http://www.ncbi.nlm.nih.gov/books/NBK470598/

Baik, B. S., Lee, W. S., Park, K. S., Yang, W. S., & Ji, S. Y. (2019). Treatment of the wide open wound in the Ehlers-Danlos syndrome. *Archives of Craniofacial Surgery*, *20*(2), 130–133. https://doi.org/10.7181/acfs.2018.02334

Barh, D., Chaitankar, V., Yiannakopoulou, E. C., Salawu, E. O., Chowbina, S., Ghosh, P., & Azevedo, V. (2014). In Silico Models. *Animal Biotechnology*, 385–404. https://doi.org/10.1016/B978-0-12-416002-6.00021-3

Biju, T. S., Priya, V. V., & Francis, A. P. (2023). Role of three-dimensional cell culture in therapeutics and diagnostics: an updated review. Drug Delivery and Translational Research, 1–15. https://doi.org/10.1007/s13346-023-01327-6

Bogachkov, Y. Y. (2021, November 1). *NIH study: Cost of rare diseases "large" relative to other ills*. https://ehlersdanlosnews.com/news/nih-study-healthcare-costs-rare-diseases-large-relative-other-ills/

Braťka, P., Fenclová, T., Hlinková, J., Uherková, L., Šebová, E., Hefka Blahnová, V., Hedvičáková, V., Žižková, R., Litvinec, A., Trč, T., Rosina, J., & Filová, E. (2022). The Preparation and Biological Testing of Novel Wound Dressings with an Encapsulated

Antibacterial and Antioxidant Substance. *Nanomaterials*, *12*(21), 3824. https://doi.org/10.3390/nano12213824

Britto, E. J., Nezwek, T. A., Popowicz, P., & Robins, M. (2023). Wound Dressings. In *StatPearls*. StatPearls Publishing. http://www.ncbi.nlm.nih.gov/books/NBK470199/

Burcharth, J., & Rosenberg, J. (2012). Gastrointestinal Surgery and Related Complications in Patients with EhlersDanlos Syndrome: A Systematic Review. *Digestive Surgery*, *29*(4), 349–357. https://doi.org/10.1159/000343738

Chiarelli, N., Ritelli, M., Zoppi, N., & Colombi, M. (2019a). Cellular and Molecular Mechanisms in the Pathogenesis of Classical, Vascular, and Hypermobile Ehlers–Danlos Syndromes. *Genes*, *10*(8), 609. https://doi.org/10.3390/genes10080609

Cho, C.-Y., Chiang, T.-H., Hsieh, L.-H., Yang, W.-Y., Hsu, H.-H., Yeh, C.-K., Huang, C.-C., & Huang, J.-H. (2020). Development of a Novel Hanging Drop Platform for Engineering Controllable 3D Microenvironments. Frontiers in Cell and Developmental Biology, 8. https://www.frontiersin.org/articles/10.3389/fcell.2020.00327

Cho, H., Won, C. H., Chang, S. E., Lee, M. W., & Park, G. (2013). Usefulness and Limitations of Skin Explants to Assess Laser Treatment. *Medical Lasers*, *2*(2), 58–63. https://doi.org/10.25289/ML.2013.2.2.58

Cousins, S., Blencowe, N. S., & Blazeby, J. M. (2019). What is an invasive procedure? A definition to inform study design, evidence synthesis and research tracking. *BMJ Open*, *9*(7), e028576. https://doi.org/10.1136/bmjopen-2018-028576

De Ieso, M. L., & Pei, J. V. (2018). An accurate and cost-effective alternative method for measuring cell migration with the circular wound closure assay. *Bioscience Reports*, *38*(5), BSR20180698. https://doi.org/10.1042/BSR20180698

DeNigris, J., Yao, Q., Birk, E. K., & Birk, D. E. (2016). Altered dermal fibroblast behavior in a collagen V haploinsufficient murine model of classic Ehlers-Danlos syndrome. *Connective Tissue Research*, *57*(1), 1–9. https://doi.org/10.3109/03008207.2015.1081901

Du, Y., Lo, E., Ali, S., & Khademhosseini, A. (2008). Directed assembly of cell-laden microgels for fabrication of 3D tissue constructs. *Proceedings of the National Academy of Sciences*, *105*(28), 9522–9527. https://doi.org/10.1073/pnas.0801866105

Duong, H., Wu, B., & Tawil, B. (2009). Modulation of 3D Fibrin Matrix Stiffness by Intrinsic Fibrinogen–Thrombin Compositions and by Extrinsic Cellular Activity. *Tissue Engineering Part A*, *15*(7), 1865–1876. https://doi.org/10.1089/ten.tea.2008.0319

Ehlers Danlos Society. (2023). Why do we need awareness? The Ehlers Danlos Society. https://www.ehlers-danlos.com/may-awareness/why-we-need-awareness/

Ehlers Danlos Support UK. (2022, January 1). *Classical Ehlers-Danlos syndrome*. Ehlers Danlos. https://www.ehlers-danlos.org/information/classical-ehlers-danlos-syndrome/

Enoch, S., & Leaper, D. J. (2008). Basic science of wound healing. *Surgery (Oxford)*, *26*(2), 31–37. https://doi.org/10.1016/j.mpsur.2007.11.005

Ericson, W. B., & Wolman, R. (2017). Orthopaedic management of the Ehlers–Danlos syndromes. *American Journal of Medical Genetics Part C: Seminars in Medical Genetics*, *175*(1), 188–194. https://doi.org/10.1002/ajmg.c.31551

Freedman, B. R., Hwang, C., Talbot, S., Hibler, B., Matoori, S., & Mooney, D. J. (2023). Breakthrough treatments for accelerated wound healing. *Science Advances*, *9*(20), eade7007. https://doi.org/10.1126/sciadv.ade7007

Fumarola, S., Allaway, R., Callaghan, R., Collier, M., Downie, F., Geraghty, J., Kiernan, S., Spratt, F., Bianchi, J., Bethell, E., Downe, A., Griffin, J., Hughes, M., King, B., LeBlanc, K., Savine, L., Stubbs, N., & Voegeli, D. (2020). Overlooked and underestimated: medical adhesive-related skin injuries. *Journal of Wound Care*, *29*(Sup3c), S1–S24. https://doi.org/10.12968/jowc.2020.29.Sup3c.S1

Gajbhiye, S., & Wairkar, S. (2022). Collagen fabricated delivery systems for wound healing: A new roadmap. *Biomaterials Advances*, *142*, 213152. https://doi.org/10.1016/j.bioadv.2022.213152

Gonzalez, A. C. de O., Costa, T. F., Andrade, Z. de A., & Medrado, A. R. A. P. (2016). Wound healing - A literature review. *Anais Brasileiros de Dermatologia*, *91*(5), 614–620. https://doi.org/10.1590/abd1806-4841.20164741

Grada, A., Mervis, J., & Falanga, V. (2018). Research Techniques Made Simple: Animal Models of Wound Healing. *Journal of Investigative Dermatology*, *138*(10), 2095-2105.e1. https://doi.org/10.1016/j.jid.2018.08.005

Greenfield, J. (2021, April). *Treatment for Ehlers-Danlos Syndrome | Brain & Spine Center*. https://weillcornellbrainandspine.org/condition/ehlers-danlos-syndrome-eds/treatment-ehlers-danlos-syndrome#:~:text=Treatment%20for%20Ehlers-Danlos%20Syndrome%20will%20depend%20upon%20the%20severity,not%20addressed%20by%20conservative%20treatment.

Grigoriev, T. E., Osidak, E. O., … Mironov, V. A. (2020). Magnetic levitational bioassembly of 3D tissue construct in space. *Science Advances*, *6*(29), eaba4174. https://doi.org/10.1126/sciadv.aba4174

Gunendran, T., & Uma Dwarakanath, N. (2023). The Analgesic Mismanagement of a Patient With Ehlers-Danlos Syndrome (Hypermobility Variant): A Case Report. *Cureus*, *15*(9), e45713. https://doi.org/10.7759/cureus.45713

Guo, S., & DiPietro, L. A. (2010). Factors Affecting Wound Healing. *Journal of Dental Research*, *89*(3), 219–229. https://doi.org/10.1177/0022034509359125

Gupta, A., & Kumar, P. (2014). Possible Simple Measures for Complex Wound Healing Problems in Ehlers-Danlos Syndrome. *Plastic and Reconstructive Surgery Global Open*, *2*(10), e241. https://doi.org/10.1097/GOX.0000000000000199

Health, C. for D. and R. (2023, September 7). *Use of International Standard ISO 10993-1, "Biological evaluation of medical devices - Part 1: Evaluation and testing within a risk management process."* https://www.fda.gov/regulatory-information/search-fda-guidance-documents/use-international-standard-iso-10993-1-biological-evaluation-medical-devices-part-1-evaluation-and

Hofmann, E., Fink, J., Pignet, A.-L., Schwarz, A., Schellnegger, M., Nischwitz, S. P., Holzer-Geissler, J. C. J., Kamolz, L.-P., & Kotzbeck, P. (2023). Human *In vitro* Skin Models for Wound Healing and Wound Healing Disorders. *Biomedicines*, *11*(4), 1056. https://doi.org/10.3390/biomedicines11041056

Holzer-Geissler, J. C. J., Schwingenschuh, S., Zacharias, M., Einsiedler, J., Kainz, S., Reisenegger, P., Holecek, C., Hofmann, E., Wolff-Winiski, B., Fahrngruber, H., Birngruber, T., Kamolz, L.-P., & Kotzbeck, P. (2022). The Impact of Prolonged Inflammation on Wound Healing. Biomedicines, 10(4), 856. https://doi.org/10.3390/biomedicines10040856

Kamolz, L.-P., & Kotzbeck, P. (2022). The Impact of Prolonged Inflammation on Wound Healing. *Biomedicines*, *10*(4), 856. https://doi.org/10.3390/biomedicines10040856

Javor, J., Ewoldt, J. K., Cloonan, P. E., Chopra, A., Luu, R. J., Freychet, G., Zhernenkov, M., Ludwig, K., Seidman, J. G., Seidman, C. E., Chen, C. S., & Bishop, D. J. (2021). Probing the subcellular nanostructure of engineered human cardiomyocytes in 3D tissue. *Microsystems & Nanoengineering*, *7*(1), 1–8. https://doi.org/10.1038/s41378-020-00234-x

Kapałczyńska, M., Kolenda, T., Przybyła, W., Zajączkowska, M., Teresiak, A., Filas, V., Ibbs, M., Bliźniak, R., Łuczewski, Ł., & Lamperska, K. (2018). 2D and 3D cell cultures – a comparison of different types of cancer cell cultures. *Archives of Medical Science : AMS*, *14*(4), 910–919. https://doi.org/10.5114/aoms.2016.63743

Kaukonen, R., Jacquemet, G., Hamidi, H., & Ivaska, J. (2017). Cell-derived matrices for studying cell proliferation and directional migration in a complex 3D microenvironment. *Nature Protocols*, *12*(11), 2376–2390. https://doi.org/10.1038/nprot.2017.107

Keer, R., & Simmonds, J. (n.d.). *Physical therapy for hypermobility*. Ehlers Danlos Support UK. Retrieved October 14, 2023, from https://www.ehlers-danlos.org/information/physical-therapy-for-hypermobility/

Landén, N. X., Li, D., & Ståhle, M. (2016). Transition from inflammation to proliferation: a critical step during wound healing. *Cellular and Molecular Life Sciences*, *73*(20), 3861–3885. https://doi.org/10.1007/s00018-016-2268-0

Laurens, N., Koolwijk, P., & de Maat, M. P. M. (2006). Fibrin structure and wound healing. *Journal of Thrombosis and Haemostasis: JTH*, *4*(5), 932–939. https://doi.org/10.1111/j.1538-7836.2006.01861.x

Law, A. L., Krebs, B., Karnik, B., & Griffin, L. (2020). Comparison of Healthcare Costs Associated With Patients Receiving Traditional Negative Pressure Wound Therapies in the Post-Acute Setting. *Cureus*, *12*(11), e11790. https://doi.org/10.7759/cureus.11790

Lee, K. Y., & Mooney, D. J. (2012). Alginate: properties and biomedical applications. *Progress in Polymer Science*, *37*(1), 106–126. https://doi.org/10.1016/j.progpolymsci.2011.06.003

Malfait, F., Castori, M., Francomano, C. A., Giunta, C., Kosho, T., & Byers, P. H. (2020). The Ehlers–Danlos syndromes. *Nature Reviews Disease Primers*, *6*(1), 1–25. https://doi.org/10.1038/s41572-020-0194-9

Malfait, F., Vroman, R., Colman, M., & Syx, D. (2021). Collagens in the Physiopathology of the Ehlers–Danlos Syndromes. In F. Ruggiero (Ed.), *The Collagen Superfamily and Collagenopathies* (pp. 55–119). Springer International Publishing. https://doi.org/10.1007/978-3-030-67592-9_3

Mao, J.-R., & Bristow, J. (2001). The Ehlers-Danlos syndrome: on beyond collagens. *Journal of Clinical Investigation*, *107*(9), 1063–1069. https://www.ncbi.nlm.nih.gov/pmc/articles/PMC209288/

Masson-Meyers, D. S., Andrade, T. A. M., Caetano, G. F., Guimaraes, F. R., Leite, M. N., Leite, S. N., & Frade, M. A. C. (2020). Experimental models and methods for cutaneous wound healing assessment. *International Journal of Experimental Pathology*, *101*(1–2), 21–37. https://doi.org/10.1111/iep.12346

Mathew-Steiner, S. S., Roy, S., & Sen, C. K. (2021). Collagen in Wound Healing. *Bioengineering*, *8*(5), 63. https://doi.org/10.3390/bioengineering8050063

Menke, N. B., Cain, J. W., Reynolds, A., Chan, D. M., Segal, R. A., Witten, T. M., Bonchev, D. G., Diegelmann, R. F., Ward, K. R., & Virginia Commonwealth University Reanimation, Engineering Shock Center, The Wound Healing Group. (2010). An in silico approach to the analysis of acute wound healing. *Wound Repair and Regeneration*, *18*(1), 105–113. https://doi.org/10.1111/j.1524-475X.2009.00549.x

Miklovic, T., & Sieg, V. C. (2023). Ehlers-danlos syndrome. In StatPearls. StatPearls Publishing. http://www.ncbi.nlm.nih.gov/books/NBK549814/

Millipore. (2024). *Cell Comb^{TM} Scratch Assay*. https://www.emdmillipore.com/US/en/product/Cell-Comb-Scratch-Assay,MM_NF-17-10191

Neil, J. E., Brown, M. B., & Williams, A. C. (2020). Human skin explant model for the investigation of topical therapeutics. *Scientific Reports*, *10*(1), 21192. https://doi.org/10.1038/s41598-020-78292-4

Parfenov, V. A., Khesuani, Y. D., Petrov, S. V., Karalkin, P. A., Koudan, E. V., Nezhurina, E. K., Pereira, F. D., Krokhmal, A. A., Gryadunova, A. A., Bulanova, E. A., Vakhrushev, I. V., Babichenko, I. I., Kasyanov, V., Petrov, O. F., Vasiliev, M. M., Brakke, K., Belousov, S. I., Grigoriev, T. E., Osidak, E. O., … Mironov, V. A. (2020). Magnetic levitational bioassembly of 3D tissue construct in space. *Science Advances*, *6*(29), eaba4174. https://doi.org/10.1126/sciadv.aba4174

Passaniti, A., Kleinman, H. K., & Martin, G. R. (2022). Matrigel: history/background, uses, and future applications. *Journal of Cell Communication and Signaling*, *16*(4), 621–626. https://doi.org/10.1007/s12079-021-00643-1

Parnell, L. K. S., & Volk, S. W. (2019). The Evolution of Animal Models in Wound Healing Research: 1993–2017. *Advances in Wound Care*, *8*(12), 692–702. https://doi.org/10.1089/wound.2019.1098

Pastar, I., Stojadinovic, O., Yin, N. C., Ramirez, H., Nusbaum, A. G., Sawaya, A., Patel, S. B., Khalid, L., Isseroff, R. R., & Tomic-Canic, M. (2014). Epithelialization in Wound Healing: A Comprehensive Review. *Advances in Wound Care*, *3*(7), 445–464. https://doi.org/10.1089/wound.2013.0473

Pozzi, S., Scomparin, A., Israeli Dangoor, S., Rodriguez Ajamil, D., Ofek, P., Neufeld, L., Krivitsky, A., Vaskovich-Koubi, D., Kleiner, R., Dey, P., Koshrovski-Michael, S., Reisman, N., & Satchi-Fainaro, R. (2021). Meet me halfway: Are *in vitro* 3D cancer models on the way to replace in vivo models for nanomedicine development? *Advanced Drug Delivery Reviews*, *175*, 113760. https://doi.org/10.1016/j.addr.2021.04.001

Randall, M. J., Jüngel, A., Rimann, M., & Wuertz-Kozak, K. (2018). Advances in the biofabrication of 3d skin in vitro: Healthy and pathological models. *Frontiers in Bioengineering and Biotechnology*, *6*. https://www.frontiersin.org/articles/10.3389/fbioe.2018.00154

Raspanti, M., Reguzzoni, M., Protasoni, M., & Basso, P. (2018). Not only tendons: The other architecture of collagen fibrils. *International Journal of Biological Macromolecules*, *107*, 1668–1674. https://doi.org/10.1016/j.ijbiomac.2017.10.037

Ravi, M., Paramesh, V., Kaviya, S. R., Anuradha, E., & Solomon, F. D. P. (2015). 3D Cell Culture Systems: Advantages and Applications. *Journal of Cellular Physiology*, *230*(1), 16–26. https://doi.org/10.1002/jcp.24683

Research, C. for B. E. and. (2023). Standards Development for Regenerative Medicine Therapies. *FDA*. https://www.fda.gov/vaccines-blood-biologics/standards- development-regenerative-medicine-therapies

Ricard-Blum, S. (2011). The Collagen Family. *Cold Spring Harbor Perspectives in Biology*, *3*(1), a004978. https://doi.org/10.1101/cshperspect.a004978

Royer, S. P., & Han, S. J. (2022). Mechanobiology in the Comorbidities of Ehlers Danlos Syndrome. *Frontiers in Cell and Developmental Biology*, *10*, 874840. https://doi.org/10.3389/fcell.2022.874840

Saba, I., Jakubowska, W., Bolduc, S., & Chabaud, S. (2018). Engineering Tissues without the Use of a Synthetic Scaffold: A Twenty-Year History of the Self-Assembly Method. BioMed Research International, 2018, e5684679. https://doi.org/10.1155/2018/5684679

Sami, D. G., Heiba, H. H., & Abdellatif, A. (2019). Wound healing models: A systematic review of animal and non-animal models. *Wound Medicine*, *24*(1), 8–17. https://doi.org/10.1016/j.wndm.2018.12.001

Schultz, G. S., Chin, G. A., Moldawer, L., & Diegelmann, R. F. (2011). Principles of Wound Healing. In R. Fitridge & M. Thompson (Eds.), *Mechanisms of Vascular Disease: A Reference Book for Vascular Specialists*. University of Adelaide Press. http://www.ncbi.nlm.nih.gov/books/NBK534261/

Shannon, J. L., Kirchner, S. J., & Zhang, J. Y. (2022). Human Skin Explant Preparation and Culture. *Bio-Protocol*, *12*(18), e4514. https://doi.org/10.21769/BioProtoc.4514

Shirley, E. D., DeMaio, M., & Bodurtha, J. (2012). Ehlers-Danlos Syndrome in Orthopaedics. *Sports Health*, *4*(5), 394–403. https://doi.org/10.1177/1941738112452385

Sobey, G. (2015). Ehlers–Danlos syndrome: how to diagnose and when to perform genetic tests. *Archives of Disease in Childhood*, *100*(1), 57–61. https://doi.org/10.1136/archdischild-2013-304822

Stamm, A., Reimers, K., Strauß, S., Vogt, P., Scheper, T., & Pepelanova, I. (2016). *In vitro* wound healing assays – state of the art. *BioNanoMaterials*, *17*(1–2), 79–87. https://doi.org/10.1515/bnm-2016-0002

Stone, K. (2012, October 23). Costs of Animal and Non-Animal Testing. *Humane Society International*. https://www.hsi.org/news-resources/time_and_cost/

Suarez-Arnedo, A., Torres Figueroa, F., Clavijo, C., Arbeláez, P., Cruz, J. C., & Muñoz-Camargo, C. (2020). An image J plugin for the high throughput image analysis of in vitro scratch wound healing assays. *PLOS ONE*, *15*(7), e0232565. https://doi.org/10.1371/journal.pone.0232565

Summerfield, A., Meurens, F., & Ricklin, M. E. (2015). The immunology of porcine skin and its value as a model for human skin. *Molecular Immunology*, *66*(1), 14–21. https://doi.org/10.1016/j.molimm.2014.10.023

Tanzer, M. L. (1973). Cross-linking of collagen. Science (New York, N.Y.), 180(4086), 561–566. https://doi.org/10.1126/science.180.4086.561

The University of Texas Medical Branch. (2008). *Anatomy of the Skin*. https://www.utmb.edu/pedi_ed/CoreV2/Dermatology/page_03.htm#:~:text=The%20dermis%20is%20a%20tough,thin%20as%20piece%20of%20paper.

Urciuolo, F., Passariello, R., Imparato, G., Casale, C., & Netti, P. A. (2022). Bioengineered Wound Healing Skin Models: The Role of Immune Response and Endogenous ECM to Fully Replicate the Dynamic of Scar Tissue Formation *In vitro*. *Bioengineering*, *9*(6), 233. https://doi.org/10.3390/bioengineering9060233

Ushiki, T. (1992). [The three-dimensional ultrastructure of the collagen fibers, reticular fibers and elastic fibers: a review]. *Kaibogaku Zasshi. Journal of Anatomy*, *67*(3), 186–199.

Van Norman, G. A. (2019). Limitations of Animal Studies for Predicting Toxicity in Clinical Trials. *JACC: Basic to Translational Science*, *4*(7), 845–854. https://doi.org/10.1016/j.jacbts.2019.10.008

Viglio, S., Zoppi, N., Sangalli, A., Gallanti, A., Barlati, S., Mottes, M., Colombi, M., & Valli, M. (2008). Rescue of Migratory Defects of Ehlers–Danlos Syndrome Fibroblasts *In vitro* by Type V Collagen but not Insulin-Like Binding Protein-1. *Journal of Investigative Dermatology*, *128*(8), 1915–1919. https://doi.org/10.1038/jid.2008.33

Wei, J. C. J., Edwards, G. A., Martin, D. J., Huang, H., Crichton, M. L., & Kendall, M. A. F. (2017). Allometric scaling of skin thickness, elasticity, viscoelasticity to mass for micro-medical device translation: from mice, rats, rabbits, pigs to humans. Scientific Reports, 7(1), 15885. https://doi.org/10.1038/s41598-017-15830-7

Wiesmann, T., Castori, M., Malfait, F., & Wulf, H. (2014). Recommendations for anesthesia and perioperative management in patients with Ehlers-Danlos syndrome(S). *Orphanet Journal of Rare Diseases*, *9*, 109. https://doi.org/10.1186/s13023-014-0109-5

Wilhelm, K. -P., Wilhelm, D., & Bielfeldt, S. (2017). Models of wound healing: an emphasis on clinical studies. *Skin Research and Technology*, *23*(1), 3–12. https://doi.org/10.1111/srt.12317

Wolf, K. J., & Kumar, S. (2019). Hyaluronic Acid: Incorporating the Bio into the Material. *ACS Biomaterials Science & Engineering*, *5*(8), 3753–3765. https://doi.org/10.1021/acsbiomaterials.8b01268

Yale Genome Editing Center. (n.d.). *Fees*. Retrieved March 1, 2024, from https://medicine.yale.edu/compmed/ags/fees/

Yates, C. C., Hebda, P., & Wells, A. (2012). Skin Wound Healing and Scarring: Fetal Wounds and Regenerative Restitution: Scarless and Scarring Healing. *Birth Defects Research Part C: Embryo Today: Reviews*, *96*(4), 325–333. https://doi.org/10.1002/bdrc.21024

Zabaglo, M., & Sharman, T. (2023). Postoperative Wound Infection. In *StatPearls*. StatPearls Publishing. http://www.ncbi.nlm.nih.gov/books/NBK560533/

Zhang, T., Yang, F., Qin, X., Yang, X., Zhang, C., Wan, Z., & Lin, H. (2022). Investigation of the In Vivo, *In vitro*, and In Silico Wound Healing Potential of Pinctada martensii Purified Peptides. *Marine Drugs*, *20*(7), 417. https://doi.org/10.3390/md20070417

Zhang, Q. (2022). *The mechanics of hydrogels: mechanical properties, testing, and applications* (H. Li & V. Silberschmidt, Eds.). Woodhead Publishing, an imprint of Elsevier.

Appendices

Appendix A: Interviews with Clinicians

Interview Introduction Script and Questions for Assessing Current Treatments for Ehlers-Danlos Patients

We are a part of a student-led senior capstone project group from Worcester Polytechnic Institute (WPI) in Massachusetts. We are undertaking interviews with clinicians and researchers in order to better understand the current knowledge gaps in the treatment of patients with Ehlers-Danlos.

Participation is entirely voluntary, and interviews will last around 30 minutes. You can choose not to answer any of the questions and may withdraw from the interview at any time.

With your consent, we would like to record audio and take notes during the interview. The interview recording, notes, and any personal data you choose to share with us will be stored securely and disposed of by May 15th, 2024.

Our student team will produce a finalized research report and other outputs using the data we collect from the interview. We would like to use quotes from you and would ask for your approval of quotes we use prior to publication. These quotes will remain anonymous unless you give us explicit verbal permission to do so. You will be able to review any quotations we are considering prior to publication. You may also withdraw permission to include your comments at any time prior to publication.

If you have any questions about the information taken away from the interview, please contact gr-hypermobility_mqp@wpi.edu or our advisor gpins@wpi.edu.

Do you have any questions before we start?

1. Could you introduce yourself further and briefly discuss your background, so we understand your perspective about EDS treatment or research?
2. What knowledge gap motivated your participation in treating EDS patients?
    a. What knowledge gaps remain in the field?

3. If you work with patients, what have you seen to be the most prevalent symptoms in EDS patients that you manage?
4. What feature of EDS have you observed that has the biggest social/mental health implication?
5. Is there a feature of EDS that has the biggest financial implication for patients?
6. What primary treatment options are available and most frequently used by EDS patients?
7. Are you familiar with any tailored treatment approaches for unique EDS patients?
8. What gap in knowledge and treatment have you seen regarding effectively improving these individuals' quality of life?
9. In your experience, what is the greatest unmet need for therapies and treatments?
10. What has been the greatest challenge in implementing or deploying this strategy? (Why hasn't this problem been solved?)
11. What would you like to see in a treatment?
12. Do you have any resources you would recommend to further understand the needs of EDS patients? (For example, literature, other professionals, etc.)
13. What is something you find yourself needing when treating/researching EDS patients? "If only I had…"
14. Is there something we should have asked you, but we didn't?
15. If we have any follow up questions, can we reconnect with you later in the term?
16. Do you have any other questions for us?

Appendix B: Synopses of Interviews with Clinicians and Researchers

Elizabeth Doherty, PhD

Elizabeth L. Doherty, PhD University of North Carolina at Chapel Hill, was interviewed on September 21st, 2023. Her research focuses on developing in vitro models to study how the extracellular matrix plays a role in the disease progression of vEDS. Doherty detailed that for her research, she uses vEDS patient-derived cells obtained from the Corriell Institute. She provided recommendations for external resources for the team to explore to learn more about existing in vitro models.

Raymond Dunn, MD

Dr. Raymond Dunn, Professor of Plastic Surgery at UMass Medical School, was interviewed on October 18th, 2023. Dr. Dunn expressed that he does not operate on EDS patients due to tissue fragility. He stated that reconstructive surgery can result in further damage for EDS patients, so it is typically avoided. Additionally, Dr. Dunn explained that wound healing is a complex process that is protracted in EDS patients. He recommended that the team explore collagen disorders other than EDS for inspiration regarding 3D in vitro models. Dr. Dunn expressed that a model could be helpful for future researchers to understand more about the wound healing mechanisms in cEDS as well as to test treatments on.

Dacre Knight, MD

Dr. Dacre Knight, a general internal medicine physician in Jacksonville, Florida, specializes in consultative and diagnostic medicine. Interviewed by the team on September 26th, 2023, Dr. Knight's research centers on clinical, social, and genetic factors related to inherited connective tissue disorders, particularly Ehlers-Danlos syndrome (EDS) and hypermobility spectrum disorders (HSD). He is dedicated to offering personalized diagnostic evaluations and

treatments to EDS patients, emphasizing the need to address gaps in knowledge within the field. Dr. Knight highlighted the risks faced by pregnant women with EDS, including an elevated risk of bleeding and the potential for early onset labor. Additionally, he stressed the insufficient understanding of pain, joint instability, and tissue fragility in EDS, suggesting these areas as potential focuses for research and treatment development. Furthermore, Dr. Knight discussed the variability in wound healing among EDS patients, leading to differences in wound care protocols. Complications such as tissue fragility, minimal scarring, thin tissue, and increased susceptibility to future injuries were noted. While treatments like prolotherapy and topical agents exist to strengthen tissues and alleviate musculoskeletal pain, their efficacy varies among patients.

Fransiska Malfait, MD, PhD

Dr. Malfait is a clinical geneticist centered in Ghent, Belgium. The team interviewed Dr. Malfait on September 26th, 2023. She has been involved in EDS diagnostic research for over 20 years. Dr. Malfait's lab works with in vitro models of cEDS including mouse and zebra fish in an effort to better understand the mechanisms of these genetic mutations. Dr. Malfait shared that the most prevalent symptom patients experience is pain, which is the main reason they seek treatment. She feels the hypermobile subtype is often focused on the most as it is the most prevalent and therefore these patients have the largest voice. She shared that she is not aware of any targeted treatments beyond physical therapy and the mechanisms of EDS wound healing are not well understood. Dr. Malfait emphasized there is a lack of research in the field and more investigations into the differing types of EDS would be beneficial. Dr. Malfait recommended that the team identify other rare skin disorders with similar phenotypes and confirmed the significance of a collagen-deficient wound model.

Jill Schofield, MD

On September 26, 2023, the team interviewed Dr. Jill Schofield, founder and director of the Center for Multisystem Disease located in Denver, Colorado. Dr. Schofield specializes in immune-mediated disorders that pose challenges due to their systemic nature, affecting multiple bodily systems. Her organization focuses on providing comprehensive care to patients grappling with various multisystem autoimmune diseases. Dr. Schofield emphasized the significant knowledge gap in addressing these complex conditions. She highlighted the specialized expertise required, particularly among neurosurgeons, vascular surgeons and interventional radiologists treating conditions like Ehlers-Danlos syndrome comorbidities, such as tethered cord syndrome, craniocervical instability, median arcuate ligament syndrome and pelvic venous insufficiency syndromes. Dr. Schofield compared these specialists with general surgeons who may lack familiarity with these nuanced disorders which are often diagnosed differently in the EDS population. Furthermore, Dr. Schofield pointed out major hurdles within the healthcare system itself that exacerbate challenges for these patients. These obstacles include navigating treatment and management of multisystemic complications, insurance coverage and the overall financial burden associated with disease management. Additionally, Dr. Schofield shed light on common symptoms experienced by patients with multisystemic diseases, which include pain, dysautonomia, substantial gastrointestinal issues, headaches and many others.

Sara Strecker, PhD

Dr. Sara Strecker, PhD/MS Senior Scientist with the Hartford HealthCare Bone and Joint Institute, was interviewed by the team on September 18th, 2023. Her research centers on how EDS affects bone density, gait, and the prevalence of comorbid conditions. Her studies have revealed lower bone mass in EDS patients and gait abnormalities, likely linked to hypermobility.

Dr. Strecker highlighted the heterogeneity of EDS and the need for better bracing methods, ligament replacements, and pain management strategies. She mentioned a need for research that investigates biocompatible ligament replacements through tenocyte cultures and the optimization of collagen synthesis. Dr. Strecker explained that while there exists a tenascin-X knockout mouse model of EDS, a need persists for representative cell models of cEDS and hEDS. Recognizing the challenges faced by patients, Dr. Strecker advocated for increased physician education and highlighted the limitations of current pain management options. Her research on provider perspectives aims to bridge the gap between patients and healthcare professionals.

Brad Tinkle, MD, PhD

Dr. Brad Tinkle is a clinical geneticist at Peyton Manning Children's Hospital in Indianapolis, Indiana with experience in EDS. He sees patients ranging from 3 to 85 years old. He was interviewed by the team on September 28th, 2023. Dr. Tinkle has worked with EDS patients, primarily those with hEDS, for 21 years. He currently sees approximately 25-30 patients a week. Dr. Tinkle sees patients with a wide variety of clinical presentations. However, the most common symptoms patients present with include musculoskeletal and dysautonomic issues. Management of the condition focuses on preventative care for younger patients and education for older ones. Dr. Tinkle occasionally sees patients that present poor wound healing because of fragile tissue. Any force applied to an EDS patient's wound can result in the skin separating, creating secondary wounds (microtears) and ultimately, atrophic scarring. The constant re-opening of the wound makes EDS patients more prone to skin infections. Additionally, wound dehiscence limits physical mobility, which can be detrimental to physical rehabilitation post-surgery. Dr. Tinkle expressed that while treatments like dermal glue and scar reduction techniques exist, there remains a lack of understanding of how to improve wound

healing in EDS patients. This knowledge gap hinders better treatment decisions and can lead to financial burdens due to prolonged recovery and complications. Dr. Tinkle emphasized the need for further research into mechanical wound closure methods, materials that stimulate collagen production, and the potential applicability of diabetic wound care techniques to EDS.

Appendix C: Objective & Design Brainstorming

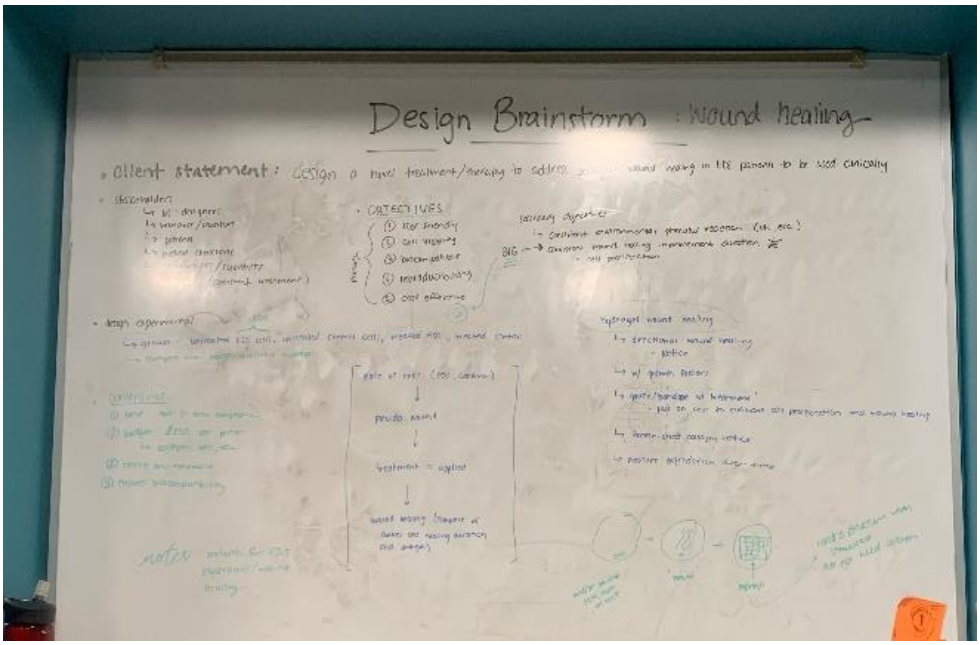

Figure 1. Brainstorm of client statement, constraints, and project objectives.

Appendix D: Primary Objectives Pairwise Comparison Charts

Designer PCC by Madison Donahue, Maya Evohr, Morgan Foltz, Abigail Holmes, and Spencer Whitford:

Primary Objectives	Reproducible	Imageable	Representative	Versatile	Usable	Affordable	Total
Reproducible	X	0	0	1	1	1	**3**
Imageable	1	X	0	1	1	1	**4**
Representative	1	1	X	1	1	1	**5**
Versatile	0	0	0	X	1	1	**2**
Usable	0	0	0	0	X	1	**1**
Affordable	0	0	0	0	0	X	**0**

Client PCC by George Pins:

Primary Objectives	Reproducible	Imageable	Representative	Versatile	Usable	Affordable	Total
Reproducible	X	0.5	0.5	1	0.5	1	**3.5**
Imageable	0.5	X	0.5	1	0.5	1	**3.5**
Representation	0.5	0.5	X	1	0.5	1	**3.5**
Versatile	0	0	0	X	0	1	**1**
Usable	0.5	0.5	0.5	1	X	1	**3.5**
Affordable	0	0	0	0	0	X	**0**

User PCC by Bryanna Samolyk:

Primary Objectives	Reproducible	Imageable	Representative	Versatile	Usable	Affordable	Total
Reproducible	X	1	0	0.5	0.5	1	**2**
Imageable	0	X	0	0.5	0	1	**1.5**
Representative	1	1	X	1	0.75	1	**4.75**
Versatile	0.5	0.5	0	X	0	1	**2**
Usable	0.5	1	0.25	1	X	1	**3.75**
Affordable	0	0	0	0	0	X	**0**

Appendix E: Secondary Objectives Pairwise Comparison Charts

Representative Secondary Objectives:

Designer PCC by Madison Donahue, Maya Evohr, Morgan Foltz, Abigail Holmes, and Spencer Whitford:

Primary Objective: Representative	Mechanical Properties	Collagen	Proliferation	Migration	Contraction	ECM Synthesis	Wound Closure	Total
Mechanical Properties	X	1	1	0	0.5	1	0	**3.5**
Collagen	0	X	0	0	0	1	0	**1**
Proliferation	0	1	X	0	0	1	0	**2**
Migration	1	1	1	X	0.5	1	0	**4.5**
Contraction	0.5	1	1	0.5	X	1	0	**4**
ECM Synthesis	0	0	0	0	0	X	0	**0**
Wound Closure	1	1	1	1	1	1	X	**6**

Client PCC by George Pins:

Primary Objective: Representative	Mechanical Properties	Collagen	Proliferation	Migration	Contraction	ECM Synthesis	Wound Closure	Total
Mechanical Properties	X	1	0.5	0	0	1	0	**2.5**
Collagen	0	X	0	0	0	0	0	**0**
Proliferation	0.5	1	X	0.5	0	1	0	**3**
Migration	1	1	0.5	X	0	0	0	**2.5**
Contraction	1	1	1	1	X	1	0.5	**5.5**
ECM Synthesis	0	1	0	1	0	X	0	**2**
Wound Closure	1	1	1	1	0.5	1	X	**5.5**

User PCC by Bryanna Samolyk:

Primary Objective: Representative	Mechanical Properties	Collagen	Proliferation	Migration	Contraction	ECM Synthesis	Wound Closure	Total
Mechanical Properties	X	0.5	1	1	1	0.5	0.5	**4.5**
Collagen	0.5	X	1	1	1	0.5	0.5	**4.5**
Proliferation	0	0	X	0.5	1	0	0	**1.5**
Migration	0	0	0.5	X	1	0	0	**1.5**
Contraction	0	0	0	0	X	0	0	**0**
ECM Synthesis	0.5	0.5	1	1	1	X	0.5	**4.5**
Wound Closure	0.5	0.5	1	1	1	0.5	X	**4.5**

Imageable Secondary Objectives:

Designer PCC by Madison Donahue, Maya Evohr, Morgan Foltz, Abigail Holmes, and Spencer Whitford:

Primary Objective: Imageable	Throughput	Light Microscopy	Measurable Wound Area	Fluorescence Microscopy	Measures Collagen	Timelapse	Total
Throughput	X	0	0	1	1	1	**3**
Light Microscopy	1	X	0	1	1	1	**4**
Measurable Wound Area	1	1	X	1	1	1	**5**
Fluorescence Microscopy	0	0	0	X	1	1	**2**
Measures Collagen	0	0	0	0	X	0	**0**
Timelapse	0	0	0	0	1	X	**1**

Client PCC by George Pins:

Primary Objective: Imageable	Throughput	Light Microscopy	Measurable Wound Area	Fluorescence Microscopy	Measures Collagen	Timelapse	Total
Throughput	X	0	0	0	0	1	**1**
Light Microscopy	1	X	0.5	1	1	1	**4.5**
Measurable Wound Area	1	0.5	X	1	1	1	**4.5**
Fluorescence Microscopy	1	0	0	X	1	1	**3**
Measures Collagen	1	0	0	0	X	1	**2**
Timelapse	0	0	0	0	0	X	**0**

User PCC by Bryanna Samolyk:

Primary Objective: Imageable	Throughput	Light Microscopy	Measurable Wound Area	Fluorescence Microscopy	Measures Collagen	Timelapse	Total
Throughput	X	1	0	0	0	1	**2**
Light Microscopy	0	X	0	0	0	1	**1**
Measurable Wound Area	1	1	X	0.25	0.25	1	**3.5**
Fluorescence Microscopy	1	1	0.75	X	0.75	1	**4.5**
Measures Collagen	1	1	0.75	0.25	X	1	**4**
Timelapse	0	0	0	0	0	X	**0**

Reproducible Secondary Objectives:

Designer PCC by Madison Donahue, Maya Evohr, Morgan Foltz, Abigail Holmes, and Spencer Whitford:

Primary Objective: Reproducible	Accurate	Precise	Scalable	Total
Accurate	X	0	1	**1**
Precise	1	X	1	**2**
Scalable	0	0	X	**0**

Client PCC by George Pins:

Primary Objective: Reproducible	Accurate	Precise	Scalable	Total
Accurate	X	0	1	**1**
Precise	1	X	1	**2**
Scalable	0	0	X	**0**

User PCC by Bryanna Samolyk:

Primary Objective: Reproducible	Accurate	Precise	Scalable	Total
Accurate	X	1	1	**2**
Precise	0	X	1	**1**
Scalable	0	0	X	**0**

Usable Secondary Objectives:

Designer PCC by Madison Donahue, Maya Evohr, Morgan Foltz, Abigail Holmes, and Spencer Whitford:

Primary Objective: Usable	Non-Daily Care	Standard Dish/ Plate	Typical Incubator	Single Scientist	Available Materials	Material Safety	Easy Assemble	Time Efficient	Induct Wound	Total
Non-Daily Care	X	0	0	0	0	0	0.5	0	0	**0.5**
Standard Dish/Plate	1	X	0	0	0	0	1	0	0	**2**
Typical Incubator	1	1	X	0	0.5	0	1	0	0	**3.5**
Single Scientist	1	1	1	X	0.5	0	1	1	0	**5.5**
Available Materials	1	1	0.5	0.5	X	0	1	1	0	**5**
Material Safety	1	1	1	1	1	X	1	1	0	**7**
Easy Assembly	0.5	0	0	0	0	0	X	0	0	**0.5**
Time Efficient	1	1	1	0	0	0	1	X	0	**4**
Wound Induction	1	1	1	1	1	1	1	1	X	**8**

Client PCC by George Pins:

Primary Objective: Usable	Non-Daily Care	Standard Dish/ Plate	Typical Incubator	Single Scientist	Available Materials	Material Safety	Easy Assemble	Time Efficient	Induct Wound	Total
Non-Daily Care	X	1	0	0	0	0	0	0	0	**1**
Standard Dish/Plate	0	X	0	0	0	0	0	0	0	**0**
Typical Incubator	1	1	X	0.5	0.5	0	0	0	0	**3**
Single Scientist	1	1	0.5	X	1	0.5	0.5	0.5	0.5	**5.5**
Available Materials	1	1	0.5	0	X	0	0	0	0	**2.5**
Material Safety	1	1	1	0.5	1	X	1	1	0.5	**7**
Easy Assembly	1	1	1	0.5	1	0	X	0.5	0	**5**
Time Efficient	1	1	1	0.5	1	0	0.5	X	0	**5**
Wound Induction	1	1	1	0.5	1	0.5	1	1	X	**7**

User PCC by Bryanna Samolyk:

Primary Objective: Usable	Non-Daily Care	Standard Dish/ Plate	Typical Incubator	Single Scientist	Available Materials	Material Safety	Easy Assemble	Time Efficient	Induct Wound	Total
Non-Daily Care	X	0	0	0	0	0	0	0	0	**0**
Standard Dish/Plate	1	X	0	1	0	0	0	0.5	0	**2.5**
Typical Incubator	1	1	X	1	1	0	1	1	0.5	**6.5**
Single Scientist	1	0	0	X	0.5	0	0.5	0.5	0	**2.5**
Available Materials	1	1	0	0.5	X	0	0	0	0	**2.5**
Material Safety	1	1	1	1	1	X	1	1	1	**8**
Easy Assembly	1	1	0	0.5	1	0	X	0.5	0	**4**
Time Efficient	1	0.5	0	0.5	1	0	0.5	X	0	**3.5**
Wound Induction	1	1	0.5	1	1	0	1	1	X	**6.5**

Appendix F. Design Gantt Chart

A Term:

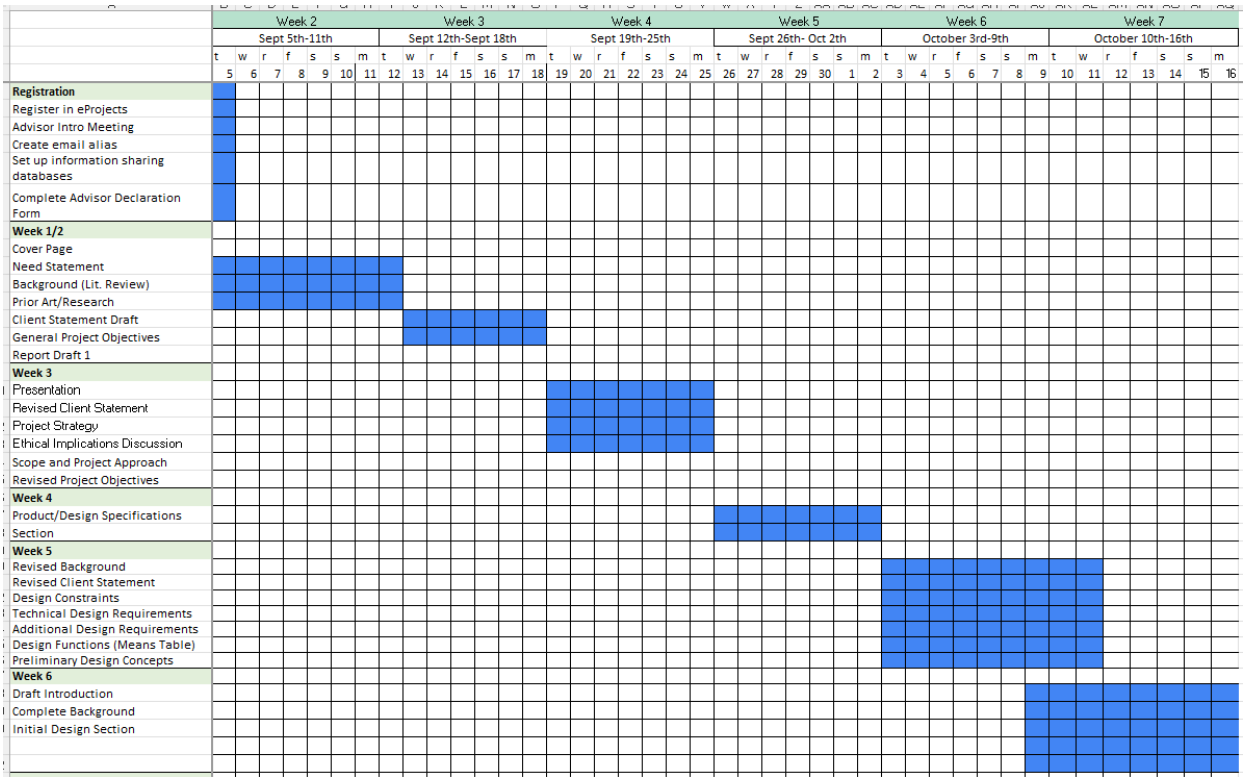

B Term:

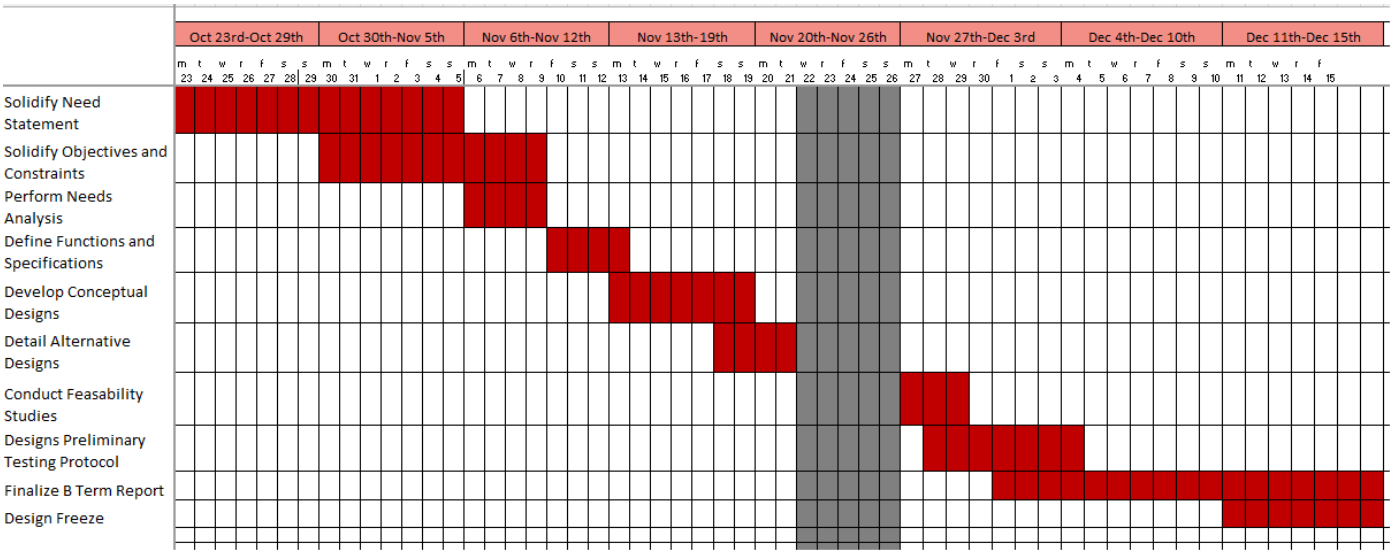

C Term:

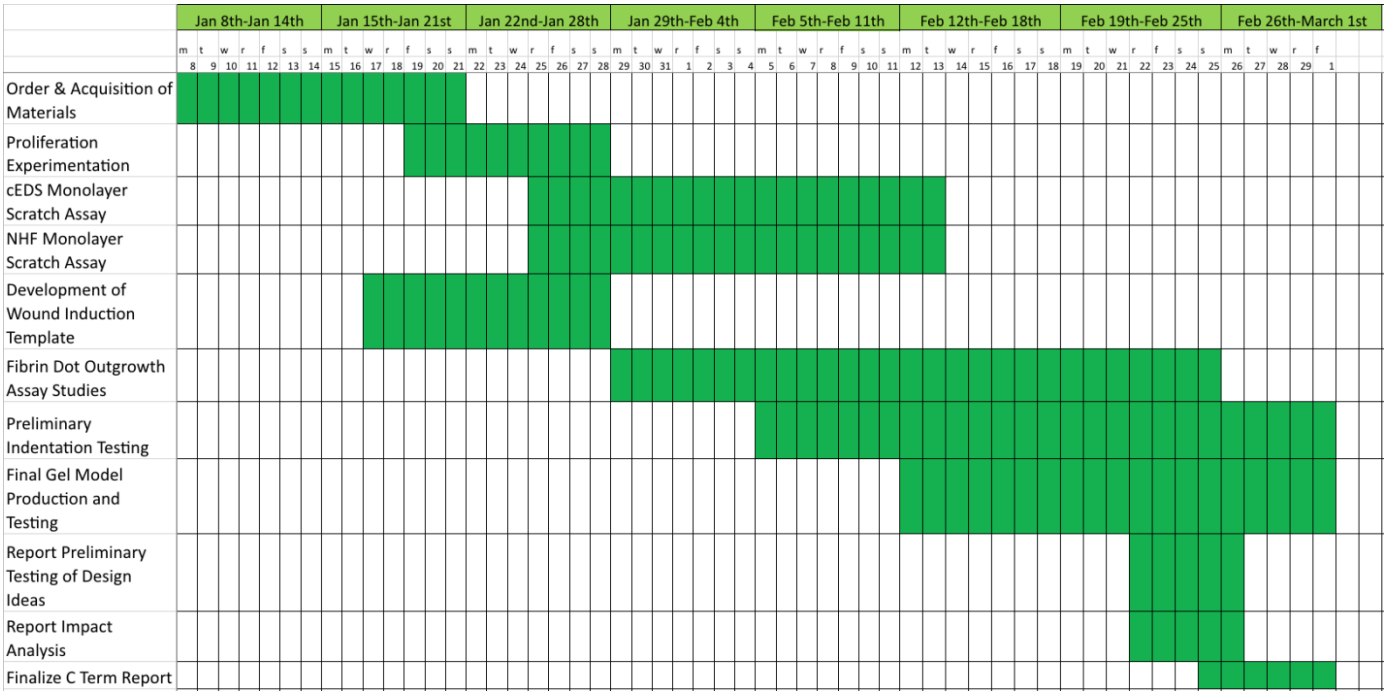
Jan 8th-Jan 14th
Jan 15th-Jan 21st
Jan 22nd-Jan 28th
Jan 29th-Feb 4th
Feb 5th-Feb 11th
Feb 12th-Feb 18th
Feb 19th-Feb 25th
Feb 26th-March 1st
Order & Acquisition of Materials
Proliferation Experimentation
cEDS Monolayer Scratch Assay
NHF Monolayer Scratch Assay
Development of Wound Induction Template
Fibrin Dot Outgrowth Assay Studies
Preliminary Indentation Testing
Final Gel Model Production and Testing
Report Preliminary Testing of Design Ideas
Report Impact Analysis
Finalize C Term Report

D Term:

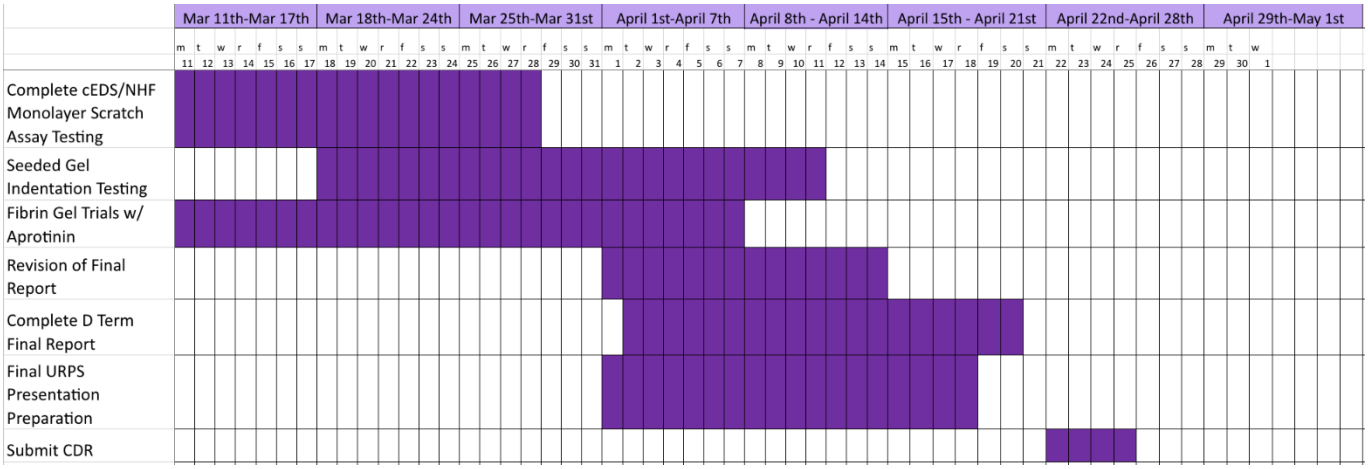
Mar 11th-Mar 17th
Mar 18th-Mar 24th
Mar 25th-Mar 31st
April 1st-April 7th
April 8th - April 14th
April 15th - April 21st
April 22nd-April 28th
April 29th-May 1st
Complete cEDS/NHF Monolayer Scratch Assay Testing
Seeded Gel Indentation Testing
Fibrin Gel Trials w/ Aprotinin
Revision of Final Report
Complete D Term Final Report
Final URPS Presentation Preparation
Submit CDR

Appendix G. Metrics Rubrics

*This provides an overview of all applicable functions and their specifications used during the model design and development process (reference **Section 4.2**). Each function contains specifications with rankings from 1-3 with 1 indicating the least favorable and 3 indicating the most favorable. These rankings will be incorporated into the design matrix (reference **Section 4.3.3**).*

Functions and Specifications

1. **Representative of EDS cell functions**

a. Proliferation

Units: The ability to have dermal fibroblast proliferation rate that is lower than the rate of unaffected dermal fibroblast proliferation (DeNigris et al., 2016)

1 – Dermal fibroblast proliferation rate equal to the rate of unaffected dermal fibroblast proliferation

2 – Dermal fibroblast proliferation rate is 2/3 the rate of unaffected dermal fibroblast proliferation

3 – Dermal fibroblast proliferation rate is 1/3 the rate of unaffected dermal fibroblast proliferation.

b. Migration

Units: The ability to have dermal fibroblast migration rate that is lower than the rate of unaffected dermal fibroblast migration (Viglio et al., 2008)

1 – Dermal fibroblast migration is equal to the rate of unaffected dermal fibroblast migration.

2 – Dermal fibroblast migration is less than 2/3 the rate of unaffected dermal fibroblast migration.

3 – Dermal fibroblast migration is less than 1/3 the rate of unaffected dermal fibroblast migration.

c. Wound Closure

Units: Time for full wound closure is longer than the time it would take for an unaffected wound matrix.

1 – Time for full wound closure is the same as an unaffected wound matrix.

2 – Time for full wound closure is 1.5 times as long as an unaffected wound matrix.

3 – Time for full wound closure is twice as long as the time for an unaffected wound matrix.

d. Tensile modulus

Units: The model exhibits representative tensile elastic modulus of skin (Wei et al., 2017)

1 – Model exhibits a tensile elastic modulus of 40 MPa or higher

2 – Model exhibits a tensile elastic modulus of 20 to 40 MPa or 0 to 5 MPa

3 - Model exhibits a tensile elastic modulus of 5 to 20 MPa

2. Allows for efficient imaging of model over time

a. Measurable Wound Area

Units: Wound area is measurable down to 0.1 mm.

1 – Wound area is measurable to the nearest 1 mm

2 – Wound area is measurable to the nearest 0.5 mm

3 – Wound area is measurable to the nearest 0.1 mm

b. Light Microscopy

Units: Magnification setting allows for cells to be visualized at least 80% clarity

1 - Model can be visualized at 4x objective

2 - Model can be visualized at 10x objective

3 – Model can be visualized at 40x objective

c. Throughput

Units: Number of models that can be imaged in under 1 hour.

1 – One model can be imaged in under 1 hour.

2 – Six models can be imaged in under 1 hour.

3 – Twelve models can be imaged in under 1 hour.

3. Allows for accurate and efficient repeated fabrication of model

a. Scalable

Units: Model can be precisely replicated enough times for statistical significance.

1 – Model can be replicated with 80% precision less than five times

2 – Model can be replicated with 80% precision 5-10 times

3 – Model can be replicated with 80% precision greater than 10 times

b. Easy Assembly

Units: Complexity of model is low enough to allow easy assembly

1 – Model requires greater than 10 components to assemble

2 – Model requires 5-10 components to assemble

3 – Model requires 5 or less components to assemble

c. Time Efficient

Units: Model formation is time efficient given the seven-week experimental timeframe

1 – Model formation from beginning to cells being seeded takes greater than 2 weeks

2 – Model formation from beginning to cells being seeded takes 1-2 weeks

3 – Model formation from beginning to cells being seeded takes less than or equal to 1 week

d. Wound Induction Efficacy

Units: Wound can be repeatedly induced within a reasonable time frame

1 – Wound induction takes longer than 5 minutes for each sample

2 – Wound induction takes 2-5 minutes for each sample

3 – Wound induction takes less than 2 minutes for each sample

e. Single Scientist

Units: Model production and regular care does not require multiple scientists

1 – Model production and regular care will require at least two scientists

2 – Model production and regular care will require one scientist but prefer two

3 –Model production and regular care will require only one scientist

f. Daily Care

Units: Model does not require hourly or daily care

1 – Model requires care more than once per 24 hours

2 – Model requires care once per 24 hours

3 – Model requires care less than once per 24 hours

4. Integrates standard and easily available materials and equipment

a. Material Safety

   Units: Model requires minimal PPE for scientist protection

   1 – Model requires greater than 3 non-standard safety precautions

   2 – Model requires 1-2 non-standard safety precautions

   3 – Model requires 0 non-standard safety precautions (only requires gloves and a BSC, standard PPE)

b. Standard Well Plate

   Units: Model fits within well plate that allows for multiple trials

   1 – Model fits in well plate with 88.0 mm diameter (petri dish)

   2 – Models fits in well plate with 35.0 mm diameter (6-well plate)

   3 – Model fits in well plate with 22.8 mm diameter (12-well plate)

c. Typical Incubator

   Units: Model is able to be incubated in a standard incubator that is readily available

   1 – Model requires more than one non-standard specification for the incubator and an incubator must be specially obtained.

   2 – Model requires one non-standard specification for the incubator that can be programmed into available incubator

   3 – Model can be incubated at 37°C and 5% CO_2 with zero non-standard specifications for the incubator

d. Available Materials

   Units: Time with which materials can be obtained

   1 – Materials take greater than six weeks to obtain

   2 – Materials take two to six weeks to obtain

   3 – Materials take less than two weeks to obtain

Appendix H: Decision Matrices

Cell Type

			Human EDS Fibroblasts			EDS Mouse/Animal Model Fibroblasts			Normal Human Fibroblasts in EDS Derived Matrix			Normal Human Fibroblasts in Chemically Altered		
	Constraints	Weight %	Score	Normalized Score	Weighted Sum	Score	Normalized Score	Weighted Sum	Score	Normalized Score	Weighted Sum	Score	Normalized Score	Weighted Sum
C	Timeline			Y			N			N			Y	
C	Budget			Y			N			N			Y	
C	Material Availibility			Y			N			Y			Y	
C	Equipment Availability			Y			N			Y			Y	
C	Sterilizable			Y			Y			Y			Y	
C	Biocompatible			Y			Y			Y			Y	
C	Nontoxic			Y			Y			Y			Y	
C	Standardization			Y			Y			Y			Y	
C	Incubator			Y			Y			Y			Y	
C	Media			Y			Y			Y			Y	
C	Proliferation			Y			Y			Y			Y	
C	Confluency			Y			Y			Y			Y	
C	Contamination			Y			Y			Y			Y	
	Objectives													
O1	**Representative**	30		3	90								2	59.94
O	Proliferation		3	1								2	0.7	
O	Migration		3	1								2	0.7	
O	Wound Closure		3	1								2	0.7	
O3	**Reproducible**	19		1	19								1	18.981
O	Scalable		3	1								3	1	
O4	**Usable**	18		2	36								1	17.982
O	Daily Care		3	1								3	1	
O	Material Safety		3	1									0	
					145									96.903

Model Style

			Micro-TUG Model			Assembling Tissue Model			Cell-Laden (Hydro/Micro) Gel Model			Microfluidic Model			Hanging Drop Model			Magnetic Suspension Model		
	Constraints	Weight %	Score	Normalized Score	Weighted Sum	Score	Normalized Score	Weighted Sum	Score	Normalized Score	Weighted Sum	Score	Normalized Score	Weighted Sum	Score	Normalized Score	Weighted Sum	Score	Normalized Score	Weighted Sum
C	Material Availibility			Y			Y			Y			Y			Y			N	
C	Equipment Availability			Y			Y			Y			Y			Y			Y	
C	Sterilizable			Y			Y			Y			Y			Y			Y	
C	Biocompatible			Y			Y			Y			Y			Y			Y	
C	Nontoxic			Y			Y			Y			Y			Y			Y	
C	Standardization			Y			Y			Y			Y			Y			Y	
C	Incubator			Y			Y			Y			Y			Y			Y	
C	Media			Y			Y			Y			Y			Y			Y	
C	Proliferation			Y			Y			Y			Y			Y			Y	
C	Confluency			Y			Y			Y			Y			Y			Y	
C	Contamination			Y			Y			Y			Y			Y			Y	
	Objectives																			
O2	**Imageable**	20		3	59.9		3	59.94		3	59.94		3	59.94		2	47			
O	Measurable Wound Area		3	1		3	1		3	1		3	1		1	0				
O	Light Microscopy		3	1		3	1		3	1		3	1		3	1				
O	Throughput		3	1		3	1		3	1		3	1		3	1				
O4	**Usable**	18		8	138		7	119.9		8	143.856		5	95.904		7	120			
O	Standard Dish/Plate		3	1		3	1		3	1		1	0		3	1				
O	Typical Incubator		3	1		3	1		3	1		3	1		3	1				
O	Single Scientist		3	1		3	1		3	1		3	1		3	1				
O	Available Materials		3	1		3	1		3	1		3	1		2	1				
O	Material Safety		3	1		3	1		3	1		3	1		3	1				
O	Easy Assembly		3	1		3	1		3	1		2	1		2	1				
O	Time Efficient		3	1		1	0		3	1		1	0		3	1				
O	Induct Wound		2	1		1	0		3	1			0		1	0				
					198			179.8			203.796			155.84			167			

Matrix Material

			Cell-Derived Matrix via Fibroblasts			Fibrin			Collagen I			Matrigel			Alginate			Polylactic Acid (PLA)			Poyglycolic Acid (PGA)			Hydroxyapatite (HA)			Hyaluronic Acid (HA)		
		Weight %	Score	Normalized Score	Weighted Sum	Score	Normalized Score	Weighted Sum	Score	Normalized Score	Weighted Sum	Score	Normalized Score	Weighted Sum	Score	Normalized Score	Weighted Sum	Score	Normalized Score	Weighted Sum	Score	Normalized Score	Weighted Sum	Score	Normalized Score	Weighted Sum	Score	Normalized Score	Weighted Sum
C	Timeline			N			Y			Y			Y			Y			Y			Y			Y			Y	
C	Budget			Y			Y			Y			Y			Y			Y			Y			Y			Y	
C	Material Availability			Y			Y			Y			Y			Y			Y			Y			Y			Y	
C	Equipment Availability			Y			Y			Y			Y			Y			Y			Y			Y			Y	
C	Sterilizable			Y			Y			Y			Y			Y			Y			Y			Y			Y	
C	Biocompatible			Y			Y			Y			Y			Y			Y			Y			Y			Y	
C	Nontoxic			Y			Y			Y			Y			Y			Y			Y			Y			Y	
C	Standardization			Y			Y			Y			Y			Y			Y			Y			Y			Y	
C	Incubator			Y			Y			Y			Y			Y			Y			Y			Y			Y	
C	Media			Y			Y			Y			Y			Y			Y			Y			Y			Y	
C	Proliferation			Y			Y			Y			Y			N			Y			Y			Y			N	
C	Confluency			Y			Y			Y			Y			Y			Y			Y			Y			Y	
C	Contamination			Y			Y			Y			Y			Y			Y			Y			Y			Y	
	Objectives																												
O1	**Representative**	30					2	60		2	50		1	30	0	0		1	40		1	39.96		1	39.96				
O	Wound Closure					3	1		2	1		2	1					3	1		3	1		3	1				
	Tensile modulus					3	1		3	1		1	0					1	0		1	0		1	0				
O2	**Imageable**	20					1	20		1	20		1	20			0		1	20		1	19.98		1	19.98			
O	Light Microscopy					3	1		3	1		3	1					3	1		3	1		3	1				
O4	**Usable**	18					4	72		4	72		4	72			0		4	72		4	71.93	3	4	71.928			
O	Available Materials					3	1		3	1		3	1					3	1		3	1		3	1				
O	Material Safety					3	1		3	1		3	1					3	1		3	1		3	1				
O	Easy Assembly					3	1		3	1		3	1					3	1		3	1		3	1				
	3 Induct Wound					3	1		3	1		3	1					3	1		3	1		3	1				
								152			142			122			0			132			131.9			131.868			

Wound Induction Method

			Scratch Pipette Tip			Scratch Rubber Policeman			Scalpel Scratch			Stamp Punch Biopsy			Thermal Wound via Hot Rod/Branding			Laser (Optical Wound)			Rotating Drill			Electric Cell-Substrate Impedance Sensing (ECIS) (Electrical Wound)		
	Constraints	Weight %	Score	Normalized Score	Weighted Sum	Score	Normalized Score	Weighted Sum	Score	Normalized Score	Weighted Sum	Score	Normalized Score	Weighted Sum	Score	Normalized Score	Weighted Sum	Score	Normalized Score	Weighted Sum	Score	Normalized Score	Weighted Sum	Score	Normalized Score	Weighted Sum
C	Timeline			Y			Y			Y			Y			Y			Y			Y			Y	
C	Budget			Y			Y			Y			Y			Y			N			Y			N	
C	Material Availibility			Y			Y			Y			Y			Y			Y			Y			Y	
C	Equipment Availability			Y			Y			Y			Y			Y			Y			Y			Y	
C	Sterilizable			Y			Y			Y			Y			Y			Y			Y			Y	
C	Biocompatible			Y			Y			Y			Y			Y			Y			Y			Y	
C	Nontoxic			Y			Y			Y			Y			Y			Y			Y			Y	
C	Standardization			Y			Y			Y			Y			Y			Y			Y			Y	
C	Incubator			Y			Y			Y			Y			Y			Y			Y			Y	
C	Media			Y			Y			Y			Y			Y			Y			Y			Y	
C	Proliferation			Y			Y			Y			Y			Y			Y			Y			Y	
C	Confluency			Y			Y			Y			Y			Y			Y			Y			Y	
C	Contamination						Y			Y			Y			Y			Y			Y			Y	
	Objectives																									
O1	**Representative**	30		1	29.97		1	29.97		1	29.97		1	19.98		1	29.97					1	29.97			
O	Wound Closure		3	1	[redacted]	3	1	[redacted]	3	1	[redacted]	2	1	[redacted]	3	1	[redacted]				3	1	[redacted]			
O4	**Usable**	20		6	119.9		6	119.9		6	119.88		6	113.2		5	99.9					6	113.22			
O	Standard Dish/Plate		3	1	[redacted]	3	1	[redacted]	3	1	[redacted]	3	1	[redacted]	2	1	[redacted]				3	1	[redacted]			
O	Single Scientist		3	1	[redacted]	3	1	[redacted]	3	1	[redacted]	3	1	[redacted]	3	1	[redacted]				2	1	[redacted]			
O	Material Safety		3	1	[redacted]	3	1	[redacted]	3	1	[redacted]	2	1	[redacted]	2	1	[redacted]				3	1	[redacted]			
O	Available Materials		3	1	[redacted]	3	1	[redacted]	3	1	[redacted]	3	1	[redacted]	2	1	[redacted]				3	1	[redacted]			
O	Time Efficient		3	1	[redacted]	3	1	[redacted]	3	1	[redacted]	3	1	[redacted]	3	1	[redacted]				3	1	[redacted]			
O	Induct Wound		3	1	[redacted]	3	1	[redacted]	3	1	[redacted]	3	1	[redacted]	3	1	[redacted]				3	1	[redacted]			
					149.9			149.9			149.85			133.2			129.87						143.19			

Appendix I: Laboratory Protocols

Protocol for complete media and trypsin of cEDS dermal fibroblasts cells

(Adapted from Cellular Engineering – Preliminary Edition, by Sakthikumar Ambady)

1. Preparation of complete media of DMEM, 10% FBS, 1% Glutamax, and 1% Penicillin-Strep.
2. Place 44 mL of DMEM basal media (VWR, 45000-316, 4.5g/L glucose and sodium pyruvate) into a 50 mL conical tube.
3. Place 0.5 mL of Glutamax 100x (Thermo Fisher, 35050061) into the same 50 mL conical tube
    a. This ensures media is 1% GMAX
4. Place 0.5 mL of Penicillin/streptomycin 100x (VWR, 45000-652) into the same 50 mL conical tube
    b. This ensures media is 1% Pen-Strep
5. Place 5 mL of FBS (Atlanta Biologicals, S11150) into the same 50 mL conical tube
    c. This ensures media is 10% FBS
6. Invert tube a few times, place in fridge for storage for later use

Preparation of complete media of EMEM ,10%FBS, 1% Glutamax, and 1% Penicillin-Strep.

1. Place 44 mL of EMEM (ATCC, 30-2003 2 mM L-glutamine, 1 mM sodium pyruvate, and 1500 mg/L sodium bicarbonate) into a 50 mL conical tube.
2. Place 0.5 mL of Glutamax 100x (Thermo Fisher, 35050061) into the same 50 mL conical tube
    d. This ensures media is 1% GMAX
3. Place 0.5 mL of Penicillin/streptomycin 100x (VWR, 45000-652) into the same 50 mL conical tube
    e. This ensures media is 1% Pen-Strep
4. Place 5 mL of FBS (Atlanta Biologicals, S11150) into the same 50 mL conical tube
    f. This ensures media is 10% FBS
5. Invert tube a few times, place in fridge for storage for later use

Preparation of Trypsin (0.04% Trypsin, 50 mL prep)

1. Place 8 mL of DPBS into a 50 mL conical tube
2. Place 42 mL of 0.25% Trypsin-EDTA (Corning, 25053CI) into the same 15 mL conical tube
3. Invert tube a few times, place mixture on cells or store as needed.

*** must be diluted in DPBS because there should not be any Ca2+ or Mg2+ within the solution

Preparation of Concentrated Aprotinin Solution (1 mg/mL in DMEM)

1. Dissolve 25 mg lyophilized aprotinin powder (Thermo Fisher Scientific, J11388.MB) in 25 mL of DMEM (VWR, 45000-316, 4.5g/L glucose and sodium pyruvate) within a sterile 50 mL conical tube
2. Invert tube a few times, pace mixture in fridge until needed

Preparation of complete media of DMEM, 10% FBS, 1% Glutamax, and 1% Penicillin-Strep and 20 μg/mL Aprotinin.

1. Place 43 mL of DMEM basal media (VWR, 45000-316, 4.5g/L glucose and sodium pyruvate) into a 50 mL conical tube.
2. Place 0.5 mL of Glutamax 100x (Thermo Fisher, 35050061) into the same 50 mL conical tube
    a. This ensures media is 1% GMAX
3. Place 0.5 mL of Penicillin/streptomycin 100x (VWR, 45000-652) into the same 50 mL conical tube
    a. This ensures media is 1% Pen-Strep
4. Place 5 mL of FBS (Atlanta Biologicals, S11150) into the same 50 mL conical tube
    a. This ensures media is 10% FBS
5. Place 1 mL of concentrated Aprotinin DMEM mixture (1 mg/mL of Aprotinin) into the same 50 mL conical tube
    a. This ensures that the final aprotinin concentration is 20 μg/mL
6. Invert tube a few times, place in fridge for storage for later use

Protocol for passaging of cEDS dermal fibroblasts and neonatal human dermal fibroblasts

1. Open the cell culture hood. Spray liberally with 70% isopropanol and clean the surface of the hood.
2. Spray 70% isopropanol into the waste suction tube with the vacuum pump in one position (by pressing on the pedal). Spray the outside tube and wipe it clean.
3. Take the culture dish out of the incubator and check the media color and consistency. Based on the cell growth, the media will be red, slightly pink, or yellow in color. Cloudy media indicates possible contamination of the culture.
4. Before bringing the culture plate into the hood **check culture plate under the microscope** to
5. Check the health and degree of confluency of the cells
6. Cells should be passaged if they are more than 80% confluent.
7. Ensure that cells are not contaminated.
8. Take a new sterile 15 ml conical centrifuge tube. Mark the cell line name on the tube.
9. Aspirate the medium.
10. Using a serological pipette, gently add 5 ml **DPBS (-)** along the side of the flask, rinse cells.
11. Aspirate DPBS (-).
12. Add 3 ml of 0.04% Trypsin-EDTA solution along the side of the plate. Close the lid.

13. Incubate the plate on the slide warmer at 37 ^{o}C for 5-10 minutes.
14. After incubation, check the cells under microscope to make sure that cells are detached, rounded and loose.
15. Add 4 ml **complete medium** to neutralize the trypsin.
16. Using the same serological pipette, disperse cells by repeated pipetting. **Avoid air bubbles**.
17. Transfer cell suspension to the sterile 15 ml conical tube. Repeat pipetting to break up cell clumps.
18. **If you plan on doing a cell count, you can use a sample of cell suspension at this point.**
19. Spin the tube at **200G** for 5-10 minutes in the centrifuge. 7 minutes is preferred
20. Aspirate the medium leaving about 0.5 ml fluid in the tube.
21. Resuspend cells in an appropriate amount of complete media based on specific number of cells as needed for the experiment.
22. Plate enough cells into a fresh plate. Make up total volume of medium to 10 ml (If you are plating 1 ml cells, add 9 ml complete media (e.g., 1 ml+9 ml, 2 ml +8 ml, 3 ml +7 ml etc.)

Protocol for freezing of cEDS dermal fibroblasts and neonatal human dermal fibroblasts

(Adapted from Cellular Engineering – Preliminary Edition, by Sakthikumar Ambady)

1. Mark three 15 ml conical tubes as follows:
    a. freezing solution A: The final composition is DMEM/10% FBS/20% DMSO
    b. freezing solution B: The final composition is DMEM/10% FBS/2X final cell concentration for freezing.
    c. freezing mixture (one per student): Once the mixture is prepared as per instructions, the final composition of the mixture in this tube will be DMEM/10% FBS/10% DMSO/1X cell concentration.
2. Prepare 5 ml of "freezing solution A" by mixing the following:
    a. DMEM basal medium: 3.5 ml
    b. DMSO: 1.0 ml
    c. FBS: 0.5 ml
3. Prepare "freezing solution B" by creating a solution that has a final composition of double the cell concentration desired for freezing
    a. Ex. 2 mL of DMEM/10% FBS with 1 million cells per mL will result in a final freezing mixture of 500k per mL of solution.
4. For the regular cell freezing with DMSO, mix the contents in "freezing solution B" by gently inverting the tube 3–4 times to ensure uniform cell suspension.
5. Using a P-1000 micropipette, quickly transfer 1 ml of cell suspension to the tube labeled "freezing mixture".
6. Using a P-1000 micropipette, measure 1 ml of freezing solution A. Introduce the solution slowly to the cells in the "freezing mixture" tube while mixing the solutions gently and gradually. Introduce about 200 µl of freezing solution A to the cell suspension, and aspirate back 200 µl cell suspension into the pipet. Repeat the process gently and

deliberately. This is called “pro-gressive mixing.” In this method, DMSO is introduced to the cells progressively to minimize shock to the cells. Once all freezing mixture A is added to the cell suspension, mix the solution by repeated pipetting to ensure a uniform suspension.

   a. This can be scaled up depending on how many cryovials of cells will be frozen, as long as the ratio of freezing mixture a to freezing mixture b remains at 1:1.

7. Transfer 1 ml of the cell-DMSO mixture from the “freezing mixture” tube to the cryovial marked “with DMSO.” Tighten the cap and transfer the cryovial to the CoolCell freezing container.
8. The CoolCell container will remain in the −20 °C freezer until all students complete their freezing procedure and then will be transferred to the −80 °C freezer. The contents in the cryovials will freeze at a rate of 1 °C per minute in the CoolCell container in the −80 °C freezer.

Protocol for thawing of cEDS dermal fibroblasts and neonatal human dermal fibroblasts

(Adapted from Cellular Engineering – Preliminary Edition, by Sakthikumar Ambady)

1. The frozen cells should be rinsed with complete medium to remove DMSO while seeding in fresh plates.
2. Take one 15 ml conical tube per cryovial (good freeze and bad freeze) and add 9 ml fresh com-plete medium to each. Keep it aside in the hood.
3. Fill a small beaker (30 ml beaker) with lukewarm tap water. The level of water should not exceed about three quarters of the height of the cryovial.
4. Take the frozen vial of cells from the CoolCell box in the −80 °C freezer or liquid N2 tank (as appli-cable) and place it in the beaker containing lukewarm water. Make sure the vials are standing upright and not floating. This is done to prevent the possibility of tap water from entering the vial. Complete thawing occurs in about 1–2 minutes.
5. As soon as the contents of the vial are completely thawed, take the vial out of the beaker, wipe the outside of the vial dry with a paper towel sprayed with 70% isopropyl alcohol, and bring it inside the hood.
6. Using a P-1000 pipette, transfer the thawed contents of the vials to the conical tubes containing 9 ml complete medium. Rinse the vial a couple of times using 1 ml medium from the same 15 ml tube to which you transferred the cells. This ensures that any remaining frozen cells at the bottom of the vial are thawed and recovered. Close the cap of the 15 ml tube.
7. Mix the 15 ml tube by gently inverting a few times.
8. Spin the tube in a centrifuge at 200 g to 250 g for 7–10 minutes.
9. While the tubes are spinning, label T-25 with details for cells from each cryovial.
10. After centrifugation, check the size and quality of the cell pellet for the good and the bad freeze. Note the observations in your lab notebook.

11. Aspirate the supernatant, leaving less than 0.5 ml of medium with the cell pellet, place 8 mL of media into the T-25.
12. Add 2 ml complete medium to each pellet, resuspend the pellet, and transfer the entire content to the corresponding T-25.
13. Transfer the flask to the incubator and allow 15 to 20 minutes for the cells to settle down.
14. After the 15-to -20-minute incubation, observe the plates under the microscope and image the cells.
15. Note your observations about the quantity and quality of cells.
16. Transfer the plates to 37 °C incubator and let them incubate overnight. 17. On the following day, check under the microscope, specifically checking for dead and floating cells. Fewer floating and dead cells indicate successful freezing and thawing. A greater-than-85% survival rate in a good freeze is expected.

Protocol for Cell Count Assay

1. Once cells have been passaged, seed cells into a 12 well plate at 5,000 cells per well in 10% FBS DMEM with supplements.
2. Image every 24 hours starting on Day 1 (24 hours after cells were initially seeded)
    a. Imaging will be conducted by placing the well mask under the plate and placing it onto the microscope. The top left and bottom right of each well visible within the mask will be imaged.
3. Imaging will occur until day 5 when assays will be terminated.

Protocol for Monolayer Scratch Assay

1. Seed cells into a 12-well plate with 80k cells (cEDS or NHF) per well and allowe to grow until 90-100% confluent.
2. Aspirate media from well-plate
3. Scrape using 200uL pipette
    a. Scrape should be a full-length scratch from the top of each well plate and through the center for consistent results.
    b. The well plate mask template should be placed underneath the well plate to ensure a centered scratch
4. Rinse with 500uL PBS
5. Aspirate PBS from well-plate
6. Add 1000uL complete DMEM to each well plate
7. Incubate at 37C
8. Image wound in the same location at t = 0, 24, 48, 72, and 96hr
9. Analyze via ImageJ

Protocol for Fibrin Stock Solutions

Materials:

Fibrinogen (Sigma-Aldrich, Cat No:F8630-1G, 65-85% clottable protein)

*Assume 65% clottable protein
Thrombin (T6634, Sigma-Aldrich, 100 U)
Calcium Chloride (CaCl2; MW: 110.99)
Sodium Chloride (NaCl; MW: 58.44)
HEPES (MW: 238.3)

Procedure:
HEPES buffered saline (HBS) preparation
Definition: HBS contains 20 mM HEPES and 0.9% (w/v) NaCl

1. Add the following reagents to 200 mL:
    a. 2.25g of NaCl
    b. 1.1915g of HEPES
2. pH solution to 7.4 using NaOH/HCl
3. Bring final volume to 250 mL
4. Store at room temperature

Fibrinogen aliquots (10 mg/mL)

1. Measure 30 mL of HBS into a 50 mL conical tube, pre-warm to 37°C
2. Weigh out the calculated amount of grams fibrinogen, and pour into the conical tube
    a. % Effective Protein = (% Protein) * (% Clottable Protein)
    b. ____*____ = ____% effective
    c. Gold Standard: 10mg/mL at 72%
    d. (10 mg/mL)(0.72) = (X mg/mL)(% Effective Protein)
    e. (10)(0.72) = (X)(___)
    f. X = _____ mg/mL
    g. (X mg/mL) * 30 mL = Y g
    h. Y = _____ mg/mL * 30 mL = _____ g
3. Put conical tube on rocker plate, adjusting the position every 30 minutes until fibrinogen goes into solution

****NEVER SHAKE/VORTEX FIBRINOGEN SOLUTION!!!! THIS WILL CAUSE FIBRINOGEN TO FALL OUT OF SOLUTION AND BIND TO ITSELF!!!!

4. Incubate conical tube at 37°C overnight to ensure fibrinogen is completely dissolved

The next morning, measure 1 mL aliquots in microcentrifuge tubes and store at -20 °C

Thrombin aliquots (4 U/ 200 µL)

1. Add 5 mL HBS to bottle of 100 U thrombin, mix well
2. Aliquot 200 µL into microcentrifuge tubes and store at -20 °C (Final concentration: 4U / 200 µL)
3. Calcium chloride preparation (40 mM)

4. Add 0.1776 g of CaCl2 to 40 mL of diH2O
5. Store at 4 °

Protocol for Fibrin Dot Outgrowth Assay

1. Add 150 µL of thrombin aliquot to 850 µL of calcium chloride solution in a 15 mL tube, mix well.
2. Add 200,000 fibroblasts to Th/$CaCl_2$ suspended in 200 µL of 10% FBS DMEM with 20 µg/mL aprotinin.
3. Mix 1000 µL Fibrinogen and with fibroblast Th/$CaCl_2$ mixture, and pipette 100µL of solution at a time into separate wells in a 12-well plate, creating dots.
    a. be quick because it will start to polymerize immediately
    b. Smaller amounts (with the same concentrations) of thrombin, cells, and fibrinogen can be mixed to limit waste as gels polymerize rapidly.
4. Gels should be allowed to polymerize for 1 hr in incubator
5. After 1 hour in incubator, add 1 mL of 10% FBS DMEM with 20 µg/mL aprotinin to each gel and place in incubator for overnight attachment

Procedure for Fibrin Gels Seeded with Fibroblasts for Indentation Testing

1. Add 150 µL of thrombin aliquot to 850 µL of calcium chloride solution in a 15 mL tube, mix well.
2. Add 200,000 fibroblasts to Th/$CaCl_2$ suspended in 200 µL of 10% FBS DMEM with 20 µg/mL aprotinin.
3. Add fibroblast/Th/$CaCl_2$ mixture into well
4. Add 1000 µL Fibrinogen and mix well (be quick because it will start to polymerize immediately)
5. Gels should be allowed to polymerize for 1 hr in incubator
6. After 1 hour in incubator, add 1 mL of 10% FBS DMEM with 20 µg/mL aprotinin to each gel and place in incubator for overnight attachment

Procedure for Fibrin Gels Seeded with Fibroblasts for Final Wound Model

1. Add 37.5 µL of thrombin aliquot to 212.5 µL of calcium chloride solution in a 15 mL tube, mix well.
2. Add 200,000 fibroblasts to Th/$CaCl_2$ suspended in 200 µL of 10% FBS DMEM with 20 µg/mL aprotinin.
3. Add fibroblast/Th/$CaCl_2$ mixture into well
4. Add 250 µL Fibrinogen and mix well (be quick because it will start to polymerize immediately)
5. Gels should be allowed to polymerize for 1 hr in incubator

6. After 1 hour in incubator, add 1 mL of 10% FBS DMEM with 20 µg/mL aprotinin to each gel and place in incubator for overnight attachment

Appendix J: Gel Indentation Structural Modulus Example Calculation

Values

$$a = Indenter\ Radius = 0.003m$$

$$A = Contact\ Area = \pi a^2$$

$$B = Fitted\ Constant$$

$$n = Indenter\ Geometry\ Constant = 1$$

$$P = Load = B(h - h_f)^n$$

$$h = Displacement$$

$$S = Elastic\ Contact\ Stiffness = (\frac{dP}{dh})_{h=h_{max}}$$

$$\beta = Indenter\ Geometry\ Constant = 1\ (Assumed)$$

$$E_r = Indentation/Reduced\ Modulus = \frac{\sqrt{\pi}}{2\beta}\frac{S}{\sqrt{A}}$$

$$v = Poisson's\ Ratio\ of\ Sample = 0.25\ (Assumed)$$ (Duong et al., 2009)

$$v_i = Poisson's\ Ratio\ of\ Indenter = 0.33\ (Aluminum)$$

$$E_i = Structural\ Modulus\ of\ Sample$$

$$E = Structural\ Modulus\ of\ Indenter = 70\ GPa\ (Aluminum)$$

$$Structural\ Modulus\ Correction = \frac{1}{E_r} = \frac{1 - v^2}{E} + \frac{1 - v_i^2}{E_i}$$

Solution

$$A = \pi a^2 = \pi(0.003)^2 = 2.83 \times 10^{-5}\ m^2$$

$$P = B(h - h_f)^n = 36.063h - 0.0603\ (Linear\ Approximation)$$

$$S = (\frac{dP}{dh})_{h=h_{max}} = 36.063\ N/m$$

$$E_r = \frac{\sqrt{\pi}}{2\beta}\frac{S}{\sqrt{A}} = \frac{\sqrt{\pi}}{2(1)}\frac{44.167\ [\frac{N}{m}]}{\sqrt{2.83 \times 10^{-5}\ [m^2]}} = 6.01\ kPa$$

$$\frac{1}{E_r} = \frac{1 - v^2}{E} + \frac{1 - v_i^2}{E_i}$$

$$\frac{1}{6.01\ kPa} = \frac{1-(0.25)^2}{E_i} + \frac{1-(0.33)^2}{7\times 10^7\ kPa}$$

$$E_i = 5.63\ kPa$$

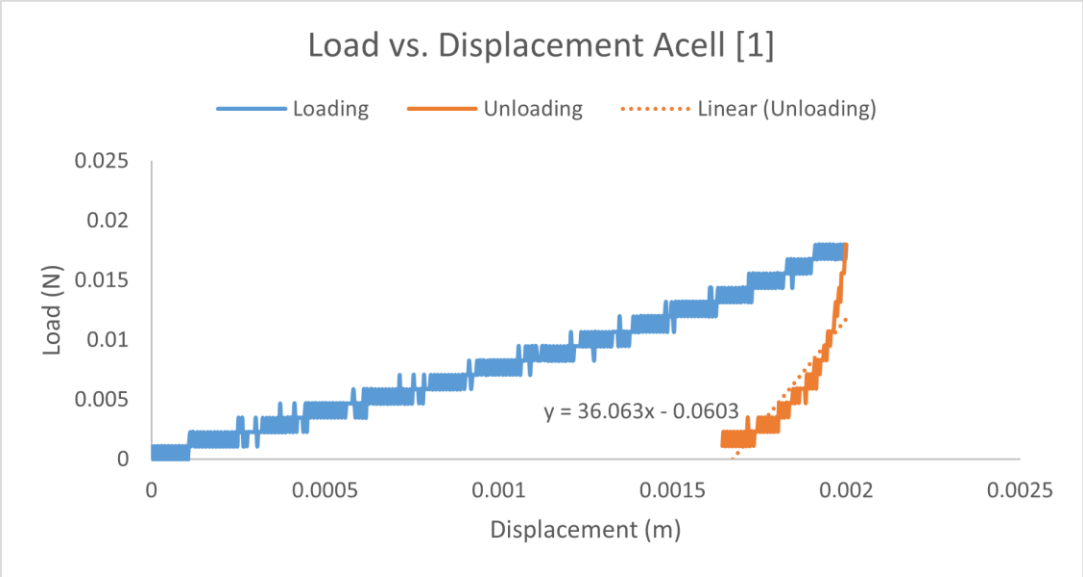

Given	Constants	Constant \	Units	Solution	Variable	Value	Units
	a	0.003	m		Er	6010.5	Pa
	A	2.8E-05	m^2		Er	6.0105	kPa
	B/S	36.063	N/m		1/Er	0.00017	1/Pa
	n	1	Unitless		1-(*v* i)^2	0.9375	Unitless
	β	1	Unitless		1-(*v*)^2	0.8911	Unitless
	v	0.33	Unitless		(1/Er)-{[1-(v)^2]/E}	0.00017	1/Pa
	v i	0.25	Unitless		Ei	5634.84	Pa
	E	7E+10	Pa		Ei	5.63484	kPa

Appendix K: Gel Indentation Data and Load vs. Displacement Graphs

Acellular				NO ACELL DAY 4 DATA, ALL FILLER DATA IN YELLOW			
Acell Ei (kPa)	Day 1 Average Ei (kPa)		Stdv	Acell Ei (kPa)	Day 4 Average Ei (kPa)		Stdv
5.63				0			
6.30				0			
		5.97	0.47254628			0	0
NHF							
NHF Ei (kPa)	Day 1 Average Ei (kPa)		Stdv	NHF Ei (kPa)	Day 4 Average Ei (kPa)		Stdv
6.32				6.99			
7.69				8.27			
		7.00	0.96486948			7.63	0.90344
cEDS							
cEDS Ei (kPa)	Day 1 Average Ei (kPa)		Stdv	cEDS Ei (kPa)	Day 4 Average Ei (kPa)		Stdv
8.34				13.66			
12.12				8.96			
		10.23	2.6696603			11.31	3.326386

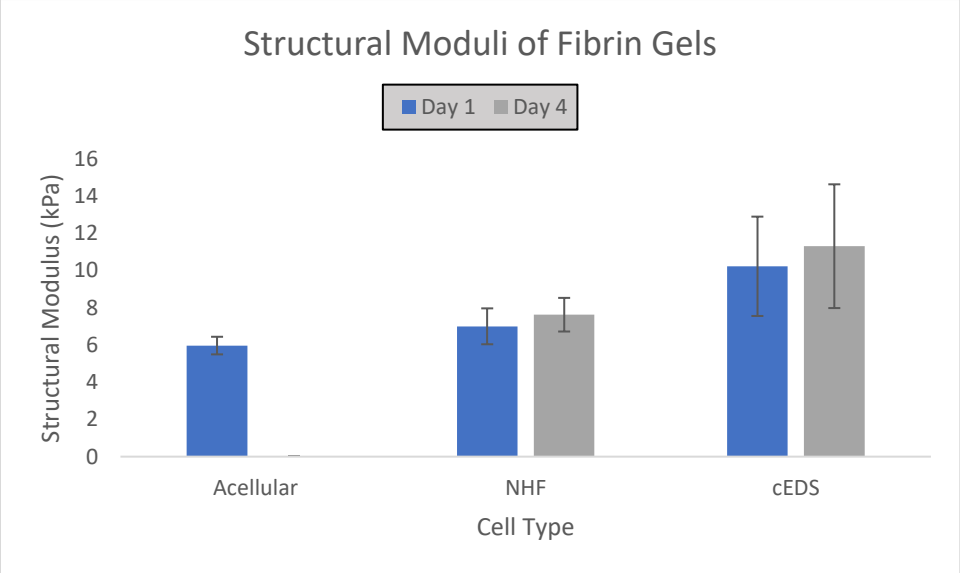

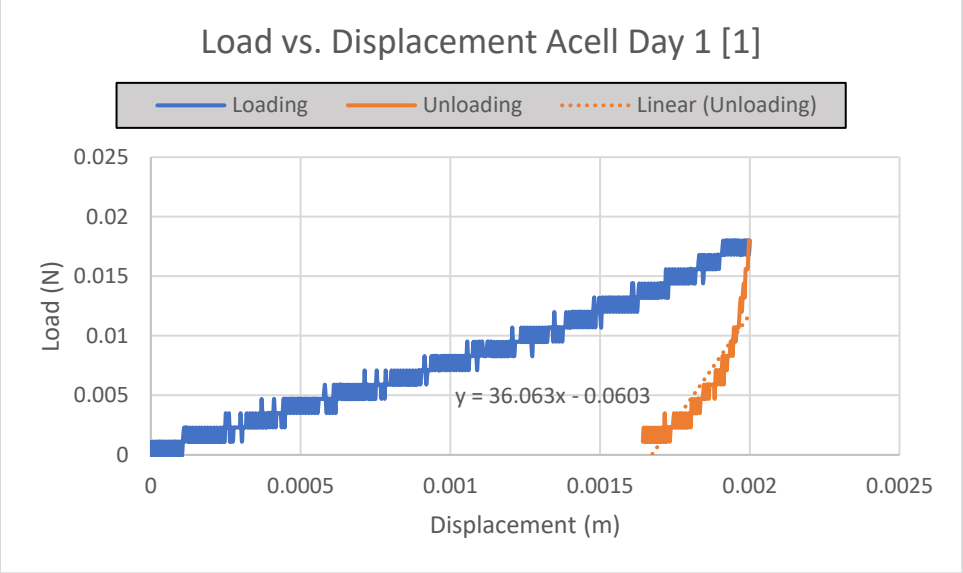

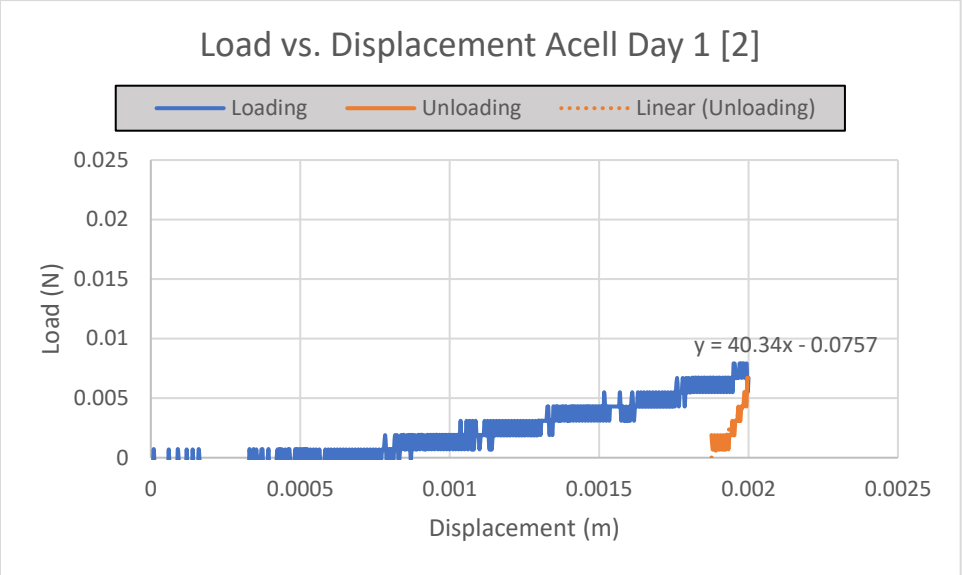
Load vs. Displacement Acell Day 1 [2]
Loading
Unloading
Linear (Unloading)
Load (N)
0.025
0.02
0.015
0.01
0.005
0
y = 40.34x - 0.0757
0
0.0005
0.001
0.0015
0.002
0.0025
Displacement (m)

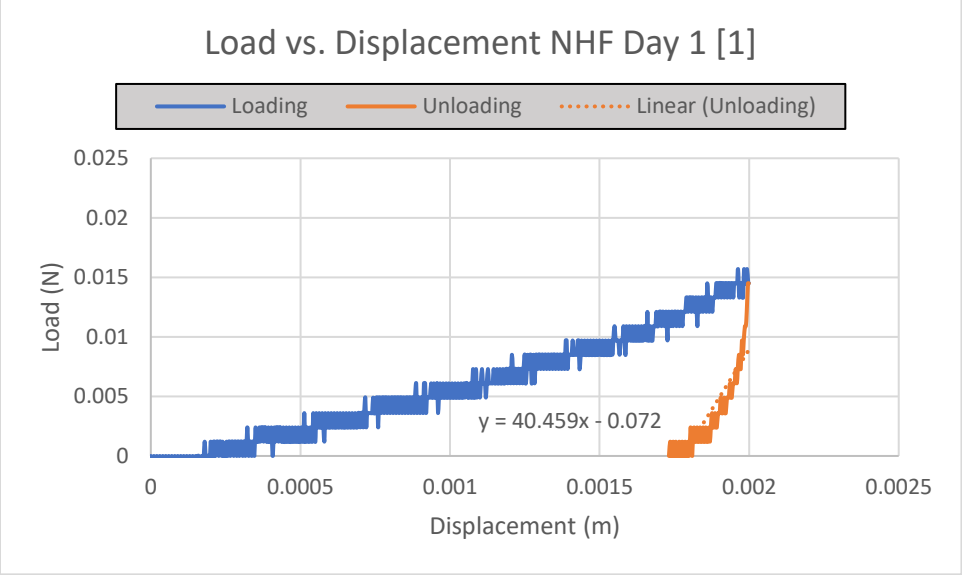
Load vs. Displacement NHF Day 1 [1]
Loading
Unloading
Linear (Unloading)
Load (N)
0.025
0.02
0.015
0.01
0.005
0
y = 40.459x - 0.072
0
0.0005
0.001
0.0015
0.002
0.0025
Displacement (m)

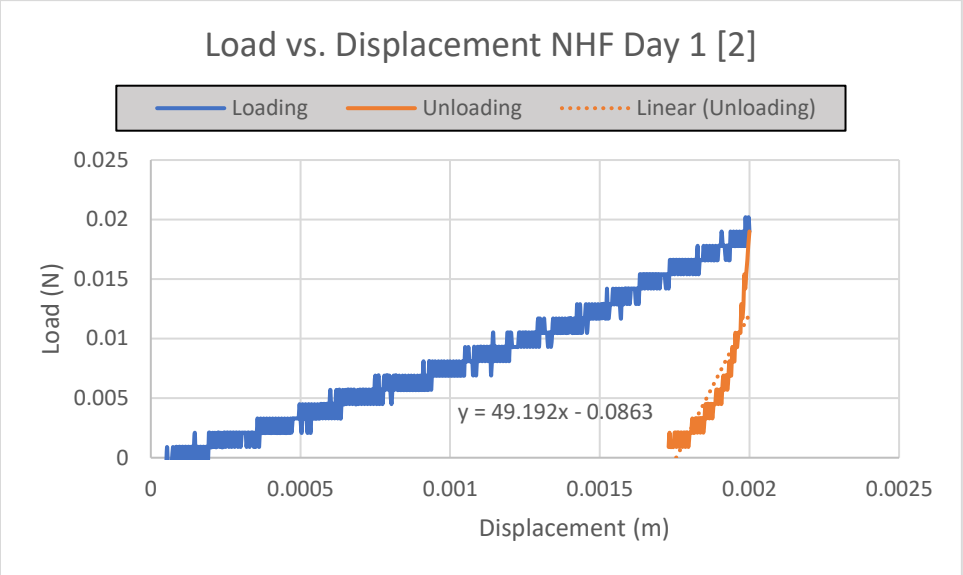
Load vs. Displacement NHF Day 1 [2]
Loading
Unloading
Linear (Unloading)
Load (N)
0.025
0.02
0.015
0.01
0.005
0
y = 49.192x - 0.0863
0
0.0005
0.001
0.0015
0.002
0.0025
Displacement (m)

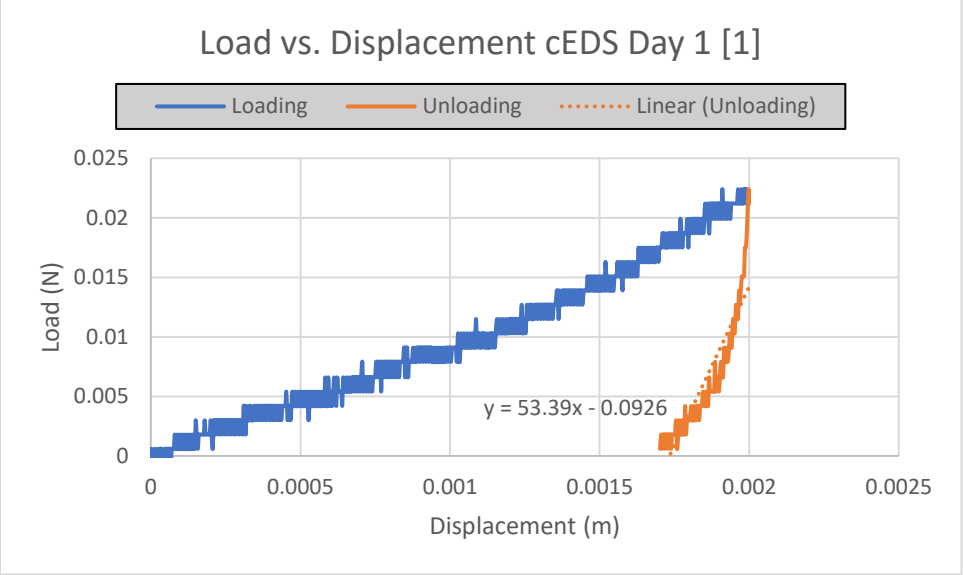
Load vs. Displacement cEDS Day 1 [1]
Loading
Unloading
Linear (Unloading)
Load (N)
0.025
0.02
0.015
0.01
0.005
0
y = 53.39x - 0.0926
0
0.0005
0.001
0.0015
0.002
0.0025
Displacement (m)

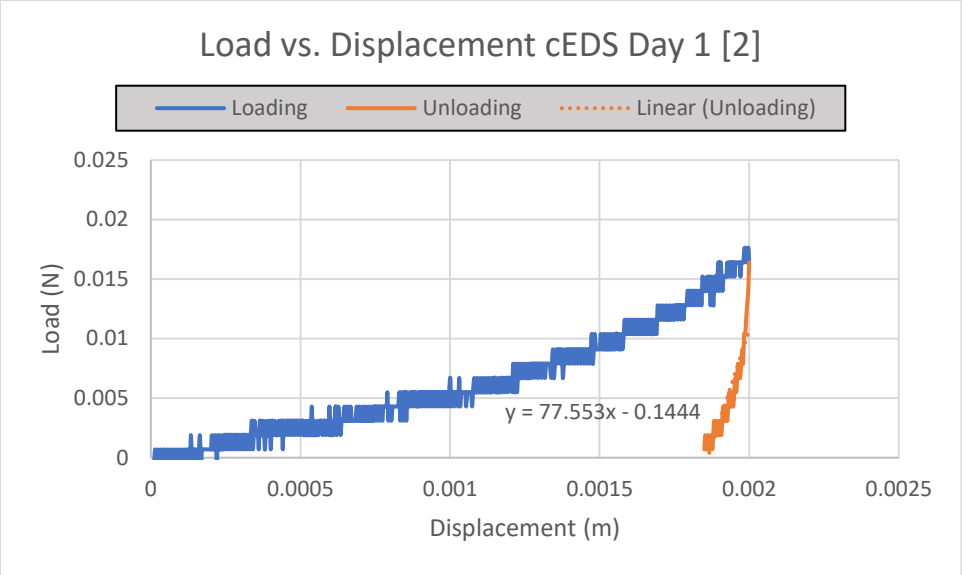
Load vs. Displacement cEDS Day 1 [2]
Loading
Unloading
Linear (Unloading)
Load (N)
0.025
0.02
0.015
0.01
0.005
0
y = 77.553x - 0.1444
0
0.0005
0.001
0.0015
0.002
0.0025
Displacement (m)

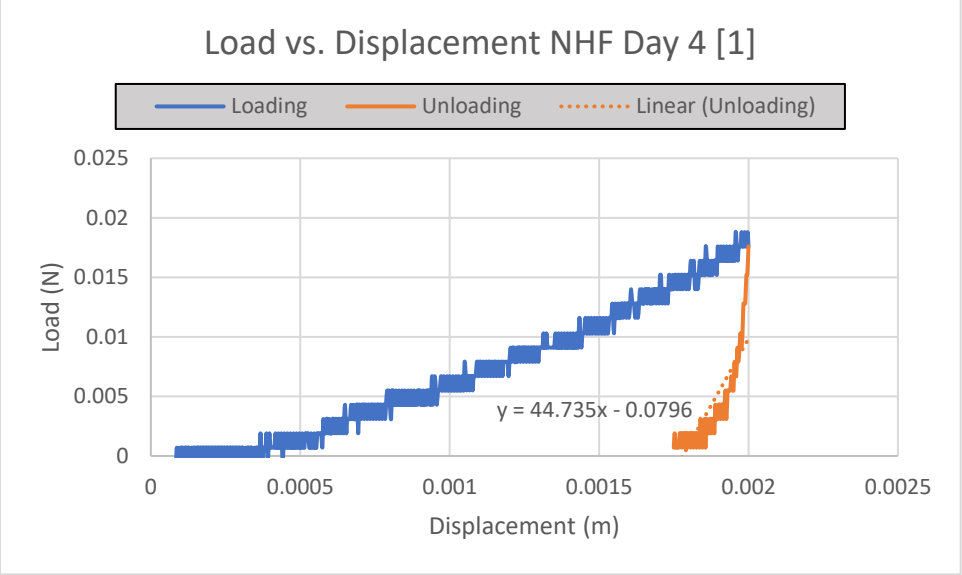
Load vs. Displacement NHF Day 4 [1]
Loading
Unloading
Linear (Unloading)
Load (N)
0.025
0.02
0.015
0.01
0.005
0
y = 44.735x - 0.0796
0
0.0005
0.001
0.0015
0.002
0.0025
Displacement (m)

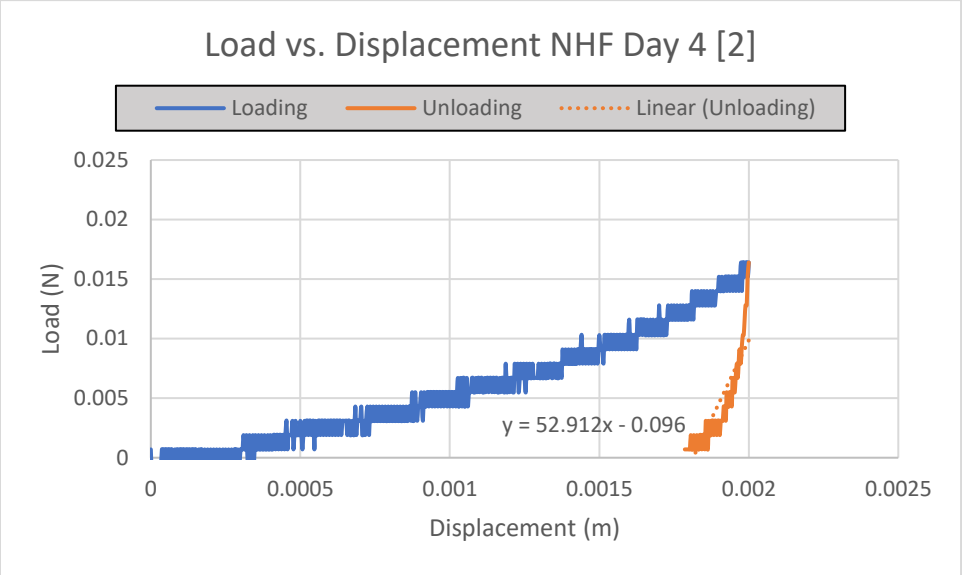
Load vs. Displacement NHF Day 4 [2]
Loading
Unloading
Linear (Unloading)
Load (N)
0.025
0.02
0.015
0.01
0.005
0
y = 52.912x - 0.096
0
0.0005
0.001
0.0015
0.002
0.0025
Displacement (m)

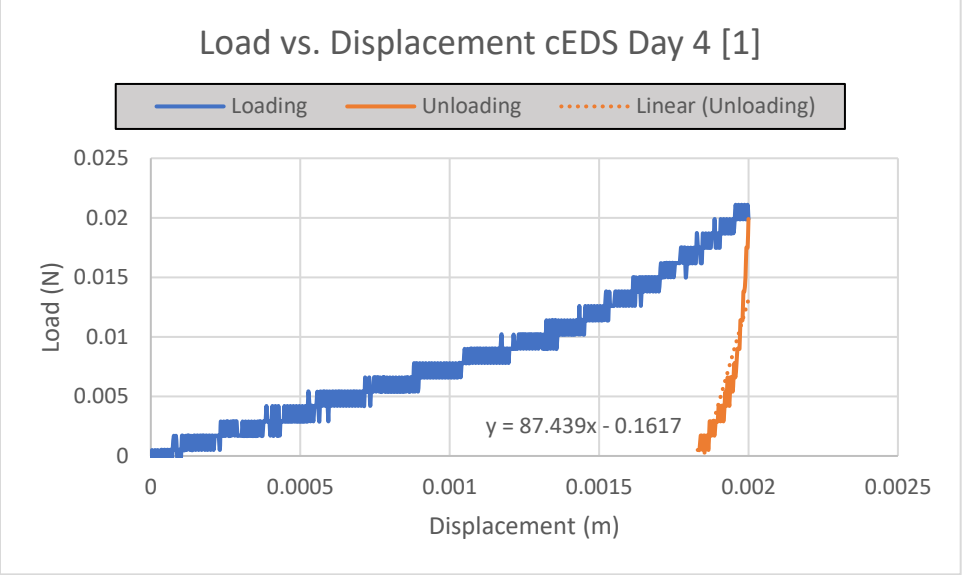
Load vs. Displacement cEDS Day 4 [1]
Loading
Unloading
Linear (Unloading)
Load (N)
0.025
0.02
0.015
0.01
0.005
0
y = 87.439x - 0.1617
0
0.0005
0.001
0.0015
0.002
0.0025
Displacement (m)

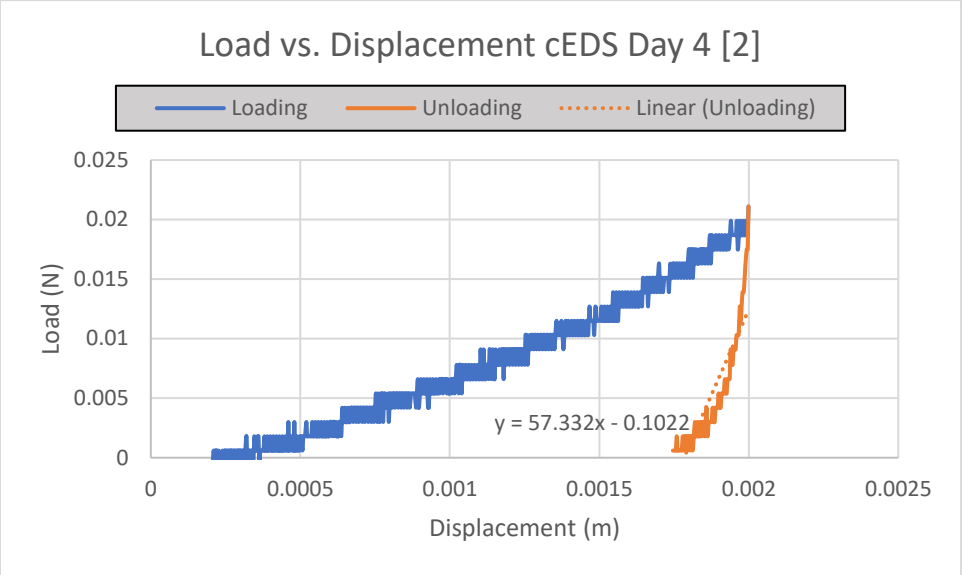
Load vs. Displacement cEDS Day 4 [2]
Loading
Unloading
Linear (Unloading)
0.025
0.02
0.015
0.01
0.005
0
Load (N)
y = 57.332x - 0.1022
0
0.0005
0.001
0.0015
0.002
0.0025
Displacement (m)

Appendix L: Statistical Analysis

Group	Test	Time	Statistic Type	Statistic Value	DF	P Value	P Value Level	Comparison	Mean Group 1	SD Group 1	N Group 1	Mean Group 2	SD Group 2	N Group 2
Scratch	t-test	Time 0	T statistic					cEDS/NHF	100.00	0.00	8	100.00	0.00	9
Scratch	t-test	Time 2	T statistic	-3.09	12.06	0.009	**	cEDS/NHF	95.44	1.59	8	99.16	3.18	9
Scratch	t-test	Time 4	T statistic	-2.60	14.84	0.020	*	cEDS/NHF	88.26	2.94	8	92.45	3.71	9
Scratch	t-test	Time 6	T statistic	-3.30	14.93	0.005	**	cEDS/NHF	80.53	3.77	8	86.76	4.00	9
Scratch	t-test	Time 8	T statistic					cEDS/NHF	70.49	5.46	8			
Scratch	t-test	Time 10	T statistic	-4.62	10.75	0.001	***	cEDS/NHF	63.40	7.27	8	76.83	4.09	9
Scratch	t-test	Time 12	T statistic	-3.27	11.06	0.007	**	cEDS/NHF	55.90	9.54	8	68.50	5.61	9
Scratch	t-test	Time 14	T statistic	-4.08	9.94	0.002	**	cEDS/NHF	47.21	11.10	8	64.87	5.46	9
Scratch	t-test	Time 16	T statistic	-3.10	10.60	0.010	*	cEDS/NHF	40.40	10.37	8	53.21	5.70	9
Scratch	t-test	Time 18	T statistic	-2.16	10.98	0.053	NS	cEDS/NHF	32.42	13.19	8	43.94	7.67	9
Scratch	t-test	Time 20	T statistic	-2.09	9.51	0.065	NS	cEDS/NHF	22.33	14.89	8	34.26	6.74	9
Scratch	t-test	Time 22	T statistic	-0.84	10.30	0.421	NS	cEDS/NHF	19.04	14.71	8	23.91	7.72	9
Scratch	t-test	Time 24	T statistic	-0.50	11.33	0.626	NS	cEDS/NHF	15.04	14.86	8	18.08	9.09	9
Proliferation	t-test	Day 1	T statistic	-2.28	2.47	0.126	NS	cEDS/NHF	14.17	5.86	3	22.33	2.02	3
Proliferation	t-test	Day 2	T statistic	-1.71	2.60	0.200	NS	cEDS/NHF	24.83	10.69	3	36.17	4.19	3
Proliferation	t-test	Day 3	T statistic	-2.40	2.05	0.136	NS	cEDS/NHF	37.00	9.10	3	49.67	1.04	3
Proliferation	t-test	Day 4	T statistic	-1.75	4.00	0.156	NS	cEDS/NHF	58.33	11.73	3	75.00	11.65	3
Proliferation	t-test	Day 5	T statistic	-1.69	3.61	0.175	NS	cEDS/NHF	72.50	17.30	3	93.17	12.29	3
Indentation	t-test	Day 1	T statistic	-2.22	1.06	0.257	NS	ACell/cEDS	5.97	0.47	2	10.23	2.67	2
Indentation	t-test	Day 1	T statistic	-1.36	1.45	0.346	NS	ACell/NHF	5.97	0.47	2	7.00	0.96	2
Indentation	t-test	Day 1	T statistic	1.61	1.26	0.315	NS	cEDS/NHF	10.23	2.67	2	7.00	0.96	2
Indentation	t-test	Day 4	T statistic	1.51	1.15	0.349	NS	cEDS/NHF	11.31	3.33	2	7.63	0.90	2
Indentation	t-test	Day 1 - Day 4	T statistic	-0.36	1.91	0.756	NS	cEDS 1/cEDS 4	10.23	2.67	2	11.31	3.33	2
Indentation	t-test	Day 1 - Day 4	T statistic	-0.67	1.99	0.573	NS	NHF 1/NHF 4	7.00	0.96	2	7.63	0.90	2
Indentation	ANOVA	Day 1	F value	3.58	2.00	0.161	NS	ACell/cEDS/NHF						

Appendix M: Materials and Model Cost

Overview of all materials costs during project not including cost of project lab usage, materials provided within the project lab such as media, media supplements, and cell passage materials.

Item	Supplier	Reference Number	Cost (USD)
cEDS Fibroblasts	Coriell Institute	GM21659	143
Fibrinogen	Sigma-Aldrich	F8630-1G	263
Thrombin	Sigma-Aldrich	T6634-100UN	101
Aproptinin	Thermofischer scientific	J11388.MB	144.65
Leather Punch	Amazon		14.98

Total Cost of Materials (USD)	666.63
Remaining Budget (USD)	333.37

Overview of model cost estimated from calculations using how much material is provided in each item compared to how much material is needed to prepare a singular wound model.

Note: Leather punch tool is a one-time cost, there for model cost is reduced to $12.25 for all subsequent models made.

Theoretical Cost of Model	
Element	**Cost (USD)**
cEDS Fibroblasts	8.3
Fibrinogen	0.66
Thrombin	2.02
Aprotinin	1.27
Leather Punch	14.98
Total Cost of Device (USD)	27.23